Stallard Scientific Editing

your trusted partner in English-language excellence

Stallard Scientific Limited
56 Brougham Street
Nelson 7010
New Zealand

Tel: +64 3 5489108
Fax: +64 3 5489106
Email: info@stallardediting.com
Web: www.stallardediting.com

Invoice

Date: 28 December 2018

Job number: 18492

Title: Quantifying light absorption and its source attribution of insoluble light-absorbing particles in Tibetan Plateau glaciers from 2013-2015

Client: Prof. Xin Wang
Lanzhou University, Lanzhou, Gansu
China

Description		Cost	Total
Scientific editing			
Word count:	7593	US$22 per 250 words	668
Intensive edit surcharge (+10%)			67
Discount for first-time client (−10%)			-67
		Total due:	**US$ 668**

Date job returned: 28 December 2018

Thank you for choosing Stallard Scientific Editing.
We look forward to working with you again in the future.

Yours sincerely,

Aaron Stallard
Managing Editor
Stallard Scientific Editing

Bank details
Bank name: ANZ
Branch name: Trafalgar Street
Branch address: 248 Trafalgar Street, Nelson 7010, New Zealand
Account name: Stallard Scientific Limited
Swift code: ANZBNZ22
Account number: 06-0665-0199616-00
Note: All bank charges should be for your account. Please mention the job number in the payment details.

Response to editor:

Dear Dr. Wang et al

Comment 1: Thank you for submitting a revised draft of your manuscript. You have adequately addressed the major science concerns that were raised by reviewers, but before the manuscript can be accepted for publication in The Cryosphere it will need careful editing for English grammar and consistency.

R: This manuscript has been edited by the Stallard Scientific Editing company (https://www.stallardediting.com). Although we have paid for this manuscript, we only get the invoice of this manuscript instead of the statement due to the new year's vacation (See Author's Response in Page 1).

Comment 2: The abstract states that "Although the mineral dust was assumed to be the highest contributor to the mass loading of ILAPs...", and yet the prior sentence reports larger mean mass concentrations for OC than for mineral dust. So why is it assumed that mineral dust is the highest contributor to mass loadings? These two sentences seem inconsistent. This is one example of why the manuscript needs careful examination from multiple people to ensure that the results are reported consistently.

R: Corrected as suggested.

Comment 3: Table 1 is cut off at the edge of the page and cannot even be read in its entirety.

R: Corrected as suggested.

Comment 4: English grammar:

R: See comment 1.

Comment 5: The paper needs careful editing by one or more people who are fluent in English. Readers will discover grammatical errors starting with the first sentence of the Introduction.

R: See comment 1.

Comment 6: Data sharing policy: Please read the journal's data policy at: https://www.the-cryosphere.net/about/data_policy.html. Prior to publication, your data should be posted in a publicly-accessible repository, and a link to the data should be provided in the Data Availability section of the manuscript. This is particularly important for new measurements such as those reported here.

R: We have provided the data sharing contents as suggested.

I do not plan to send out your manuscript again for additional peer review. After your manuscript is *carefully* cleaned up, I expect we will be able to publish it in The Cryosphere.

Quantifying the light absorption and source attribution of insoluble light-absorbing particles on Tibetan Plateau glaciers between 2013 and 2015

Xin Wang[1,*], Hailun Wei[1], Jun Liu[1], Baiqing Xu[1,2,*], Mo Wang[2], Mingxia Ji[1], and Hongchun Jin[3]

[1] Key Laboratory for Semi-Arid Climate Change of the Ministry of Education, College of Atmospheric Sciences, Lanzhou University, Lanzhou, 730000, China

[2] Key Laboratory of Tibetan Environment Changes and Land Surface Processes, Institute of Tibetan Plateau Research, Chinese Academy of Sciences, Beijing 100085, China

[3] KuWeather Science and Technology, Haidian, Beijing, 100085, China

Corresponding authors: X. Wang (wxin@lzu.edu.cn) and B. Xu (baiqing@itpcas.ac.cn)

样式定义 ... [1]
带格式的: 左侧: 3.17 厘米, 右侧: 3.17 厘米
删除的内容: its
带格式的: 字体颜色: 黑色, 英语(英国)
带格式的: 字体颜色: 黑色, 英语(英国)
带格式的: 字体颜色: 黑色, 英语(英国)
删除的内容: in
带格式的: 字体颜色: 黑色, 英语(英国)
删除的内容: from
带格式的: 字体颜色: 黑色, 英语(英国)
删除的内容: -
带格式的: 字体颜色: 黑色, 英语(英国)
带格式的: 字体: 小四, 字体颜色: 黑色, 英语(英国)
删除的内容: ,*,
删除的内容: ,*,
带格式的: 字体颜色: 黑色, 英语(英国)
带格式的 ... [2]
带格式的: 字体颜色: 黑色, 英语(英国)
带格式的: 字体: (默认) Times New Roman, (中文) +西文正文 (Calibri), 五号, 字体颜色: 黑色, 英语(英国)
带格式的: 正文, 两端对齐, 在相同样式的段落间不添加空格, 无孤行控制
带格式的: 字体: (中文) +西文正文 (Calibri), 字体颜色: 黑色, 英语(英国)
带格式的 ... [3]
带格式的: 字体: 小四, 字体颜色: 黑色, 英语(英国)
删除的内容: Correspondence to
带格式的 ... [4]
删除的内容:),
带格式的: 默认段落字体, 字体颜色: 黑色, 英语(英国)
带格式的: 英语(英国)
带格式的 ... [5]

Abstract. The deposition of insoluble light-absorbing particles (ILAPs) on snow and ice surfaces can significantly reduce albedo, thereby accelerating the melting process. In this study, 67 ice samples were collected from seven glaciers located on the Tibetan Plateau (TP) between May 2013 and October 2015. The mixing ratios of black carbon (BC), organic carbon (OC), and mineral dust (MD) were measured with an integrating sphere / integrating sandwich spectrophotometer (ISSW) system, which assumes that the light absorption of MD is due to iron oxide. Our results indicate that the mass-mixing ratios of BC, OC, and MD exhibit considerable variability (BC: 10–3100 ng g^{-1}; OC: 10–17,000 ng g^{-1}; MD: 10–3500 ng g^{-1}), with respective mean values of 220 ± 400 ng g^{-1}, 1360 ± 2420 ng g^{-1}, and 240 ± 450 ng g^{-1} over the course of the field campaign. We observed that for wavelengths of 450–600 nm, the measured light absorption can be largely attributed to the average light absorption of BC (50.7%) and OC (33.2%). Chemical elements and selected carbonaceous particles were also analysed for source attributions of particulate light absorption, based on a positive matrix factorisation (PMF) receptor model. Our findings indicate that on average, industrial pollution (33.1%), biomass/biofuel burning (29.4%), and MD (37.5%) constitute the principal sources of ILAPs deposited on TP glaciers.

删除的内容: Amounts
带格式的 ... [6]
删除的内容: deposited on the surface of
带格式的 ... [7]
带格式的 ... [8]
删除的内容: the snow
删除的内容: and accelerate
带格式的 ... [10]
删除的内容: snow
带格式的 ... [9]
带格式的 ... [11]
删除的内容: in
带格式的 ... [12]
删除的内容: over
删除的内容: from
带格式的 ... [13]
带格式的 ... [14]
删除的内容: to
带格式的 ... [15]
删除的内容: ratio
带格式的 ... [16]
删除的内容: was
带格式的 ... [17]
删除的内容: using
带格式的 ... [18]
删除的内容: /
带格式的 ... [19]
删除的内容: associated with the chemical ... [20]
带格式的 ... [21]
删除的内容: The
带格式的 ... [22]
删除的内容: indicated
带格式的 ... [23]
删除的内容:
带格式的 ... [24]
删除的内容: showed a large variation of
带格式的 ... [25]
删除的内容: -
带格式的 ... [26]
删除的内容: -
带格式的 ... [27]
删除的内容: ,

1 Introduction

The absorption efficiency of black carbon (BC) is higher in snow than in the atmosphere because of the higher degree of sunlight scattering in the former (Chylek et al., 1984), and a wealth of evidence confirms that the snow albedo is dominated by BC at visible wavelengths (Warren and Wiscombe, 1980, 1985; Brandt et al., 2011; Hadley and Kirchstetter, 2012). For instance, a mixing ratio of 10 ng g^{-1} of BC in snow can reduce albedo by 1%, an amount equivalent to the impact of 500 ng g^{-1} of dust at 500 nm (Warren and Wiscombe, 1980; Warren, 1982; Wang et al., 2017), and Conway et al. (1996) reported a reduction in snow albedo of 0.21 and concomitant 50% increase in ablation due to 500 ng g^{-1} of BC contamination. Similarly, in their experiments using a geometric-optics surface-wave approach, Liou et al. (2011) described an albedo reduction of as much as 5–10% caused by small amounts of BC mixed internally with snow grains. Overall, BC accounts for 85% of the total absorption by insoluble light-absorbing impurities (ILAPs) in snow at wavelengths of 400–700 nm (Bond et al., 2013). Furthermore, the 'efficacy' of this BC forcing is twice as effective as that of CO_2 due to snow albedo change and may have contributed to the large-scale warming of the Northern Hemisphere over the last century (Hansen and Nazarenko, 2004).

The Tibetan Plateau (TP) and neighbouring uplands together contain the largest area of snow and ice outside the polar regions (Qin et al., 2006). However, over the last decade, ~82% of TP glaciers have retreated, and 10% of the permafrost area has been lost as a result of climate warming (Qiu, 2008; Yao et al., 2012). Xu et al. (2009a, b) reported that the deposition of BC on snow and ice surfaces has potentially led to an earlier onset of the melting season, whereas the consequent loss of ice is projected to impact atmospheric circulation and ecosystem viability at regional and global scales and in multiple ways (Qian et al., 2011; Skiles et al., 2012; Sand et al., 2013). Therefore, BC is considered to be a significant factor in the recent shrinkage of TP glaciers (Xu et al., 2006, 2009a; Qian et al., 2015; Li et al., 2016).

In addition to BC, organic carbon (OC) and mineral dust (MD) have also been identified as ILAPs contributing to springtime snowmelt and surface warming through snow-darkening effects (Painter et al., 2010, 2012; Huang et al., 2011; Kaspari et al., 2014; Wang et al., 2013, 2014;

带格式的 ... [37]
删除的内容: Ample
带格式的 ... [38]
删除的内容: indicated
带格式的 ... [39]
删除的内容: is largely dominant by black carbon ... [40]
带格式的 ... [41]
删除的内容: -
带格式的 ... [42]
删除的内容: snow
带格式的 ... [43]
删除的内容: which has a similar effect
删除的内容: that
带格式的 ... [44]
删除的内容: -
带格式的 ... [45]
带格式的 ... [46]
删除的内容:). Chylek et al. (1984) indicated that ... [47]
带格式的 ... [48]
删除的内容: measured
带格式的 ... [49]
删除的内容: snow albedo
带格式的 ... [50]
删除的内容: a
删除的内容: the
带格式的 ... [51]
带格式的 ... [52]
删除的内容: rate of natural snow attributed to
带格式的 ... [53]
删除的内容: -
删除的内容: Liou et al. (2011) developed
带格式的 ... [54]
带格式的 ... [55]
删除的内容: to demonstrate the snow
带格式的 ... [56]
删除的内容: by
带格式的 ... [57]
删除的内容: ~
带格式的 ... [58]
删除的内容: due to
带格式的 ... [59]
删除的内容: mixed

Yasunari et al., 2015). However, the optical properties of OC in snow are still largely unknown because of limited field data and technical limitations. For instance, pre-industrial OC concentrations derived from sites in Antarctica are unexpectedly high (80–360 ng g^{-1}) relative to those reported from Greenland (10–40 ng g^{-1}) and alpine sites (45–98 ng g^{-1}) (Federer et al., 2008; Preunkert et al., 2011). Furthermore, there remain significant uncertainties in estimating the light-absorption capacities of different types of OC from the chemical and optical analysis of new snow samples in western North America (Dang et al., 2014). Although the contribution of OC to climate warming is generally lower than that of BC, the impact of OC is nonetheless significant, particularly over southeastern Siberia, northeastern East Asia, and western Canada (Yasunari et al., 2015). As summarized by Flanner et al. (2009) in relation to modelling future climate, consideration of the OC content of snow is key to better estimating the impact of ILAPs' absorption of solar radiation from the ultraviolet to visible wavelengths.

It is well established that the light-absorption capacity of MD is linked to the iron oxides (hereafter referred to as Fe) (Alfaro et al., 2004; Lafon et al., 2004, 2006; Moosmuller et al., 2012). The yellow-red colour of Fe (primarily hematite and goethite) affects the ability of mineral dust to absorb sunlight at short wavelengths and alters its radiative properties, potentially influencing climate (Takahashi et al., 2011; Jeong et al., 2012; Zhou et al., 2017). For example, Painter et al. (2007) concluded that the duration of seasonal snow cover in alpine regions is shortened by 18–35 days owing to the redeposition of disturbed desert dust. On the TP, goethite constitutes the dominant form of Fe (81%–98% mass) deposited on glacier surfaces (Cong et al., 2018). Over the grasslands of Inner Mongolia and northern China, light absorption is dominated by OC, whereas the snow-particulate light absorption is provided primarily by local soil and desert dust derived from the northern TP (Wang et al., 2013).

To date, numerous surveys have sought to evaluate the light-absorption capacity of ILAPs (Xu et al., 2009a, b; Doherty et al., 2010; Huang et al., 2011; Wang et al., 2013; Dang et al., 2014) and their potential source attribution in snow and ice (Hegg et al., 2010; Zhang et al., 2013a; Doherty et al., 2014; Jenkins et al., 2016; Li et al., 2016; Pu et al., 2017). In their 2009 study, Hegg et al. (2010) used a positive matrix factorisation (PMF) receptor model to establish that ILAPs deposited

删除的内容: absent due to
带格式的 ... [92]
删除的内容: small-scale
带格式的 ... [93]
删除的内容: campaigns
带格式的 ... [94]
删除的内容: the
带格式的 ... [95]
删除的内容: extracted at Antarctic
带格式的 ... [96]
删除的内容: higher ranging from
带格式的 ... [97]
删除的内容: to
带格式的 ... [98]
删除的内容: -
带格式的 ... [99]
删除的内容: than
删除的内容: for
带格式的 ... [100]
删除的内容: -
带格式的 ... [101]
删除的内容: Alpine
带格式的 ... [102]
删除的内容: $^{-1}$) for pre-industrial ice
带格式的 ... [103]
带格式的 ... [104]
删除的内容: [Please check that this is your ... [105]
删除的内容: are still
带格式的 ... [106]
带格式的 ... [107]
删除的内容:
带格式的 ... [108]
删除的内容: by
带格式的 ... [109]
删除的内容: associated with both
带格式的 ... [110]
删除的内容: analyses from
带格式的 ... [111]
删除的内容: across
带格式的 ... [112]
删除的内容: the global
带格式的 ... [113]

in Arctic snow originate predominantly from biomass burning, pollution, and marine sources. Similarly, Doherty et al. (2014) assessed chemical and optical data from 67 North American sites and concluded that the source attribution of particulate light absorption in seasonal snow is dominated by biomass/biofuel burning, soil dust, and fossil fuel pollution.

Until now, ILAP light absorption and emission sources for the TP have been poorly understood. Increasing the in situ measurement of ILAPs in snow and ice is therefore crucial to assessing the factors driving ongoing glacier retreat. Between 2013 and 2015, we collected ice samples from seven TP glaciers during both the wet and dry seasons. By using an integrating sphere/integrating sandwich spectrophotometer (ISSW) system coupled with chemical analysis, we evaluated the particulate light absorption of BC, OC, and MD before exploring the relative contributions of their respective emission sources via a PMF receptor model.

2 Site description and methods

2.1 Site description and sample collection

Figure 1 depicts the topography and sampling locations of each glacier included in our study (Liu et al., 2014), arranged along a roughly north–south transect, and Figure S1 provides photographs of each sampling site. To minimise potential ILAP contamination from local sources, sampling sites were located at least 50 km from the main road and adjacent city areas. During our 2013–2015 field seasons, we collected a total of 67 columnar ice samples from the seven glacier surfaces. Owing to their broad geographic distribution, our glacial dataset represents climatic and land-surface conditions ranging from semi-arid in the northern TP to humid in the southern.

Samples 1–19 were collected from the centre of Qiyi (QY) Glacier (39°14′N, 97°45′E) (Fig. 1a) during the 2013–2015 wet seasons. QY Glacier is a small valley glacier (area 2.98 km^2, length 3.8 km) located in the Qilian Mountains on the northern TP and is classified as a typical 'wet island' in an otherwise arid region on account of its multiple landcover types (e.g., forests, bush/scrub, steppes, and meadows). Further south, samples 20–22 were collected from the southeastern Qiumianleiketage (QM) Glacier (36°70′N, 90°73′E) during the dry season. Located in the

删除的内容: is mainly originated
带格式的 ... [156]
删除的内容: based on a positive matrix ... [158]
带格式的 ... [157]
带格式的 ... [159]
删除的内容: found
带格式的 ... [160]
删除的内容: based on the chemical and optical ... [161]
带格式的 ... [162]
删除的内容: Up to
删除的内容: understand.
带格式的 ... [163]
删除的内容: the
带格式的 ... [164]
删除的内容: of ILAPs remain
带格式的 ... [165]
删除的内容: [Please check that this is your ... [166]
带格式的 ... [167]
删除的内容: -
带格式的 ... [168]
删除的内容: measurements
带格式的 ... [169]
删除的内容: most urgent task to explore the
带格式的 ... [170]
删除的内容: , especially in the TP regions. Here
带格式的 ... [171]
删除的内容: performed a large survey on ... [172]
带格式的 ... [173]
删除的内容: on
带格式的 ... [174]
删除的内容: in the TP regions
删除的内容: monsoon
带格式的 ... [176]
删除的内容: non-monsoon
带格式的 ... [175]
带格式的 ... [177]
删除的内容: from 2013-2015.
带格式的 ... [178]
删除的内容: /
删除的内容: … ... [179]
带格式的 ... [180]
删除的内容: associated

Kunlun Mountains of the TP (Fig. 1b). QM Glacier has a length of 2.6 km and an area of 1.73 km².

Samples 23–32 were collected from the northern part of Meikuang (MK) Glacier (35°42′N, 94°12′E), located in the eastern Kunlun Mountains, during both the wet and the dry seasons. This region is characterised by alluvial deposits and sand dunes. MK Glacier is 1.8 km long and 1.1 km² in area (Fig. 1c). Immediately east of MK Glacier, samples 33–44 were collected from the southwestern reaches of Yuzhufeng (YZF) Glacier (35°38′N, 94°13′E), located on the highest peak (6178 m) of the eastern Kunlun Mountains. This high-altitude region is characterised by a cold, arid climate and by fern, forest, and scrubby vegetation.

Samples 45–49 were obtained from the centre of Hariqin (HRQ) Glacier (33°14′N, 92°09′E), a north-facing system located on the northern flank of the Tanggula Mountains, central Qinghai–Tibetan Plateau (Fig. 1e). HRQ Glacier drops from an elevation of 5820 m a.s.l. to its terminus at 5400 m, where it forms the headwaters of the Dongkemadi River. To the southwest of HRQ Glacier, the 2.8-km-long Xiaodongkemadi (XD) Glacier (33°04′N, 92°04′E) covers an area of 1.77 km² and descends from 5900 m elevation to its terminus at 5500 m (Fig. 1f). The surrounding landscape is predominantly cold steppe and tundra. Samples 50–60 were collected from the southern reaches of XD glacier.

Gurenhekou (GR) Glacier (30°19′N, 90°46′E) is a relatively small (area: 1.4 km²; length: 2.5 km; width: 0.6 km) cold-based alpine glacier located approximately 90 km north of Lhasa in southern Tibet (Fig. 1g). The glacier ranges in elevation from 6000 m to its terminus at 5600 m. Both Kang et al. (2009) and Bolch et al. (2010) suggested that GR is influenced by both the continental climate of central Asia and the Indian monsoon system. Samples 61–67 were collected from the eastern part of the glacier.

According to Wang et al. (2015), the mean annual accumulation of snow/ice at our TP drilling sites is approximately 2 m. Therefore, for each glacier sampled between 2013 and 2015, we used a 1.2-m-long vertical tube lined with a clean, 20-cm-diameter plastic bag to collect ice deposited via

带格式的 ... [238]
删除的内容: Qinghai-Tibet Plateau (Fig. 1b). The ... [239]
删除的内容: [In other cases, you use 'Tibetan ... [241]
带格式的 ... [242]
删除的内容: the QM glacier is
删除的内容: ,
删除的内容: the
删除的内容: is
带格式的 ... [240]
带格式的 ... [243]
带格式的 ... [244]
带格式的 ... [245]
带格式的 ... [246]
带格式的 ... [247]
删除的内容: -
删除的内容: in
带格式的 ... [249]
删除的内容: glacier during both monsoon and ... [250]
带格式的 ... [248]
带格式的 ... [251]
删除的内容: ,
带格式的 ... [252]
删除的内容: 42’
带格式的 ... [253]
删除的内容: 12’
带格式的 ... [254]
删除的内容:). The MK glacier is
带格式的 ... [255]
删除的内容: where is characterized
带格式的 ... [256]
删除的内容: The
带格式的 ... [257]
删除的内容: glacier
带格式的 ... [258]
删除的内容: in length with an area of
带格式的 ... [259]
删除的内容: ↵ ... [260]
带格式的 ... [261]
删除的内容: -
删除的内容: in
带格式的 ... [262]
带格式的 ... [263]

both wet and dry deposition (Fig. 2). Owing to their relatively high altitude, wet deposition over these glaciers is dominated by fresh snowfall, with considerably less derived from rainfall. Nonetheless, the majority of samples consist of ice rather than snow, reflecting the prevalence of multiple melting processes. Following collection, ice samples were maintained at a temperature of −20 °C during transportation to the State Key Laboratory of Cryospheric Sciences, Cold and Arid Regions Environmental and Engineering Research Institute in Lanzhou, China.

In the laboratory, samples were cut vertically into four pieces following established clean-sampling protocols (Fig. S2), after which one of the four pieces was cut at 10-cm resolution. Where multiple melting events have produced a non-uniform surface layer (e.g., sites 13 and 26), we cut samples to be longer or shorter than the average. Any dirty layers were cut and analysed separately. A total of 189 samples were used in this study. To minimise the loss of ILAPs to the container walls, each sample was placed in a clean glass beaker and melted quickly in a microwave oven, immediately after which the water was filtered through Nuclepore filters (pore size 0.2 μm) following the procedure reported in Doherty et al. (2010). Further details of the filtration process are given in Wang et al. (2013) and Doherty et al. (2014).

2.2 Optical analysis

To calculate the mass-mixing ratio of BC in our samples, we employed an updated integrating sphere/integrating sandwich spectrophotometer (ISSW). Although this instrument is similar to that developed by Grenfell et al. (2011), a chief difference is that we used two integrating spheres to reduce diffuse radiation during measurement instead of the integrating sandwich diffuser employed by those authors. The ISSW spectrophotometer measures the light attenuation spectrum from 400 to 700 nm, with the total light attenuation spectrum being extended by linear extrapolation to cover the full spectral range (300–750 nm). Nominally, light attenuation is sensitive solely to ILAPs trapped on the filter as a result of the diffuse radiation field and the sandwich structure of the two integrated spheres in the ISSW (Doherty et al., 2014). Specifically, the system detects the light transmitted by an ice sample, $S(\lambda)$, and compares this value to that transmitted by a blank filter, $S_0(\lambda)$. The relative attenuation (Atn) is then expressed as:

删除的内容: during monsoon and non-monsoon ... [338]
带格式的 ... [337]
删除的内容: altitudes of these glaciers, the
删除的内容: in
删除的内容: Due
带格式的 ... [340]
删除的内容: the
带格式的 ... [339]
带格式的 ... [341]
带格式的 ... [342]
带格式的 ... [343]
删除的内容: areas were predominant
带格式的 ... [344]
删除的内容: new fallen snow, while much
删除的内容: formed by
带格式的 ... [346]
删除的内容: precipitation
带格式的 ... [345]
带格式的 ... [347]
删除的内容: However, most of the samples were ... [348]
删除的内容: [Please note that snow is a form of ... [349]
带格式的 ... [350]
删除的内容: Then, the column
带格式的 ... [351]
删除的内容: kept frozen under -
带格式的 ... [352]
删除的内容: °C and transported to laboratory ... [353]
带格式的 ... [354]
删除的内容: . Firstly, each sample was
带格式的 ... [355]
删除的内容: from the top to the bottom as shown ... [356]
带格式的 ... [357]
删除的内容: , resulting in a total of 189 samples ... [358]
带格式的 ... [359]
删除的内容: due to the multi-melting processes ... [360]
带格式的 ... [361]
删除的内容: other samples (e.g. sites 13 and 26) ... [362]
带格式的 ... [363]
删除的内容: put into
带格式的 ... [364]
删除的内容: . The melted water then
带格式的 ... [365]

$$\mathrm{Atn} = \ln[S_0(\lambda)/S(\lambda)] \quad (1)$$

The mass absorption efficiency (MAE) and absorption Ångström exponents (Å) employed here for BC, OC, and Fe are described in detail by Wang et al. (2013). Using this technique, we are able to estimate the following parameters: equivalent BC (C_{BC}^{equiv}), maximum BC (C_{BC}^{max}), estimated BC (C_{BC}^{est}), the fraction of light absorption by non-BC ILAPs (f_{non-BC}^{est}), the absorption Ångström exponent of non-BC ILAPs ($Å_{non\text{-}BC}$), and the total absorption Ångström exponent ($Å_{tot}$). These parameters are defined as follows:

1. C_{BC}^{equiv} (ng g^{-1}): *equivalent BC* is the amount of BC that would be needed to produce absorption by all insoluble particles in snow for wavelengths of 300–750 nm.

2. C_{BC}^{max} (ng g^{-1}): *maximum BC* is the maximum possible BC mixing ratio in snow, assuming that all light absorption is due to BC at wavelengths of 650–700 nm.

3. C_{BC}^{est} (ng g^{-1}): *estimated BC* is the estimated true mass of BC in snow derived by separating the spectrally resolved total light absorption and non-BC fractions.

4. f_{non-BC}^{est} (%): the *fraction of light absorption by non-BC light-absorbing particles* is the integrated absorption due to non-BC light-absorbing particles. This value is weighted by the down-welling solar flux at wavelengths of 300–750 nm.

5. $Å_{non\text{-}BC}$: *non-BC absorption Ångström exponent*, derived from the light absorption by non-BC components for wavelengths of 450–600 nm.

6. $Å_{tot}$: *absorption Ångström exponent* calculated for all insoluble particles deposited on the filter between 450 and 600 nm.

Both the composition and the size distribution of aerosols are well-known parameters influencing the absorption Ångström exponent. Doherty et al. (2010) reported that the absorption Ångström exponent of OC is close to 5, consistent with the previously reported range of 4–6 (Kirchstetter et al., 2004), and several studies have included absorption Ångström exponents of 2–5 for MD (Fialho et al., 2005; Lafon et al., 2006; Zhou et al., 2017; Cong et al., 2018). Typical absorption Ångström exponents for urban and industrial fossil fuel emissions fall within the range 1.0–1.5 (Millikan, 1961; Bergstrom et al., 2007), which is slightly lower than that of biomass-burning aerosols (1.5–2.5) (Kirchstetter et al., 2004; Bergstrom et al., 2007). In this study, we note

删除的内容: =
带格式的 ... [399]
带格式的 ... [400]
删除的内容:
带格式的 ... [398]
带格式的 ... [401]
删除的内容: MACs
带格式的 ... [403]
删除的内容: the
带格式的 ... [402]
带格式的 ... [404]
删除的内容: used
带格式的 ... [405]
删除的内容: this study could be found in
删除的内容: By using
删除的内容: [Please consider spelling this term ... [407]
带格式的 ... [408]
删除的内容: can
带格式的 ... [406]
带格式的 ... [409]
删除的内容: included
带格式的 ... [410]
带格式的 ... [411]
带格式的 ... [412]
带格式的 ... [413]
带格式的 ... [414]
删除的内容:)
带格式的 ... [415]
删除的内容: [Your list of parameters in this ... [416]
带格式的 ... [417]
删除的内容: 1
带格式的 ... [418]
带格式的 ... [419]
删除的内容: -
带格式的 ... [420]
删除的内容: by
带格式的 ... [421]
删除的内容: the
带格式的 ... [422]
删除的内容: -
带格式的 ... [423]
删除的内容: 2
带格式的 ... [424]
带格式的 ... [425]

that the absorption Ångström exponent ($Å_{tot}$) comprises both BC and non-BC impurities trapped on the filters. Calculations of $Å_{tot}$ and of $Å_{non\text{-}BC}$ are described by Doherty et al. (2014). Specifically, $Å_{non\text{-}BC}$ is calculated as a linear combination of the contributions to light absorption made by OC and Fe:

$$Å_{non\text{-}BC} = F_{OC} \times Å_{OC} + F_{Fe} \times Å_{Fe} \quad (2)$$

2.3 Chemical analysis

Major metallic elements (Al, Cr, Mn, Fe, Ni, Cu, Zn, Cd, and Pb) were analysed on an X-7 Thermo Electrical inductively coupled plasma mass spectrometer (ICP-MS) at the Institute of Tibetan Plateau Research, Beijing, China. The detection limits are 0.238 ng ml^{-1} for Al, 0.075 ng ml^{-1} for Cr, 0.006 ng ml^{-1} for Mn, 4.146 ng ml^{-1} for Fe, 0.049 ng ml^{-1} for Ni, 0.054 ng ml^{-1} for Cu, 0.049 ng ml^{-1} for Zn, 0.002 ng ml^{-1} for Cd, and 0.002 ng ml^{-1} for Pb. Prior to measurement, melted samples were acidified (pH < 2) with ultra-pure HNO_3 and left to settle for 48 hours. The relative deviation between most of the measured values and the standard reference values is within 10%. Details of these procedures are given in Li et al. (2009) and Cong et al. (2010).

We used a Dionex 320 ion chromatograph to measure major anions (Cl^-, NO_2^-, NO_3^-, and SO_4^{2-}) and cations (Na^+, NH_4^+, K^+, Mg^{2+}, and Ca^{2+}) in filtrated water samples. The apparatus, which is housed at the Institute of Tibetan Plateau Research in Beijing, is equipped with a CS12 column for cations and an AS11 column for anions and has a detection limit for all measured ions of 1 μg · l^{-1}. We also measured concentrations of Sea salt, MD, and biosmoke K ($K_{Biosmoke}$) to assess the mass contributions of the major components in our ice samples. Specifically, Sea salt was estimated according to the protocol described by Pio et al. (2007):

$$\text{Sea salt} = Na^+_{ss} + Cl^- + Mg^{2+}_{ss} + Ca^{2+}_{ss} + K^+_{ss} + SO^{2-}_{4ss}$$
$$= Na^+_{ss} + Cl^- + 0.12 \times Na^+_{ss} + 0.038 \times Na^+_{ss} + 0.038 \times Na^+_{ss} + 0.25 \times Na^+_{ss} \quad (3)$$

$$Na_{ss} = Na_{Total} - Al \times (Na/Al)_{Crust} \quad (4)$$

删除的内容: is due to the mix state of

带格式的 ... [460]

带格式的 ... [461]

删除的内容: , and the calculations

删除的内容: The

带格式的 ... [462]

删除的内容: could be found in the study of

带格式的 ... [463]

带格式的 ... [464]

删除的内容: due to

带格式的 ... [465]

删除的内容: , and the equation is listed as follows

带格式的 ... [466]

删除的内容: =

带格式的 ... [469]

删除的内容: ×

带格式的 ... [470]

删除的内容: ×

带格式的 ... [471]

删除的内容:

带格式的 ... [467]

带格式的 ... [472]

带格式的 ... [468]

带格式的 ... [473]

删除的内容: The major

带格式的 ... [474]

带格式的 ... [475]

删除的内容: analyzed by

带格式的 ... [476]

删除的内容: -

删除的内容: spectrometry

带格式的 ... [478]

删除的内容: -

带格式的 ... [479]

删除的内容: , X-7 Thermo Elemental

带格式的 ... [477]

带格式的 ... [480]

删除的内容: in

带格式的 ... [481]

删除的内容: Al,

带格式的 ... [482]

删除的内容: -

带格式的 ... [483]

where $(Na/Al)_{Crust}$ = 0.33 and represents the Na/Al ratio in the dust material (Wedepohl, 1995).

The MD content is calculated assuming an Al concentration for dust of 7% (Zhang et al., 2013b):

$$MD = Al/0.07 \qquad (5)$$

We determined $K_{Biosmoke}$ according to the following equation (Pu et al., 2017):

$$K_{Biosmoke} = K_{Total} - K_{Dust} - K_{Ss} \qquad (6)$$

$$K_{Dust} = Al \times (K/Al)_{Crust} \qquad (7)$$

$$K_{Ss} = Na_{Ss} \times 0.038 \qquad (8)$$

where $(K/Al)_{Crust}$ is 0.37, representing the K/Al ratio of the dust material (Wedepohl, 1995), and Na_{Ss} is estimated using Equation (4).

2.4 Enrichment factor

To evaluate the relative contributions of trace elements from natural (e.g., mineral and soil dust) versus anthropogenic sources (e.g., fossil fuels and vehicle exhaust), we conducted an inter-annual comparison of enrichment factor (EF) values, which represent the enrichment of a given element relative to its concentration in Earth's crust. The primary uncertainty in these calculations originates from differences in chemical composition between snow and the reference crustal material. The EF is defined as the concentration ratio of a given metal to that of Al, which is a reliable measure of crustal dust, normalised to the same concentration ratio characteristic of the upper continental crust (Wedepohl, 1995). EF is calculated by the equation:

$$EF = \frac{(X/Al)_{snow}}{(X/Al)_{crust}} \qquad (9)$$

带格式的 ... [530]

删除的内容: ,

带格式的 ... [531]

带格式的 ... [532]

删除的内容: materials

删除的内容:

带格式的 ... [533]

带格式的 ... [534]

删除的内容: was estimated as

带格式的 ... [535]

删除的内容: was

带格式的 ... [536]

删除的内容: by a straightforward method, and ... [537]

带格式的 ... [538]

删除的内容: in

带格式的 ... [539]

带格式的 ... [540]

带格式的 ... [541]

删除的内容: =

带格式的 ... [542]

删除的内容:

带格式的 ... [543]

带格式的 ... [544]

带格式的 ... [545]

删除的内容: as follows

带格式的 ... [546]

删除的内容: $K_{Biosmoke}$=K_{Total}-K_{Dust}-K_{Ss} ... [547]

带格式的 ... [548]

带格式的 ... [549]

删除的内容: =

删除的内容: ·

带格式的 ... [551]

删除的内容:

带格式的 ... [550]

带格式的 ... [552]

带格式的 ... [553]

删除的内容: =Na_{Ss}

带格式的 ... [554]

删除的内容: ·

带格式的 ... [555]

删除的内容:

带格式的 ... [556]

删除的内容: Where

删除的内容: [You use both "×" and "·" for

2.5 Source apportionment

PMF 5.0 is a receptor model used to determine ILAP source apportionment when source emission profiles are unavailable (Paatero and Tapper, 1994). We employed a PMF procedure similar to that described by Hegg et al. (2009, 2010), in which mass concentrations and chemical species uncertainties are provided as the input. Our final data set contained 189 samples with 18 elements; only those elements with high recovery were used for PMF analysis. For each sample, uncertainty values (Unc) for individual variables were estimated from an empirical equation expressed as:

$$\mathrm{Unc} = \sqrt{(\sigma \times c)^2 + (\mathrm{MDL}^2)} \qquad (10)$$

Where σ is the standard deviation, c represents the mass concentrations of the relative species, and the MDL depicts the method detection limited.

Although we ran the PMF model for between three and six factors, including six random seeds, we found that the most meaningful results for our TP sites were generated by a three-factor solution. Indeed, *Q* values (modified values) for this three-factor solution (both robust and true) were closest to the theoretical values of any factor number for which the model was run.

3 Results and discussion

3.1 Aerosol optical depth

Aerosol optical depth (AOD) represents both the transport pathways and deposition of dry aerosols, which in turn provide vital information on potential ILAP sources. As shown in Figure 3, QY, QM, MK, and YZF glaciers are located on the northern TP, whereas XD, HRQ, and GR glaciers are located in the plateau's southern regions. Therefore, to elaborate on the sources of ILAPs for each TP study site, we assessed the spatial distribution of averaged 500 nm AOD, derived from Aqua-MODIS between 2013 and 2015. According to Ramanathan et al. (2007), anthropogenic AOD—also referred to as atmospheric brown cloud (ABC)—on the south side of the Himalayas is greater than 0.3. Consequently, AOD (500 nm) values of >0.3 and <0.1 are considered representative of anthropogenic haze and background conditions, respectively.

We observed considerably higher AOD over the western TP than over the central TP. For example, values for QY, QM, MK, and YZF glaciers ranged from 0.25 to 0.3, suggestive of anthropogenic influence, whereas values for HRQ, XD, and GR glaciers were considerably lower

带格式的 ... [583]
删除的内容: The Positive Matrix Factorization (
删除的内容:)
删除的内容: generally accepted
带格式的 ... [585]
删除的内容: considered as
删除的内容: of the ILAPs
带格式的 ... [584]
带格式的 ... [586]
带格式的 ... [587]
带格式的 ... [588]
删除的内容: unknown
带格式的 ... [589]
删除的内容: Details of the
删除的内容: used in this study are
带格式的 ... [591]
删除的内容: the previous work as discussed in
带格式的 ... [590]
带格式的 ... [592]
删除的内容:). Generally, the
带格式的 ... [593]
删除的内容: concentration
带格式的 ... [594]
删除的内容: the uncertainties of the
带格式的 ... [595]
删除的内容: were used
带格式的 ... [596]
删除的内容: The
删除的内容: used for the PMF analysis
删除的内容: whereby
带格式的 ... [597]
带格式的 ... [598]
带格式的 ... [599]
删除的内容: that have
带格式的 ... [600]
删除的内容: . The
带格式的 ... [601]
删除的内容: For each sample, uncertainty value ... [602]
带格式的 ... [603]
删除的内容: was run
带格式的 ... [604]
删除的内容: 3 to 6

(<0.125). Although the elevated AOD over the western TP might serve to enhance glacial retreat there (Engling and Gelencser, 2010), we note that AOD over the TP in general was significantly lower than in southern Asia, particularly over the Indo-Gangetic Plain during the cold season. This pattern aligns closely with previous measurements (Cong et al., 2009; Ming et al., 2010; Yang et al., 2012; Lüthi et al., 2015).

3.2 Regional averages of optical parameters

Table 1 compiles the ice C_{BC}^{est}, C_{BC}^{max}, C_{BC}^{equiv}, f_{non-BC}^{est}, $\mathring{A}_{tot}$ and $\mathring{A}_{non-BC}$ data for each glacier. The lowest median C_{BC}^{est} (23–26 ng g^{-1}) was observed on HRQ and GR glaciers, southern TP, during the wet season, whereas the highest values (187–165 ng g^{-1}) occurred on MK and YZF glaciers on the central TP. Relative to the wet season, the measured concentrations of C_{BC}^{est} were markedly higher during the dry season for all seven glaciers. The lowest overall BC concentration was recorded on XD Glacier (C_{BC}^{est} = ~10 ng g^{-1}), whereas the maximum values of C_{BC}^{est} (3100 ng g^{-1}), C_{BC}^{max} (3600 ng g^{-1}), and C_{BC}^{equiv} (4700 ng g^{-1}) all corresponded to GR Glacier. Median $\mathring{A}_{tot}$ typically exceeded 1.0 at all seven sites (Fig. 4, Table 1).

The ice samples exhibited $\mathring{A}_{tot}$ and $\mathring{A}_{non-BC}$ values of 1.4–3.7 and 1.9–5.8, respectively (Table S1). As shown in Figure 4a, the median values of $\mathring{A}_{tot}$ for QY, MK, XD, and GR glaciers were 2.62, 2.64, 2.18, and 2.46, respectively, and the estimated contributions of non-BC ILAPs to absorption were approximately 41%, 44%, 36%, and 48%, respectively. Relatively high values were observed in samples from QM (2.76), YZF (2.95), and HRQ (2.87) glaciers. Accordingly, the estimated f_{non-BC}^{est} values for those regions were 44%, 48%, and 48%, respectively. With the exception of HRQ Glacier, our data set exhibits a clear south-to-north increase in $\mathring{A}_{non-BC}$ over the TP (Fig. 4b). Histograms depicting $\mathring{A}_{tot}$ by region are shown in Figure 5.

XD Glacier exhibited the greatest degree of $\mathring{A}_{tot}$ variability, not only in the higher values (~2–4), but also at the lower end of the range (<2). This broad distribution is indicative of the complicated sources of particulate light absorption. For instance, Wang et al. (2013) reported that higher $\mathring{A}_{tot}$ values (approximately 3.5–4.5) are strongly correlated with local soils, whereas fossil fuel combustion has an absorption Ångström exponent of <2 (Millikan, 1961; Fialho et al., 2005).

删除的内容: thus contribute
带格式的 ... [655]
删除的内容: the
带格式的 ... [656]
带格式的 ... [657]
删除的内容: of Himalayan glaciers
删除的内容:). In contrast, the lower values of ... [659]
删除的内容: regions
删除的内容: much
带格式的 ... [658]
带格式的 ... [660]
带格式的 ... [661]
带格式的 ... [662]
删除的内容: that over Southern
删除的内容: especially
带格式的 ... [663]
带格式的 ... [664]
删除的内容: is close to
删除的内容: over the TP regions
带格式的 ... [665]
带格式的 ... [666]
带格式的 ... [667]
带格式的 ... [668]
删除的内容: **the**
带格式的 ... [669]
删除的内容: The general information of
带格式的 ... [670]
带格式的 ... [671]
带格式的 ... [672]
带格式的 ... [673]
删除的内容: of the ice samples are given in Table ... [674]
带格式的 ... [675]
删除的内容: lower
带格式的 ... [676]
删除的内容: values of
带格式的 ... [677]
删除的内容: could be
带格式的 ... [678]
删除的内容: ng g^{-1},
带格式的 ... [679]
删除的内容: $^{-1}$ during the monsoon season in the
带格式的 ... [680]
删除的内容: on

A significant fraction of the total absorption on XD Glacier, therefore, is attributed not only to BC (49%; Fig. 7), but also to non-BC absorbers (51%) linked to OC and MD. In contrast, $Å_{tot}$ values for all other sites typically ranged from 2 to 3. The valuesof $Å_{non\text{-}BC}$ and $Å_{tot}$ for each site are also given in Figure S3.

Figure 6 shows the regional variability in BC, OC, and Fe concentrations during the wet and dry seasons. Although we observed clear differences in median and average ILAP concentrations among the seven glaciers, we also note that overall, ILAPs exhibited a similar pattern of variability throughout our study area. With the exception of QY and QM glaciers, we collected ice samples during both the wet and the dry seasons. On average, BC and OC concentrations at HRQ, XD, and GR glaciers were several orders of magnitude higher during the dry season than during the wet season. This pattern is consistent with the findings from the middle Himalayas of Cong et al. (2015), who reported that the dry season is characterised by a distinctly higher carbonaceous aerosol level than that of the wet season, despite similar air mass pathways.

Lüthi et al. (2015) demonstrated that the atmospheric brown cloud over Southern Asia can cross the Himalayas, transporting polluted air masses to the TP and potentially impacting regional glacier mass balance. In our data set, however, there is no apparent difference in ILAP mixing ratios between the wet and dry seasons for two adjacent (MK and YZF) glaciers. We attribute this pattern to the fact that with the exception of long-range pathways, local air pollutants can also impact ILAP availability on the central TP. For instance, although the prevailing air masses over the MK and YZF glaciers originate from the arid western TP and Taklimakan Desert regions, Huang et al. (2018) concluded that the concentration of trace elements at YZF Glacier, and thus that YZF Glacier is less influenced by human activity. In close agreement with Ming et al. (2013), our median values of C^{est}_{BC} and C_{OC} (referred to as the mass concentration of OC) exhibit a gradually decreasing trend from north to south, and the mass concentrations of BC are higher for northern TP glaciers than for their southern counterparts.

To help quantify the regional ILAP status of each glacier, Table 2 contains statistics on snow and ice samples collected both during our present investigation and during previous studies of TP

删除的内容: Therefore, a

删除的内容: was not only

带格式的 ... [746]

带格式的 ... [747]

删除的内容: %, shown in

带格式的 ... [748]

删除的内容:),

删除的内容: [Fig. 6 does not yet seem to have ... [749]

删除的内容: contributed by

删除的内容: accounting for

删除的内容: in the XD glacier.

删除的内容: a common feature in the

带格式的 ... [750]

带格式的 ... [751]

带格式的 ... [752]

删除的内容: due

带格式的 ... [753]

带格式的 ... [754]

删除的内容: depicted as red dots and blue ... [759]

带格式的 ... [755]

删除的内容: regions was that the major ... [756]

带格式的 ... [757]

删除的内容: in each site

带格式的 ... [758]

删除的内容: also given

带格式的 ... [760]

删除的内容: Fig. S3.

删除的内容: . [Please consider putting this in the ... [761]

带格式的 ... [762]

删除的内容: variations of

删除的内容: concentration in each glacier

带格式的 ... [765]

删除的内容: monsoon

带格式的 ... [766]

删除的内容: non-monsoon

带格式的 ... [763]

带格式的 ... [764]

带格式的 ... [767]

删除的内容: there were significant

带格式的 ... [768]

删除的内容: between the

带格式的 ... [769]

glaciers. During our visit to YZF Glacier, we collected twelve ice samples from depths between 15 and 45 cm (Table S1). As shown in Figure S4, C_{BC}^{est} values for this region typically ranged from ~100 to 1000 ng g^{-1}, with several values of <100 ng g^{-1}. A striking feature of this data set is the relatively high C_{BC}^{max} (1600 ng g^{-1}) and C_{OC} (9160 ng g^{-1}) in the surface layer at site 41. Judging by the high value of $f_{non\text{-}BC}^{est}$ (0.56) for this site, we suggest that these data indicate that light absorption at this site is influenced not only by BC but also potentially by OC and MD.

For YZF Glacier, $Å_{tot}$ typically varied between ~2 and 3.7, and the average $f_{non\text{-}BC}^{est}$ is close to 50%, which together suggest that ILAPs at this site are heavily influenced by anthropogenic air pollution. We also observed large variations in C_{OC}, with values ranging from ~10 to 17,000 ng g^{-1}. With the exception of site 23, C_{BC}^{est} values for MK Glacier were considerably lower than those of YZF Glacier (range 20–670 ng g^{-1}; median 130 ng g^{-1}; Fig. S5). MK Glacier gave a median C_{OC} of ~600 ng g^{-1}, whereas the fraction of total particulate light absorption attributable to non-BC constituents was typically ~16%–62%. $Å_{non\text{-}BC}$ (5.12) at this site is very similar to that of YZF Glacier (5.06).

C_{BC}^{est} values for QY Glacier (Fig. S6) are similar to those of MK Glacier, ranging from ~20 to 720 ng g^{-1} (excluding the highest value of 1900 ng g^{-1} at site 13). The fraction of total particulate light absorption due to the non-BC constituent $f_{non\text{-}BC}^{est}$ was typically ~20%–70%, with a median value of 41%. Together with the lower $Å_{tot}$ (2.6), this information indicates that BC plays a dominant role in influencing light absorption in this region. Compared with the other TP glaciers, we note that the vertical ILAP profiles on QY Glacier were collected during the 2014 and 2015 wet seasons (Table S1). The mixing ratios of OC and Fe were 80–10,100 ng g^{-1} and 20–340 ng g^{-1}, respectively. Figure S7 shows that the vertical profiles of the mass-mixing ratios of BC, OC, and Fe were more variable for XD Glacier than for the other six glaciers. With the exception of the surface layer at sites 53 and 54, C_{BC}^{est} typically ranged from 10 to 280 ng g^{-1}, indicating that XD Glacier is the cleanest site in our study. At sites 56–58, $f_{non\text{-}BC}^{est}$ was less than 38%, and $Å_{tot}$ ranged from 1 to 2.5, consistent with the combustion of fossil fuels due to industrial activity.

3.3 Scavenging and washing efficiencies

删除的内容: this field campaign,
删除的内容: were collected in the YZF glacier ... [830]
带格式的 ... [828]
带格式的 ... [829]
带格式的 ... [831]
删除的内容: of these ice samples collected in the ... [832]
带格式的 ... [833]
删除的内容: to
带格式的 ... [834]
删除的内容: Fig.
带格式的 ... [835]
删除的内容: most values of
带格式的 ... [836]
删除的内容: in
带格式的 ... [837]
删除的内容: -
删除的内容: -
带格式的 ... [838]
删除的内容: a few
带格式的 ... [839]
删除的内容: lower than
带格式的 ... [840]
删除的内容: -
带格式的 ... [841]
带格式的 ... [842]
删除的内容: One notable
带格式的 ... [843]
删除的内容: that
带格式的 ... [844]
删除的内容: highest concentrations of
带格式的 ... [846]
删除的内容: for the surface layer were 1600 ng g- ... [847]
带格式的 ... [848]
删除的内容: -
带格式的 ... [845]
带格式的 ... [849]
删除的内容: We pointed out
带格式的 ... [850]
删除的内容: the
带格式的 ... [851]
删除的内容: in the surface glacier
带格式的 ... [852]

Previous studies have demonstrated how ILAPs become trapped and integrated into the snowpack as a result of melting and sublimation, thereby enriching surface concentrations of these particles (Conway et al., 1996; Painter et al., 2012; Doherty et al., 2013). For instance, Doherty et al. (2013) reported that ILAP scavenging by snow meltwater leads to elevated concentrations of BC in the surface layer. Similarly, Flanner et al. (2007, 2009) concluded that amplified ablation due to the concentration of BC in melting snow serves to further reduce the snow albedo, thus providing a positive feedback to radiative forcing. However, the impact of multiple melting processes on ILAPs located at greater depths in the glacier surface remains unclear.

On QY Glacier, we observed a marked increase in ILAP mixing ratios with depth. Although this result may appear inconsistent with those of Doherty et al. (2013), we note that Xu et al. (2012) observed high concentrations of BC at the snow surface and at depth, which those authors attributed to meltwater percolation and the deposition of superimposed ice in the snowpack. A further prominent feature in our data set is the elevated surface mixing ratio of C_{BC}^{est} at sites 52–54 on XD Glacier, relative to deeper layers, which we attribute to the dry/wet deposition of BC on the surface samples. We propose that the clear difference in vertical profiles between QY and XD glaciers is a function of ILAP deposition. Specifically, QY Glacier was sampled during the wet season, when higher temperatures and stronger melting potentially serve to concentrate ILAPs in the basal layers. In contrast, because we sampled XD Glacier during both the wet and dry seasons, ILAP concentrations decrease with depth during the dry season as a function of scavenging (Figs. S7a–g) but increase during the wet season because of the concentration effect (Figs. S7h–j). Because the single-layer samples are not shown, the vertical profiles of C_{BC}^{est} for QM, HRQ, and GR glaciers are plotted in Figure S8. With the exception of those sites included in Figure S8d–e, i, and h, the sampled glaciers exhibit the trapping and scavenging effects of a higher surface-layer BC content resulting from melting processes.

3.4 ILAP contributions to particulate light absorption

The fractional contributions of BC, OC, and Fe (presumably in the form of goethite) to total absorption (450 nm) are depicted for each glacier in Figure 7, with further details of BC, OC, and

删除的内容: illustrated that the

删除的内容: could

带格式的 ... [914]

带格式的 ... [915]

带格式的 ... [916]

删除的内容: at the surface of

带格式的 ... [917]

删除的内容: due to

带格式的 ... [918]

删除的内容: to enrich the

带格式的 ... [919]

删除的内容: found

带格式的 ... [920]

删除的内容: the ILAPs could be scavenged with ... [921]

删除的内容: to lead to a much higher

带格式的 ... [922]

带格式的 ... [923]

删除的内容: the surface snow. Flanner et al. ... [924]

带格式的 ... [925]

删除的内容: would amplify snow-

带格式的 ... [926]

删除的内容: reduction, and therefore provide

带格式的 ... [927]

删除的内容: it still

带格式的 ... [928]

删除的内容: what happens

带格式的 ... [929]

删除的内容: vertical

带格式的 ... [930]

删除的内容: d, f, h–j… but increase during the ... [931]

已移动(插入) [3]

带格式的 ... [932]

带格式的 ... [933]

删除的内容: deeper layer of snow and ice during ... [934]

带格式的 ... [935]

删除的内容: In this study, the mixing ratios of ... [936]

已上移 [3]: the vertical profiles of C_{BC}^{est}

带格式的 ... [937]

带格式的 ... [938]

删除的内容: are plotted in Fig. S8 for all ice ... [939]

带格式的 ... [940]

删除的内容: **Contributions**

带格式的 ... [941]

Fe concentrations given in Table S1. BC plays a dominant role in particulate light absorption, with average values ranging from ~44% to 54% across all seven glacier sites. Although OC represents the second highest absorber, we noted significant variability (between 25% and 46% on average) in its contribution to total light absorption during the 2013–2015 field campaign. For those glaciers located on the eastern TP (QY, YZF, and HRQ glaciers), the relative contributions of BC and OC to total absorption are broadly similar. The highest fraction of BC (54%) was measured on QM Glacier, on the western TP.

Complementing the BC and OC contributions, light absorption on TP glaciers is also influenced by Fe. According to our data, the average fraction of total light absorbed by Fe ranges from approximately 11% to 31% across all seven glaciers, with the highest values recorded on GR Glacier. This finding indicates that MD plays a key role in the spectral absorption properties of ILAPs on TP glaciers. The relative contributions of BC, OC, and Fe to total light absorption for all surface-ice samples are presented in Figure S9 and Table 1.

3.5 Enrichment factor

EF values ranging from 0.1 to 10 represent significant input from crustal sources, whereas values of >10 indicate major contributions from anthropogenic activity. According to our EF analysis (Fig. 8), mean values for Fe are less than 5 for all seven glaciers, suggesting a primarily crustal origin. This result supports the findings of previous studies in northern China (Wang et al., 2013) and North America (Doherty et al., 2014), which indicate that light-absorbing particles in snow are dominated by local soil dust. Similar to Fe, other trace metals with mean EF values of ≥5.0 are moderately to highly enriched because of anthropogenic emissions (Hsu et al., 2010). For example, Pacyna and Pacyna (2001) reported that Cr is derived chiefly from the combustion of fossil fuels, which is also a primary source of Cu, Pb and Zn, however, are linked to traffic-related combustion and coal burning (Christian et al., 2010; Contini et al., 2014). In summary, the high EF values for Cu, Zn, and Cd in our ice samples provide clear evidence that TP glaciers are being affected by anthropogenic pollution.

删除的内容: are
删除的内容: played
带格式的 ... [952]
带格式的 ... [953]
删除的内容: %-
带格式的 ... [954]
删除的内容: in
带格式的 ... [955]
删除的内容: regions.
带格式的 ... [956]
删除的内容: was
带格式的 ... [957]
删除的内容: in glacier regions, and there are ... [958]
带格式的 ... [959]
删除的内容: of OC
带格式的 ... [960]
删除的内容: (~25%-46%
带格式的 ... [961]
删除的内容: average). The
带格式的 ... [962]
删除的内容: due to BC and OC were relatively ... [963]
带格式的 ... [964]
删除的内容: accounting for 54% in the
带格式的 ... [965]
删除的内容: glaciers, which is located in
带格式的 ... [966]
删除的内容: regions. So the
带格式的 ... [967]
带格式的 ... [968]
删除的内容: due to ILAPs in the TP glacier ... [969]
删除的内容: The
带格式的 ... [971]
删除的内容: absorption due to Fe was ~11%-
带格式的 ... [970]
带格式的 ... [972]
删除的内容: in
带格式的 ... [973]
删除的内容: light absorption of Fe in the GR ... [974]
带格式的 ... [975]
删除的内容: mineral dust
带格式的 ... [976]
删除的内容: played

3.6 Source apportionment

We employed mass concentrations of principal elements and ILAPs, together with their respective uncertainties, to populate the PMF 5.0 model, the details of which are described by Hegg et al. (2009, 2010) and Pu et al. (2017). Model-derived factor loadings (defined as the apportionment of species mass to individual factors) for the three-factor solution of each source profile are shown in Figure 9, both as measured mass concentrations and the % total mass allocated to each factor. The first factor (top panel) exhibits relatively high loadings of Cl^-, Cl salt, SO_4^{2-}, and NO_3^-, which are well-known markers for urban and/or local industrial pollution (Alexander et al., 2015). Although Cl^- and Na^+ are usually considered potential products of sea salt, high loadings of Cl^- relative to Cl salt reflect a further source, such as industrial emissions or coal combustion (Hailin et al., 2008; Kulkarni, 2009). High concentrations of NH_4^+ are also linked to coal combustion (Pang et al., 2007).

Compared with the first factor, Al (90.3%) and Fe (87.3%) are generally regarded as chief indicators of urban and/or regional MD (Pu et al., 2017), and the second factor can therefore be readily interpreted as a natural MD source. We note that C_{BC}^{max} exhibits a high mass loading on this factor. Since both K^+ and $K_{Biosmoke}$ are primary indicators of biomass burning (Zhang et al., 2013a), we attribute the highest loadings of K^+ and $K_{Biosmoke}$ to this source (Fig. 9c). Nonetheless, the lowest mass loading of C_{BC}^{max} in this factor was unexpected, as C_{BC}^{max} is related not only to biomass burning but also to local MD associated with industrial activity (Bond et al., 2006). Consequently, we interpret the third factor as representing primarily the burning of biomass.

Figure 10 illustrates the chemical composition and mean ILAP source apportionment for the seven TP glaciers. We reiterate that the apportionment refers to the amount of light absorbed by insoluble particles on the glacier surface. On average, the observed source apportionment by MD is close to 37.5%, with industrial emissions and biomass burning contributing 33.1% and 29.4%, respectively. Specifically, the largest biomass contribution to light absorption is found on QY Glacier, which is located close to centres of human land use (Guan et al., 2009; Li et al., 2016). For MK, QM, GR, and XD glaciers, the MD contribution is significantly larger (>47.9%) than those of

带格式的 ... [1012]
删除的内容: Given the importance of the climate ... [1013]
删除的内容: the chemical components
带格式的 ... [1015]
删除的内容: the
删除的内容: in ice associated
删除的内容: the uncertainty datasets were used
带格式的 ... [1014]
带格式的 ... [1016]
带格式的 ... [1017]
删除的内容: the techniques have already been ... [1021]
带格式的 ... [1018]
删除的内容: run
带格式的 ... [1019]
删除的内容: . The
带格式的 ... [1020]
带格式的 ... [1022]
删除的内容: The
删除的内容: [Please check that this is your ... [1023]
带格式的 ... [1024]
删除的内容: 3
删除的内容: the
带格式的 ... [1025]
带格式的 ... [1026]
删除的内容: profiles based on the PMF 5.0 model
带格式的 ... [1027]
删除的内容: given
带格式的 ... [1028]
删除的内容: Fig.
带格式的 ... [1029]
删除的内容: (in
带格式的 ... [1030]
删除的内容: concentration
带格式的 ... [1031]
删除的内容:). It was evident that the
带格式的 ... [1032]
删除的内容: was obviously characterized by
带格式的 ... [1033]
带格式的 ... [1034]
删除的内容:
带格式的 ... [1036]
删除的内容: the

industrial pollution and biomass burning, particularly in the case of MK Glacier. In these regions, the percentage of light absorption due to soil dust ranges from 20.4% to 31.1%, whereas light absorption due to biomass burning is 18.5% to 35.8%.

Industrial pollution is a major component of apportionment for both YZF and MK glaciers, where the attribution of total anions by chloride, nitrate, and sulphate is significantly higher than that of other chemical species. On HRQ Glacier, the largest contribution of sulphate is 45.4%. As depicted in Figure 10, the primary sources of light absorption by insoluble surficial particles are MD and industrial pollution. The sole exception is YZF Glacier, which exhibits a relatively large contribution from the burning of biomass. Together, these results are highly consistent with those of previous studies (Andersson et al., 2015), which reported that BC deposited on TP glaciers is derived overwhelmingly from the combustion of coal.

4 Conclusions

We employed the ISSW technique, coupled with chemical analysis, to assess ILAPs at seven glacier sites on the Tibetan Plateau. Specifically, we analysed 67 vertical profiles in ice samples collected during both the wet and dry seasons between 2013 and 2015. Our findings from HRQ, XD, and GR glaciers show that on average, BC and OC concentrations were several orders of magnitude higher during the dry season than during the wet season. It remains unclear, however, whether the ILAPs in the MK and YZF glaciers were comparable during the monsoon and non-monsoon seasons, and thus we suggest this as a suitable focus for future research. The lowest concentrations of BC in our data set originate from XD, HRQ and GR glaciers, which give median concentrations of 33 ng g^{-1}, 24 ng g^{-1}, and 28 ng g^{-1}, respectively. Moreover, we observed a pronounced decline in ILAP concentration with depth on XD Glacier, which we attribute to scavenging during the wet season. An opposite trend, driven by meltwater 'washing' effects, characterises the warmer wet season.

Both BC and OC play central roles in particulate light absorption on TP glaciers, with average values of ~44%–54% and ~25%–46%, respectively. By using a PMF receptor model, we ascertained that the ILAP budget of northern TP glaciers reflects a significant portion of

删除的内容: especially

带格式的 ... [1103]

删除的内容: glacier

带格式的 ... [1104]

删除的内容: percent

带格式的 ... [1105]

删除的内容: the

带格式的 ... [1106]

删除的内容: ranged

带格式的 ... [1107]

删除的内容: -

带格式的 ... [1108]

删除的内容: while the

带格式的 ... [1109]

删除的内容: by

删除的内容: was in the range of

带格式的 ... [1110]

带格式的 ... [1111]

删除的内容: -

带格式的 ... [1112]

带格式的 ... [1113]

删除的内容: constituted

带格式的 ... [1114]

删除的内容: fraction in the YZF glacier. ... [1115]

带格式的 ... [1116]

删除的内容: were much similar. The

带格式的 ... [1117]

删除的内容: the

带格式的 ... [1118]

删除的内容: were

删除的内容: the

带格式的 ... [1119]

带格式的 ... [1120]

删除的内容: in the YZF and MK glaciers. In the

删除的内容: [Please check that this is your ... [1121]

带格式的 ... [1122]

删除的内容: glacier

带格式的 ... [1123]

删除的内容: the

带格式的 ... [1124]

删除的内容: was up to

带格式的 ... [1125]

anthropogenic pollutants. The largest contributors of light-absorbing insoluble particles for TP glaciers, however, include local MD and industrial pollution sources, followed by the burning of biomass. In summary, both natural MD and anthropogenic emissions constitute non-negligible sources of ILAPs for TP glaciers.

Data availability. All datasets and codes used in this study can be obtained by contacting Xin Wang (wxin@lzu.edu.cn).

The Supplement related to this article is available online at https://XXXX-supplement.

Author contributions. BX and MW designed the experiments. XW prepared the manuscript with contributions from all co-authors.

Competing interests. The authors declare that they have no conflicts of interest.

Acknowledgements. This research was supported by the National Key Research and Development Program on Monitoring, Early Warning and Prevention of Major Natural Disaster (2018YFC1506005), the National Natural Science Foundation of China (grants 41775144, 41522505, 41771091, 41675065 and 41875091), and the Fundamental Research Funds for the Central Universities (lzujbky-2018-k02).

Edited by: Mark Flanner

Reviewed by: two anonymous referees

删除的内容: the light absorption by
带格式的 ... [1186]
删除的内容: in
带格式的 ... [1187]
删除的内容: originated from the
删除的内容: mineral dust
带格式的 ... [1189]
删除的内容: biomass
删除的内容: source. Therefore, the
带格式的 ... [1188]
带格式的 ... [1190]
带格式的 ... [1191]
删除的内容: mineral dust
带格式的 ... [1192]
删除的内容: source
带格式的 ... [1193]
删除的内容: emission source are both
带格式的 ... [1194]
删除的内容: to the
带格式的 ... [1195]
删除的内容: in the
带格式的 ... [1196]
删除的内容: ↵ ... [1197]
带格式的 ... [1198]
删除的内容: **5 Data availability** ↵
带格式的 ... [1199]
带格式的 ... [1200]
删除的内容: All datasets and codes used to ... [1201]
带格式的 ... [1202]
删除的内容: ↵
带格式的 ... [1203]
带格式的 ... [1204]
带格式的 ... [1205]
删除的内容: ↵ ... [1206]
带格式的 ... [1207]
删除的内容: under grant (
删除的内容: (grants 41775144 and 41522505) ... [1208]
带格式的 ... [1209]
带格式的 ... [1210]
带格式的 ... [1211]
带格式的 ... [1212]

Table 1. Statistics of the ILAPs in each glacier measured using an ISSW spectrophotometer associated with the chemical analysis.

Region	Latitude	Longitude		C_{BC}^{equiv}	C_{BC}^{max}	C_{BC}^{est}	$f_{non\text{-}BC}^{est}$	$Å_{tot}$	OC	AI	Fe
	(N)	(E)		(ng g^{-1})	(ng g^{-1})	(ng g^{-1})	(%)		(ppm)	(ppm)	(ppm)
Qiyi glacier	39°14’28”	97°45’27”	average	414	299	238 (116, 313)	42 (15, 66)	2.59	1.21	0.19	0.18
			median	176	128	94 (29, 124)	41 (17, 70)	2.62	0.66	0.08	0.09
			minimum	26	29	25 (13, 35)	21 (—, 53)	0.8	0.08	0.01	0.02
			maximum	2651	2230	1877 (1182, 2109)	73 (41, —)	3.73	11.59	3.35	2.41
Qiumianleiketage glacier	36°41’47”	90°43’44”	average	421	296	238 (139, 402)	44 (24, 81)	2.80	1.43	0.21	0.23
			median	307	215	172 (64, 218)	44 (24, 81)	2.76	1.06	0.15	0.18
			minimum	139	93	62 (19, 93)	37 (12, 64)	2.45	0.54	0.09	0.11
			maximum	995	662	558 (143, 678)	56 (27, 86)	3.08	3.97	0.55	0.63
Meikuang glacier	35°40’24”	94°11’10”	average	493	328	260 (119, 331)	42 (15, 37)	2.65	2.14	0.19	0.22
			median	197	156	133 (76, 153)	44 (16, 69)	2.64	0.61	0.09	0.13
			minimum	24	23	19 (17, 24)	16 (—, 17)	1.37	0.13	0.02	0.03
			maximum	4696	2817	2292 (109, 2938)	62 (23, 85)	3.56	16.89	1.36	1.22
Yuzhufeng glacier	35°38’43”	94°13’36”	average	457	312	233 (94, 295)	51 (—, 37)	2.84	1.51	0.17	0.44
			median	317	201	160 (116, 204)	48 (26, 87)	2.95	1.02	0.10	0.21
			minimum	52	35	24 (8, 35)	15 (—, 37)	1.82	0.07	0.02	0.05
			maximum	2630	1608	1169 (72, 1603)	110 (6, 49)	3.7	9.16	0.81	3.51
Hariqin glacier	33°08’23”	92°05’34”	average	476	327	256 (100, 385)	48 (26, 82)	2.79	1.59	0.17	0.17
			median	54	37	23 (9, 30)	48 (26, 82)	2.87	0.22	0.04	0.05
			minimum	36	24	13 (4, 22)	19 (—, 41)	1.96	0.08	0.01	0.03
			maximum	3990	2702	2131 (682, 2784)	64 (32, 84)	3.52	9.64	1.11	1.05
Xiaodongkemadi	33°04’08”	92°04’24”	average	253	171	152 (76, 177)	37 (15, 63)	2.28	0.95	0.13	0.17

Region	Latitude	Longitude		C_{BC}^{equiv}	C_{BC}^{max}	C_{BC}^{est}	$f_{non\text{-}BC}^{est}$	$\mathring{A}_{tot}$	ISOC	Al	Fe
	(N)	(E)		(ng g^{-1})	(ng g^{-1})	(ng g^{-1})	(%)		(ppm)	(ppm)	(ppm)
			median	62	47	53 (37, 65)	36 (13, 59)	2.18	0.19	0.03	0.06
			minimum	13	12	9 (6, 18)	8 (—, 19)	1.08	0.01	0.01	0.01
			maximum	2770	1849	1637 (596, 2031)	86 (25, 90)	3.63	6.97	2.40	2.13
Gurenhekou glacier	30°11'17"	90°27'23"	average	382	292	247 (212, 591)	46 (16, 71)	2.42	0.62	0.15	0.18
			median	61	46	30 (19, 44)	48 (18, 75)	2.46	0.13	0.05	0.10
			minimum	28	23	15 (10, 24)	27 (7, 52)	1.34	0.02	0.01	0.03
			maximum	4674	3634	3080 (1876, [illegible])	61 (26, 85)	2.92	5.22	1.35	0.91

Table 2. Statistics of the ILAPs in snow and ice in the studied TP glaciers and other related glaciers.

Glacier name	Sampling time	Season	Altitude/ m a.s.l.	BC (ng g^{-1})	OC (ng g^{-1})	MD (μg g^{-1})	Sample type	References
Qiyi	2005.7	Monsoon	4850	22±2	——	——	Snow pit	Ming et al., 2009
	2001.7-8	Monsoon	4600	6.65±3.3	87.52±37.59	——	Fresh snow	Xu et al., 2006
	2001.7-8	Monsoon	4600	52.64±17.83	195.5±85	——	Aged snow	Xu et al., 2006
	2013.8-9	Monsoon	4700	238±349	1210±2023	1.42±1.17	Ice	This study
Qiumianleiketage	2014.5	Non-monsoon	5300	238±168	1431±1130	2.92±2.09	Ice	This study
Meikuang	2001.7-8	Monsoon	5200	446	124	——	Surface snow	Xu et al., 2006
	2015.10	Monsoon	5050	290±241	3745±5100	5.27±6.81	Ice	This study
	2015.5	Non-monsoon	5050	250±468	1718±3639	1.85±2.38	Ice	This study
Yuzhufeng	2014,2015.10	Monsoon	5350	265±270	1596±2052	2.93±3.19	Ice	This study
	2014.5	Non-monsoon	5350	213±188	1421±1173	1.9±1.77	Ice	This study
Hariqin	2015.10	Monsoon	5650	91±126	930±1880	1.23±1.77	Ice	This study
	2015.5	Non-monsoon	5650	1077±1489	4860±6759	8.38±10.59	Ice	This study
Xiaodongkemadi	2014.8-2015.7	Monsoon	5400-5750	41.77±6.36	157.97±42.3	1.89±0.92	Fresh snow	Li et al., 2017
		Monsoon	5400-5750	246.84±118.3	611.45±467.7	39.43±24.35	Aged snow	Li et al., 2017
		Monsoon	5400-5750	3335±3767	9857±10923	880±1038	Granular ice	Li et al., 2017
	2015.10	Monsoon	5600	57±37	250±233	0.68±0.3	Ice	This study
	2013-2015.5	Non- monsoon	5600	178±381	1174±2014	2.18±6.15	Ice	This study
Gurenhekou	2015.10	Monsoon	5610	85±177	330±648	1.17±1.49	Ice	This study
	2014.5	Non-monsoon	5610	1116±1700	2148±2668	7.7±9.99	Ice	This study
Palong-Zanbu-No. 4	1998-2005	Monsoon	4800-5600	5.27±2.23	70.8±39.3	——	Ice core	Xu et al., 2009a
		Non-monsoon	4800-5600	11.51±4.7	97.5±49.9	——	Ice core	Xu et al., 2009a
Zuoqiupu	1956-2006	Monsoon	5100-5400	2.37±1.55	11.55±11.5	——	Ice core	Xu et al., 2009b
		Non-monsoon	5100-5400	8.33±3.29	26.71±13.74	——	Ice core	Xu et al., 2009b
Zhadang	2012.8	Monsoon	5500-5800	51.9±7.2	——	6.38±1.54	Snow pit	Qu et al., 2014
	2014.6	Monsoon	5800	79	515.08	——	Snow pit	Li et al., 2016
	2015.5	Non-monsoon	5790	303	822	——	Snow pit	Li et al., 2018
	2015.6-9	Monsoon	5570-5790	281	743	——	Surface snow	Li et al., 2018
Urumqi No.1	2004.7-8	Monsoon	4130	500	1200	——	Surface snow	Xu et al., 2012
	2013.8	Monsoon	3800-4100	30±5	——	17±6	Fresh snow	Ming et al., 2016
Muji	2012.6-10	Monsoon	4700-5500	375±3	175±15	——	Snow pit	Yang et al., 2015
Qiangyong	2001	——	5400	43.1	117.3	——	Surface snow	Xu et al., 2006
Kangwure	2001	——	6000	21.8	161.1	——	Surface snow	Xu et al., 2006
Namunani	2004	——	5780-6080	4.4±2.1	51.1±20.6	——	Surface snow	Xu et al., 2006
Demula	2014.5	Non-monsoon	5404	17	185	——	Snow pit	Li et al., 2016

Yulong	2015.5	Non-monsoon	4400-4800	372±58	2003±308	9.47±2.36	Aged snow	Niu et al., 2017
	2015.8	Monsoon	4400-4800	2309±125	3211±168	97.12±50.78	Aged snow	Niu et al., 2017
Laohugou No. 12	2015.8	Monsoon	4400-4800	2198±1004	2190±1203	114±67	Aged snow	Zhang et al., 2017
	2015.10	Non-monsoon	4400-4800	1218±212	504±50	63±2	Aged snow	Zhang et al., 2017

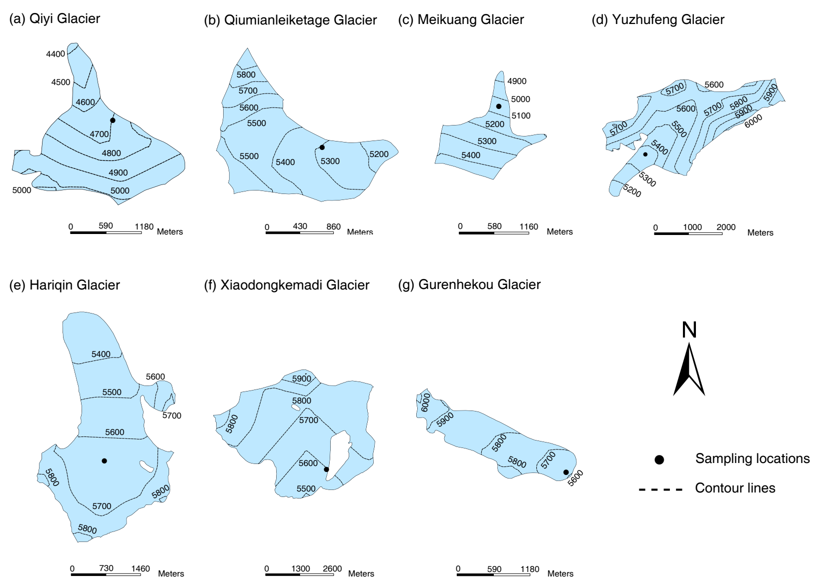

Figure 1. Geographical locations of (a) Qiyi Glacier (39.24°N, 97.76°E), (b) Qiumianleiketage Glacier (36.70°N, 90.73°E), (c) Meikuang Glacier (35.67°N, 94.19°E), (d) Yuzhufeng Glacier (35.65°N, 94.23°E), (e) Hariqin Glacier (33.14°N, 92.09°E), (f) Xiaodongkemadi Glacier (33.07°N, 92.07°E), (g) Gurenhekou Glacier (30.19°N, 90.46°E). The black dots indicate sampling locations.

带格式的: 字体: (中文) +西文正文 (Calibri), 小四
带格式的: 正文, 两端对齐, 无孤行控制
带格式的 ... [1213]
删除的内容:
带格式的: 字体: Times New Roman, 英语(英国)
带格式的: 字体: Times New Roman, 英语(英国)
带格式的 ... [1216]
带格式的 ... [1214]
带格式的 ... [1215]
删除的内容: glacier (97.76° E,
删除的内容: glacier (90.73° E,
带格式的: 字体: Times New Roman, 英语(英国)
删除的内容:
带格式的 ... [1217]
删除的内容: glacier (94.19° E,
带格式的: 字体: Times New Roman, 英语(英国)
删除的内容:
带格式的 ... [1218]
删除的内容: glacier (94.23° E,
带格式的: 字体: Times New Roman, 英语(英国)
删除的内容:
带格式的 ... [1219]
删除的内容: glacier (92.09° E,
带格式的: 字体: Times New Roman, 英语(英国)
删除的内容:
带格式的 ... [1220]
删除的内容: glacier (92.07° E,
带格式的: 字体: Times New Roman, 英语(英国)
删除的内容:
带格式的 ... [1221]
删除的内容: glacier (90.46° E,
带格式的: 字体: Times New Roman, 英语(英国)
删除的内容:
带格式的 ... [1222]
删除的内容: dot is the
带格式的: 字体: Times New Roman, 英语(英国)
删除的内容: [Please note that the British spelling ... [1223]
带格式的: 英语(英国)
带格式的: 正文, 两端对齐, 无孤行控制

Figure 2. The equipment for collecting new snow samples from the surfaces of the seven studied TP glaciers.

带格式的: 字体: (中文) +西文正文 (Calibri), 英语(英国)

带格式的: 正文, 两端对齐, 无孤行控制

带格式的: 字体: (中文) +西文正文 (Calibri), 小四

带格式的: 正文, 无孤行控制

带格式的: 字体: (中文) +西文正文 (Calibri), 英语(英国)

删除的内容: in

带格式的: 正文, 两端对齐, 无孤行控制

带格式的: 字体: (中文) +西文正文 (Calibri), 英语(英国)

带格式的: 字体: (中文) +西文正文 (Calibri), 英语(英国)

带格式的: 字体: (中文) +西文正文 (Calibri), 英语(英国)

带格式的: 字体: (中文) +西文正文 (Calibri), 英语(英国)

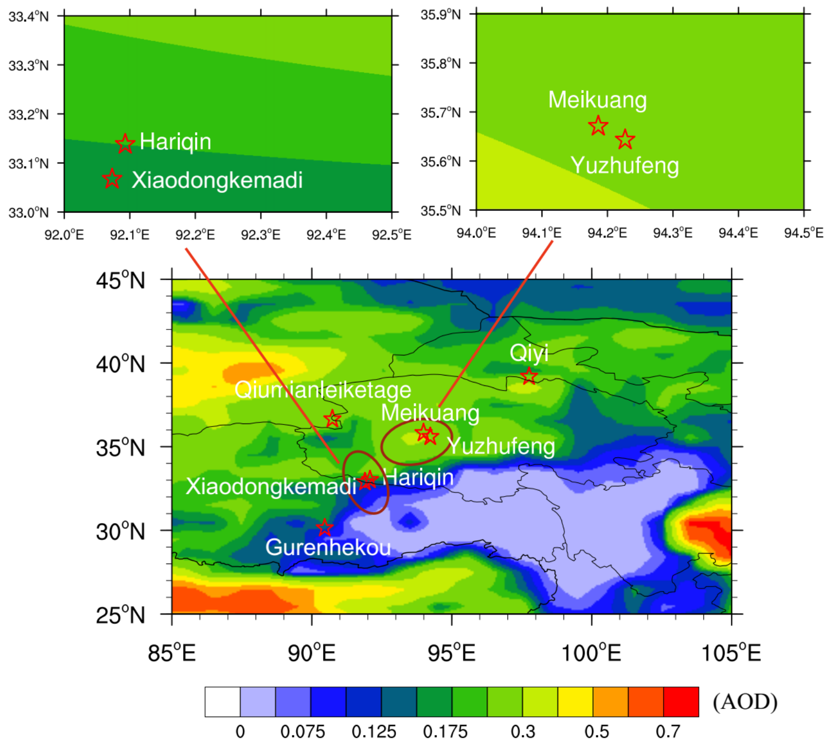

Figure 3. Spatial distribution of the averaged AOD over the TP between 2013 and 2015, retrieved from Aqua-MODIS at 500 nm. The red stars represent sampling locations (see also Table 1).

带格式的: 字体: (中文) +西文正文 (Calibri), 英语(英国)

带格式的: 正文, 两端对齐, 无孤行控制

带格式的: 字体: (默认) DengXian, (中文) +西文正文 (Calibri), 小四

带格式的: 字体: (中文) +西文正文 (Calibri), 英语(英国)

带格式的: 英语(英国)

删除的内容: over Tibetan Plateau from 2013 to 2015.

删除的内容: are the

带格式的: 英语(英国)

删除的内容:):

带格式的: 英语(英国)

带格式的: 英语(英国)

带格式的: 正文, 两端对齐, 无孤行控制

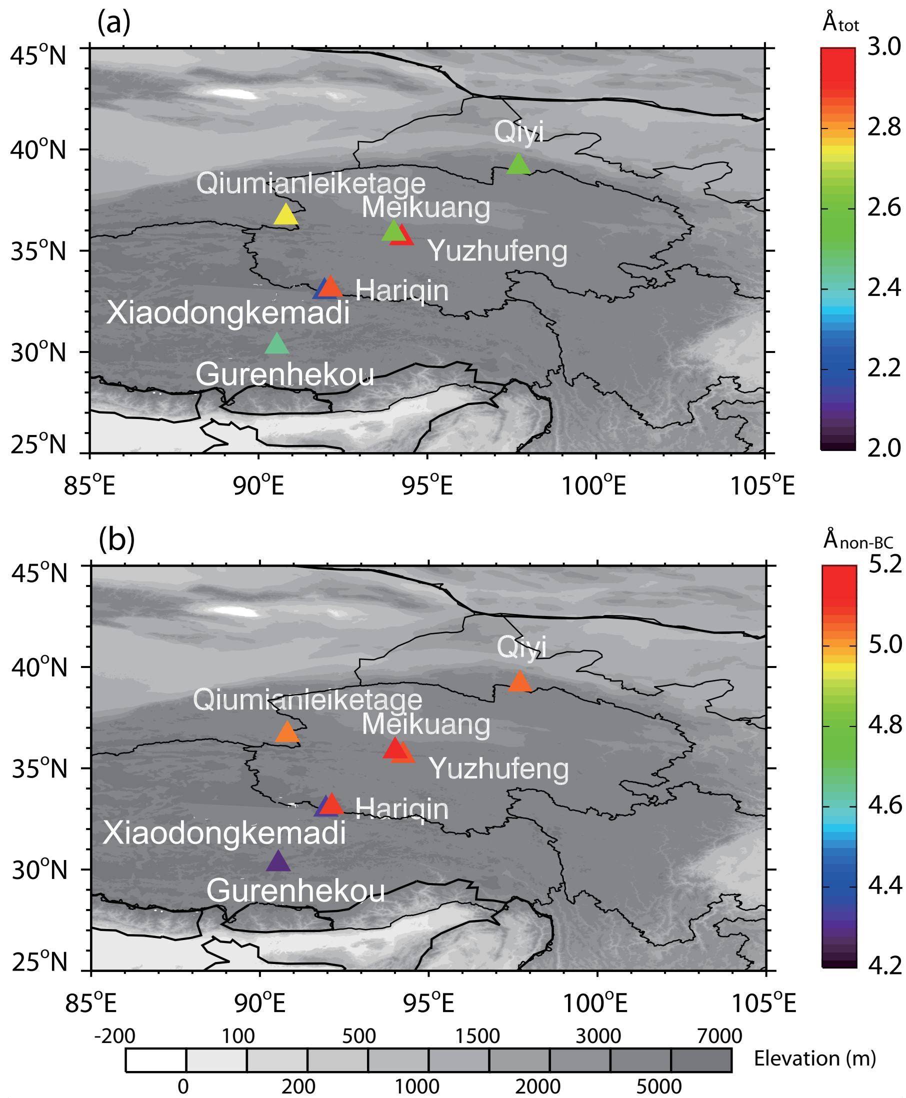

Figure 4. Spatial distribution of the median absorption Ångström exponent for (a) total particulate constituents ($Å_{tot}$), and (b) non-BC particulate constituents ($Å_{non-BC}$) for each glacier.

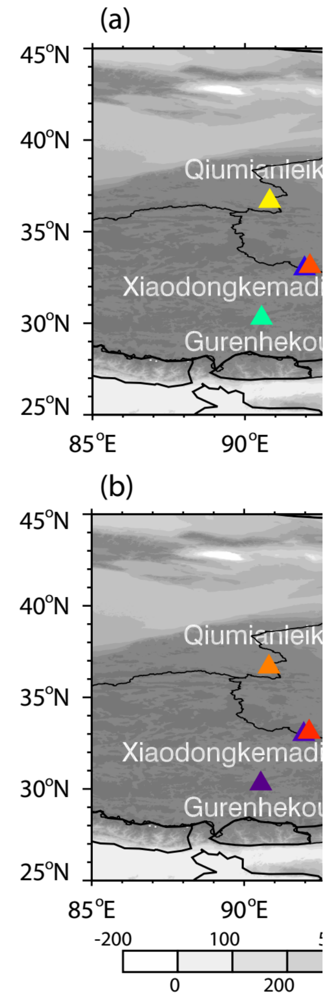

删除的内容:

带格式的: 字体: (默认) DengXian, (中文) +西文正文 (Calibri), 小四

带格式的: 字体: (中文) +西文正文 (Calibri), 英语(英国)

删除的内容: The spatial

带格式的: 英语(英国)

删除的内容: in each glacier.

删除的内容: [Please consider adding a space between the terms ‘elevation’ and ‘(m)’ in your scale, both here and in Figures 7 and 10. Also, ‘Elevation’ is preferable to ‘elevation’.]

带格式的: 字体: (中文) 宋体, (中文) 中文(中国), (其他) 英语(英国)

带格式的: 正文, 两端对齐, 无孤行控制

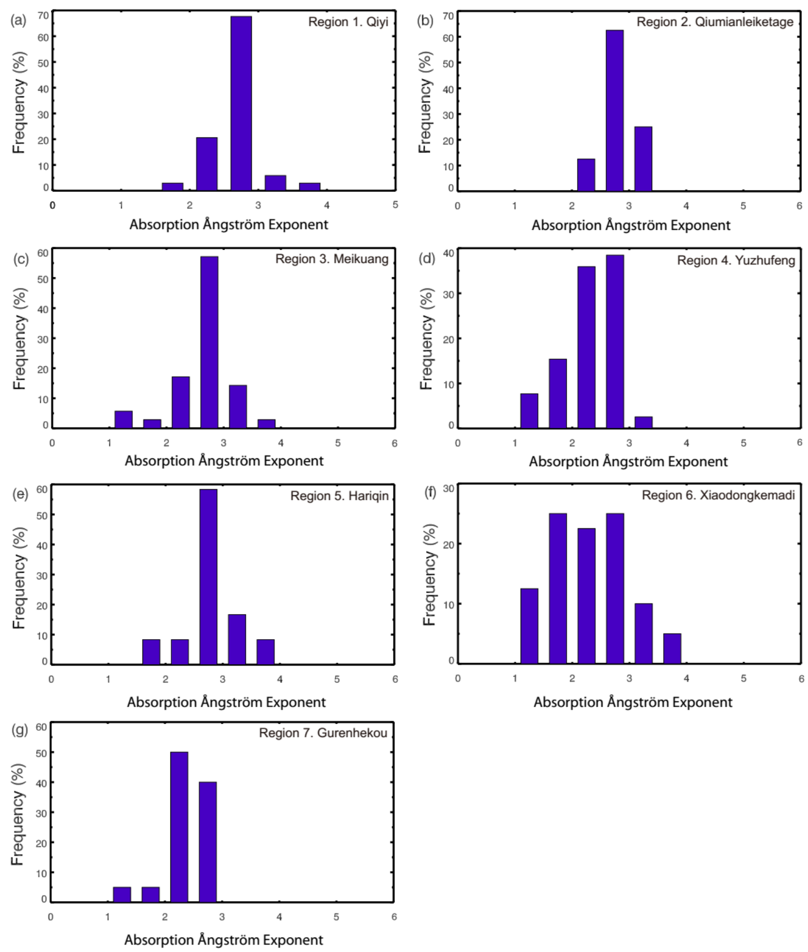

Figure 5. Histograms of the frequency of $\mathring{A}_{tot}$ (450–600 nm) in ice from each glacier. Samples from all vertical profiles are included.

带格式的: 字体: (默认) DengXian, (中文) +西文正文 (Calibri), 小四

带格式的: 字体: (中文) +西文正文 (Calibri), 英语(英国)

删除的内容: -

带格式的: 英语(英国)

删除的内容: for

带格式的: 英语(英国)

删除的内容: samples in

带格式的: 英语(英国)

删除的内容: of the

带格式的: 英语(英国)

删除的内容: region

带格式的: 英语(英国)

带格式的: 字体: (中文) 宋体, 小四, (中文) 中文(中国), (其他) 英语(英国)

带格式的: 字体: (中文) +西文正文 (Calibri), 英语(英国)

带格式的: 正文, 两端对齐, 无孤行控制

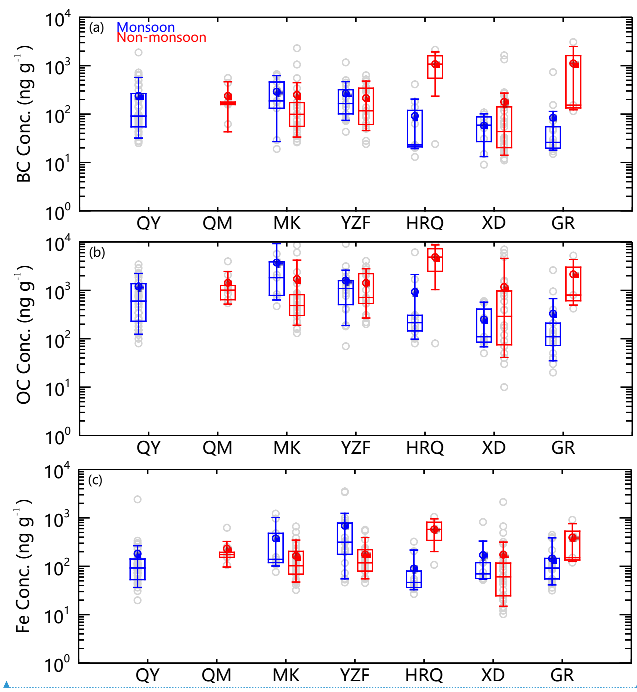

Figure 6. Box plots depicting the regional variability in (a) BC concentration, (b) ISOC concentration, and (c) Fe concentration on the seven glaciers. The solid dots represent the average ILAP concentrations for each glacier, and the bars represent the 10th, 25th, median, 75th, and 90th percentiles of the data.

带格式的: 字体: (默认) DengXian, (中文) +西文正文 (Calibri), 小四

带格式的: 字体: (中文) +西文正文 (Calibri), 英语(英国)

带格式的: 正文, 无孤行控制

删除的内容: of

带格式的: 英语(英国)

删除的内容: variations

带格式的: 英语(英国)

删除的内容: of

带格式的: 英语(英国)

删除的内容: Error

带格式的: 英语(英国)

删除的内容: are

带格式的: 英语(英国)

删除的内容: The dot symbol represents the average concentrations of the ILAPs in ice samples in each glacier.

删除的内容: [Please check that this is your intended meaning.]

带格式的: 字体: (中文) 宋体, (中文) 中文(中国), (其他) 英语(英国)

带格式的: 正文, 两端对齐, 无孤行控制

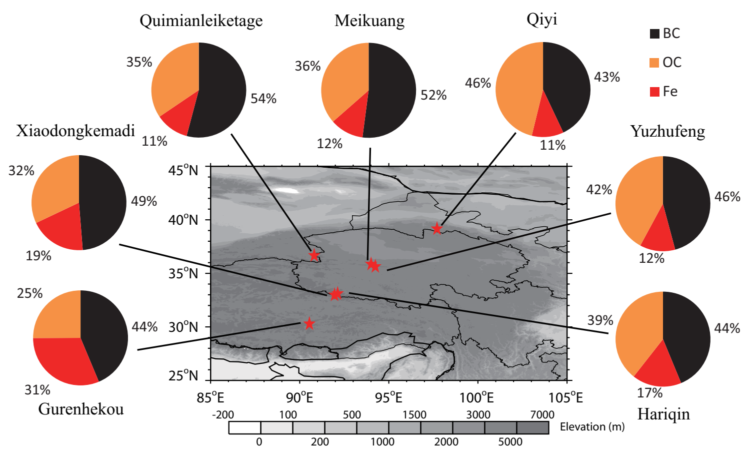

Figure 7. The median relative contributions of BC, OC, and Fe to light absorption for each glacier.

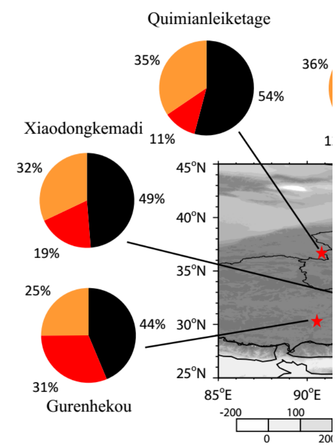

删除的内容:

带格式的: 字体: (默认) 宋体, 小四

带格式的: 字体: (默认) 宋体, 小四, 英语(英国)

删除的内容: of

删除的内容: total

带格式的: 字体: 五号, 英语(英国)

删除的内容: by BC, OC, and Fe

带格式的: 字体: 五号, 英语(英国)

删除的内容: ice samples in

带格式的: 字体: 五号, 英语(英国)

带格式的: 字体: 五号, 英语(英国)

带格式的: 字体: 五号, 英语(英国)

带格式的: 字体: 五号, 英语(英国)

带格式的: 字体: (默认) 宋体, (中文) 宋体, 五号, (中文) 中文(中国), (其他) 英语(英国)

带格式的: 字体: (中文) +西文正文 (Calibri), 英语(英国)

带格式的: 正文, 两端对齐, 无孤行控制

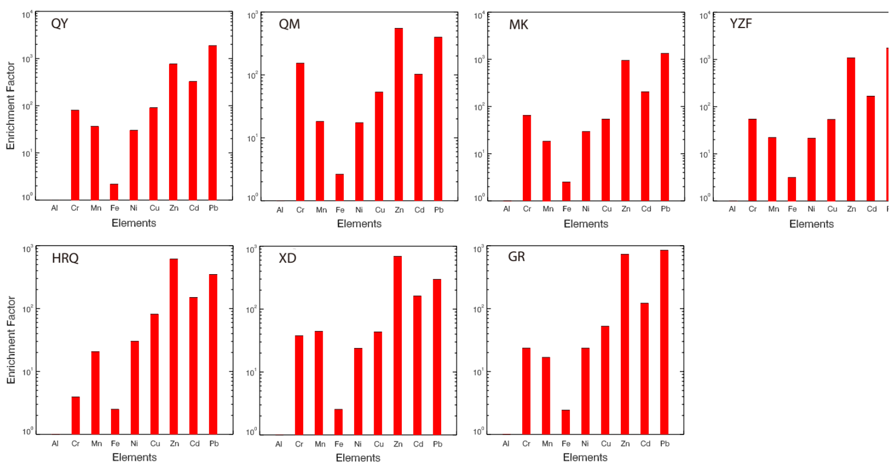

Figure 8. The average enrichment factors of trace metals in surface-ice samples from each glacier.

带格式的: 字体: (默认) 宋体, 小四

带格式的: 字体: (默认) 宋体, 小四, 英语(英国)

删除的内容: at

带格式的: 英语(英国)

删除的内容: Average

删除的内容: region

带格式的: 英语(英国)

删除的内容:

带格式的: 英语(英国)

带格式的: 英语(英国)

带格式的: 英语(英国)

带格式的: 字体: 小四, 英语(英国)

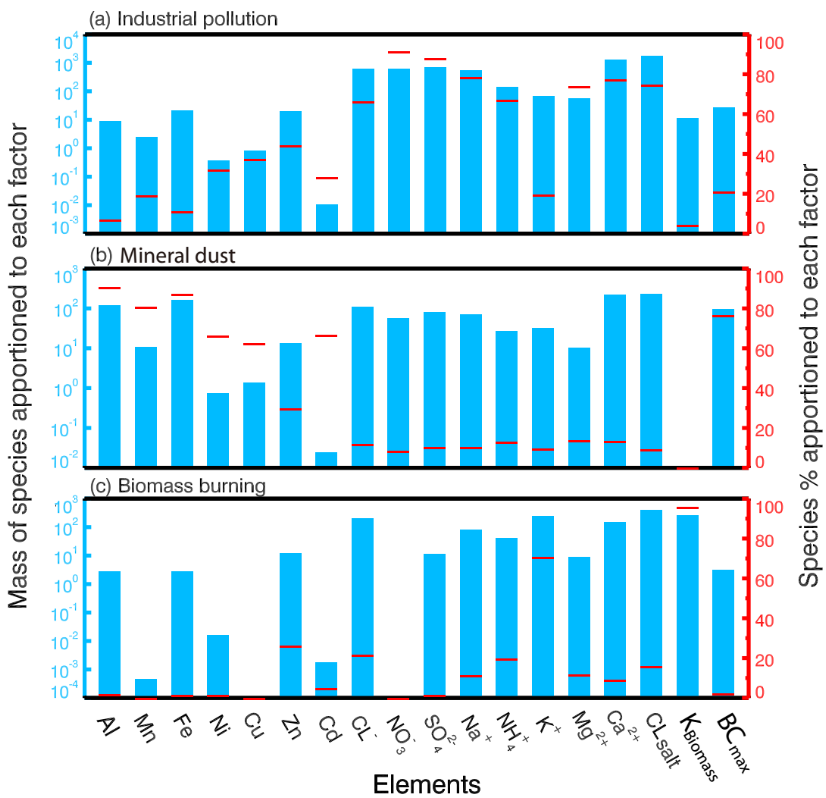

Figure 9. Source profiles for the three factors/sources that were resolved by the PMF 5.0 model. The blue columns and red horizontal bars depict the mass and percentage of the relative species, respectively.

带格式的: 字体: (默认) 宋体, 小四

带格式的: 英语(英国)

带格式的: 字体颜色: 自动设置, 英语(英国)

带格式的: 默认段落字体, 字体: 11 磅, 英语(英国)

带格式的: 英语(英国)

带格式的: 默认段落字体, 字体: 11 磅, 英语(英国)

删除的内容: [Consider explaining/defining what the blue columns and red horizontal bars depict.]

带格式的: 默认段落字体, 字体: (默认) 宋体, (中文) 宋体, 小四, (中文) 中文(中国), (其他) 英语(英国)

带格式的: 英语(英国)

带格式的: 字体: (默认) 宋体, 小四, 英语(英国)

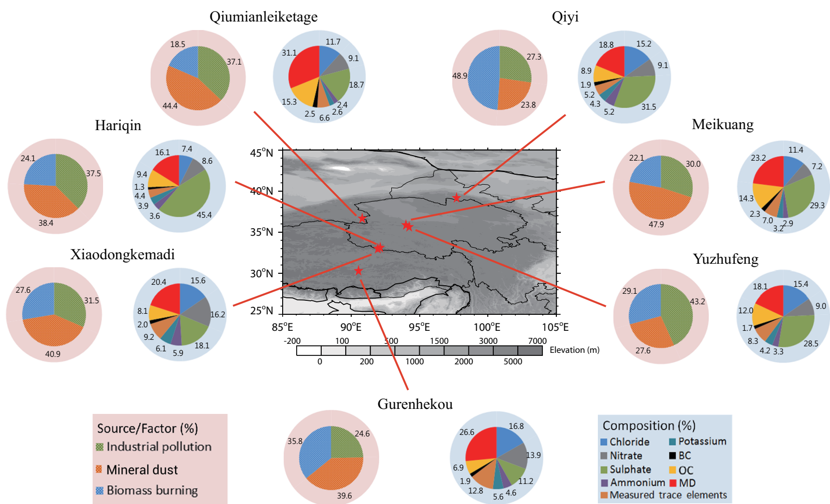

Figure 10. Chemical composition and source apportionment for the seven TP glaciers. Note that the apportionment applies to the light absorbed by insoluble particles on the glacier surfaces.

带格式的: 字体: (默认) 宋体, 小四, 英语(英国)

带格式的: 英语(英国)

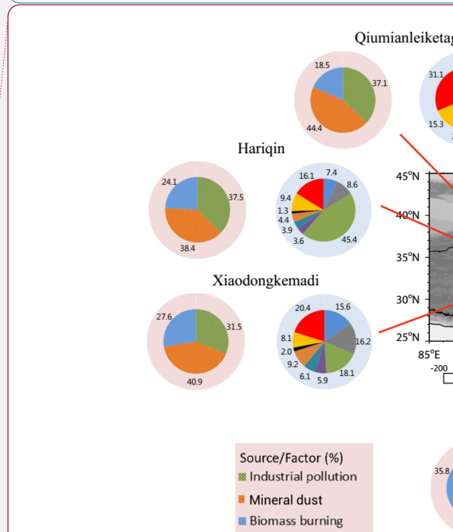

删除的内容:

带格式的: 字体: (默认) 宋体, 小四

带格式的: 英语(英国)

带格式的: 英语(英国)

删除的内容: in the TP regions.

带格式的: 英语(英国)

删除的内容: is of

带格式的: 英语(英国)

删除的内容: absorption

带格式的: 英语(英国)

删除的内容: in

带格式的: 英语(英国)

删除的内容: surface glaciers

带格式的: 英语(英国)

References

Alexander, B., and Mickley, L. J.: Paleo-perspectives on potential future changes in the oxidative capacity of the atmosphere due to climate change and anthropogenic emissions, Current Pollution Reports, 1, 57-69, 2015.

Alfaro, S. C., Lafon, S., Rajot, J. L., Formenti, P., Gaudichet, A., and Maille, M.: Iron oxides and light absorption by pure desert dust: An experimental study, J. Geophys. Res.-Atmos., 109, Artn D08208, 10.1029/2003jd004374, 2004.

Bergstrom, C.: Measuring the value and prestige of scholarly journals, College and Research Libraries News, 68, 314-316, 2007.

Bolch, T., Yao, T., Kang, S., Buchroithner, M. F., Scherer, D., Maussion, F., Huintjes, E., and Schneider, C.: A glacier inventory for the western Nyainqentanglha Range and the Nam Co Basin, Tibet, and glacier changes 1976–2009, The Cryosphere, 4, 419-433, https://doi.org/10.5194/tc-4-419-2010, 2010.

Bond, T. C., and Bergstrom, R. W.: Light absorption by carbonaceous particles: An investigative review, Aerosol Sci. Technol., 40, 27-67, 2006.

Bond, T. C., Doherty, S. J., Fahey, D. W., et al.: Bounding the role of black carbon in the climate system: A scientific assessment, J. Geophys. Res.-Atmos., 118, 5380-5552, 2013.

Brandt, R. E., Warren, S. G., and Clarke, A. D.: A controlled snowmaking experiment testing the relation between black carbon content and reduction of snow albedo, J. Geophys. Res.-Atmos., 116, Artn D08109, 10.1029/2010jd015330, 2011.

Christian, T. J., Yokelson, R. J., Cárdenas, B., Molina, L. T., Engling, G., and Hsu, S. C.: Trace gas and particle emissions from domestic and industrial biofuel use and garbage burning in Central Mexico, Atmos. Chem. Phys., 10, 565-584, 2010.

Chylek, P., Ramaswamy, V. & Srivastava, V.: Graphitic carbon content ofaerosols, clouds and snow, and its climatic implications, Sci. Total Environ., 36, 117–120, 1984.

Cong, Z., Gao, S., Zhao, W., Wang, X., Wu, G., Zhang, Y., Kang, S., Liu, Y., and Ji, J.: Iron oxides in the cryoconite of glaciers on the Tibetan Plateau: abundance, speciation and implications, The Cryosphere, 12, 3177-3186, 10.5194/tc-12-3177-2018, 2018.

Cong, Z. Y., Kang, S. C., Smirnov, A., and Holben, B.: Aerosol optical properties at Nam Co, a remote site in central Tibetan Plateau, Atmos. Res., 92, 42-48, 10.1016/J.Atmosres.2008.08.005, 2009.

Cong, Z. Y., Kang, S. C., Zhang, Y. L., and Li, X. D.: Atmospheric wet deposition of trace elements to central Tibetan Plateau, Appl. Geochem., 25, 1415-1421, 2010.

Cong, Z., Kang, S., Kawamura, K., Liu, B., Wan, X., Wang, Z., Gao, S., and Fu, P.:

Carbonaceous aerosols on the south edge of the Tibetan Plateau: concentrations, seasonality and sources, Atmos. Chem. Phys., 15, 1573-1584, 2015.

Contini, D., Cesari, D., Genga, A., Siciliano, M., Ielpo, P., and Guascito, M. R.: Source apportionment of size-segregated atmospheric particles based on the major water-soluble components in Lecce (Italy), Sci. Total Environ., 472, 248-261, 2014.

Conway, H., Gades, A., and Raymond, C. F.: Albedo of dirty snow during conditions of melt, Water Resour. Res., 32, 1713-1718, 10.1029/96wr00712, 1996.

Dang, C., and Hegg, D. A.: Quantifying light absorption by organic carbon in Western North American snow by serial chemical extractions, J. Geophys. Res.-Atmos., 119, 10.1002/2014jd022156, 2014.

Doherty, S. J., Warren, S. G., Grenfell, T. C., Clarke, A. D., and Brandt, R. E.: Light-absorbing impurities in Arctic snow, Atmos. Chem. Phys., 10, 11647-11680, 2010.

Doherty, S. J., Grenfell, T. C., Forsström, S., Hegg, D. L., Brandt, R. E., and Warren, S. G.: Observed vertical redistribution of black carbon and other insoluble light-absorbing particles in melting snow, J. Geophys. Res.-Atmos., 118, 5553-5569, 2013.

Doherty, S. J., Dang, C., Hegg, D. A., Zhang, R. D., and Warren, S. G.: Black carbon and other light-absorbing particles in snow of central North America, J. Geophys. Res.-Atmos., 119, 12807-12831, 2014.

Engling, G. and Gelencser, A.: Atmospheric Brown Clouds: From Local Air Pollution to Climate Change, Elements, 6, 223-228, 2010.

Federer, U., Kaufmann, P. R., Hutterli, M., Schüpbach, S., and Stocker, T. F.: Continuous flow analysis of total organic carbon in polar ice cores, Environ. Sci. Technol., 42, 8039–8043, 2008.

Fialho, P., Hansen, A. D. A., and Honrath, R. E.: Absorption coefficients by aerosols in remote areas: a new approach to decouple dust and black carbon absorption coefficients using seven-wavelength Aethalometer data, J. Aerosol Sci., 36, 267-282, 2005.

Flanner, M. G., Zender, C. S., Randerson, J. T., and Rasch, P. J.: Present-day climate forcing and response from black carbon in snow, J. Geophys. Res.-Atmos., 112, D11202, doi: 10.1029/2006jd008003, 2007.

Flanner, M. G., Zender, C. S., Hess, P. G., Mahowald, N. M., Painter, T. H., Ramanathan, V., and Rasch, P. J.: Springtime warming and reduced snow cover from carbonaceous particles, Atmos. Chem. Phys., 9, 2481-2497, 2009.

Grenfell, T. C., Doherty, S. J., Clarke, A. D., and Warren, S. G.: Light absorption from particulate impurities in snow and ice determined by spectrophotometric analysis of filters, Appl. Opt., 50, 2037-2048, 2011.

Guan, X., Huang, J., Guo, N., Bi, J., and Wang, G.: Variability of soil moisture and its relationship with surface albedo and soil thermal parameters over the Loess Plateau, Adv. Atmos. Sci., 26, 692-700, 2009.

Hadley, O. L., and Kirchstetter, T. W.: Black-carbon reduction of snow albedo, Nat. Clim. Change, 2, 437-440, 2012.

Hansen, J., and Nazarenko, L.: Soot climate forcing via snow and ice albedos, P. Natl. Acad. Sci. USA, 101, 423-428, 2004.

Hegg, D. A., Warren, S. G., and Grenfell, T. C.: Source attribution of black carbon in Arctic snow, Environ. Sci. Technol., 43, 4016-4021, 2009.

Hegg, D. A., Warren, S. G., and Grenfell, T. C.: Sources of light-absorbing aerosol in arctic snow and their seasonal variation, Atmos. Chem. Phys., 10, 10923-10938, 2010.

Hsu, S. C., Liu, S. C., Arimoto, R., et al.: Effects of acidic processing, transport history, and dust and sea salt loadings on the dissolution of iron from Asian dust, J. Geophys. Res.-Atmos., 115, 2010.

Huang, J., Li, Y. F., Li, Z., and Xiong, L. F.: Spatial variations and sources of trace elements in recent snow from glaciers at the Tibetan Plateau, Environ. Sci. Pollut. R., 25, 7875-7883, 2018.

Huang, J. P., Fu, Q., Zhang, W., Wang, X., Zhang, R. D., Ye, H., and Warren, S. G.: Dust and Black Carbon in Seasonal Snow across Northern China, Bull. Amer. Meteor. Soc., 92, 175-181, 2011.

Jenkins, M., Kaspari, S., Kang, S. C., Grigholm, B., and Mayewski, P. A.: Tibetan plateau geladaindong black carbon ice core record (1843-1982): recent increases due to higher emissions and lower snow accumulation, Advances in Climate Change Research, 7(3), 132-138, 2016.

Jeong, D., Kim, K., and Choi, W.: Accelerated dissolution of iron oxides in ice, Atmos. Chem. Phys., 12, 11125-11133, 10.5194/acp-12-11125-2012, 2012.

Kang, S., Chen, F., Gao, T., Zhang, Y., Yang, W., Yu, W., and Yao, T.: Early onset of rainy season suppresses glacier melt: a case study on Zhadang glacier, Tibetan Plateau, J. Glaciol., 55(192), 755–758, 2009.

Kaspari, S., Painter, T. H., Gysel, M., Skiles, S. M., and Schwikowski, M.: Seasonal and elevational variations of black carbon and dust in snow and ice in the Solu-Khumbu, Nepal and estimated radiative forcings, Atmos. Chem. Phys., 14, 8089-8103, 2014.

Kirchstetter, T. W., Novakov, T., Hobbs, P. V.: Evidence that the spectral dependence of light absorption by aerosols is affected by organic carbon, J. Geophys. Res.-Atmos., 109, D21, 10.1029/2004JD004999, 2004.

Kulkarni, S.: Assessment of source-receptor relationships of aerosols: an integrated forward and backward modeling approach, Dissertations and Theses-Gradworks, 2009.

Lafon, S., Rajot, J. L., Alfaro, S. C., and Gaudichet, A.: Quantification of iron oxides in desert aerosol, Atmos. Environ., 38, 1211-1218, 10.1016/J.Atmosenv.2003.11.006, 2004.

Lafon, S., and Lee, A. B.: Diffusion maps and coarse-graining: a unified framework for dimensionality reduction, graph partitioning and data set parameterization, IEEE T. Pattern anal., 28, 1393-1403, 2006.

Li C. L., Kang S. C., Zhang Q.: Elemental composition of Tibetan Plateau top soils and its effect on evaluating atmospheric pollution transport, Environ. Pollut., 157, 8-9, 2009.

Li, C. L., Bosch, C., Kang, S. C., Andersson, A., Chen, P. F., Zhang, Q. G., Cong, Z. Y.,Chen, B., Qin, D. H., and Gustafsson, O.: Sources of black carbon to the Himalayan-Tibetan Plateau glaciers, Nat. Commun., 7, 12574, 10.1038/ncomms12574, 2016.

Liou, K. N., Takano, Y., and Yang, P.: Light absorption and scattering by aggregates: Application to black carbon and snow grains, J. Quant. Spectrosc. Ra., 112, 1581-1594, 10.1016/J.Jqsrt.2011.03.007, 2011.

Liu S. Y., Guo, W. Q., Xu J. L., et al.: The Second Glacier Inventory Dataset of China (Version 1.0), Cold and Arid Regions Science Data Center at Lanzhou, 10.3972/glacier.001.2013.db, 2014.

Lüthi, Z. L., Škerlak, B., Kim, S.-W., Lauer, A., Mues, A., Rupakheti, M., and Kang, S.: Atmospheric brown clouds reach the Tibetan Plateau by crossing the Himalayas, Atmos. Chem. Phys., 15, 6007-6021, https://doi.org/10.5194/acp-15-6007-2015, 2015.

Millikan, R. C.: Optical properties of soot, J. Opt. Soc. Am., 51, 698-699, 1961.

Ming, J., Xiao, C. D., Du, Z. C., and Yang, X. G.: An overview of black carbon deposition in High Asia glaciers and its impacts on radiation balance, Adv. Water Resour., 55, 80-87, 2013.

Ming, J., Xiao, C. D., Sun, J. Y., Kang, S. C., and Bonasoni, P.: Carbonaceous particles in the atmosphere and precipitation of the Nam Co region, central Tibet, J. Environ. Sci., 22, 1748-1756, 10.1016/S1001-0742(09)60315-6, 2010.

Moosmuller, H., Engelbrecht, J. P., Skiba, M., Frey, G., Chakrabarty, R. K., and Arnott, W. P.: Single scattering albedo of fine mineral dust aerosols controlled by iron concentration, J. Geophys. Res.-Atmos., 117, Artn D11210, 10.1029/2011jd016909, 2012.

Paatero, P., and Tapper, U.: Positive matrix factorization: a non-negative factor model with optimal utilization of error estimates of data values, Environmetrics, 5, 111-126, 1994.

Pacyna, J. M. and Pacyna, E. G.: An assessment of global and regional emissions of trace metals to the atmosphere from anthropogenic sources worldwide, Environ. Rev., 9, 269-298, 2001.

Painter, T. H., Barrett, A. P., Landry, C. C., Neff, J. C., Cassidy, M. P., Lawrence, C. R., McBride, K. E., and Farmer, G. L.: Impact of disturbed desert soils on duration of mountain snow cover, Geophys. Res. Lett., 34, L12502, 10.1029/2007gl030284, 2007.

Painter, T. H., Deems, J. S., Belnap, J., Hamlet, A. F., Landry, C. C., and Udall, B.: Response of Colorado River runoff to dust radiative forcing in snow, P. Natl. Acad. Sci. USA, 107, 17125-17130, 2010.

Painter, T. H., Bryant, A. C., and Skiles, S. M.: Radiative forcing by light absorbing impurities in snow from MODIS surface reflectance data, Geophys. Res. Lett., 39, L17502, 10.1029/2012gl052457, 2012.

Pang, H., He, Y., Theakstone, W. H., and Zhang, D. D.: Soluble ionic and oxygen isotopic compositions of a shallow firn profile, Baishui glacier No. 1, southeastern Tibetan Plateau, Ann. Glaciol., 46, 325-330, 2007.

Pio, C. A., Legrand, M., Oliveira, T., Afonso, J., Santos, C., Caseiro, A., Fialho, P., Barata, F., Puxbaum, H., Sanchez-Ochoa, A., Kasper-Giebl, A., Gelencser, A., Preunkert, S., and Schock, M.: Climatology of aerosol composition (organic versus inorganic) at nonurban sites on a west-east transect across Europe, J. Geophys. Res., 112, D23S02, 10.1029/2006JD008038, 2007.

Preunkert, S., Legrand, M., Stricker, P., Bulat, S., Alekhina, I., Petit, J. R., Hoffmann, H., May, B., and Jourdain B.: Quantification of Dissolved Organic Carbon at very low levels in natural ice samples by a UV induced oxidation method, Environ. Sci. Technol., 45, 673–678, 2011.

Pu, W., Wang, X., Wei, H. L., Zhou, Y., Shi, J. S., Hu, Z. Y., Jin, H. C., and Chen, Q. L.: Properties of black carbon and other insoluble light-absorbing particles in seasonal snow of northwestern China, The Cryosphere, 11, 1213-1233, 2017.

Qian, Y., Flanner, M. G., Leung, L. R., and Wang, W.: Sensitivity studies on the impacts of Tibetan Plateau snowpack pollution on the Asian hydrological cycle and monsoon climate, Atmos. Chem. Phys., 11, 1929-1948, 2011.

Qian, Y., Yasunari, T. J., Doherty, S. J., Flanner, M. G., Lau, W. K. M., & Jing, M.: Light-absorbing particles in snow and ice: measurement and modeling of climatic and hydrological impact, Adv. Atmos. Sci., 32, 64-91, 2015.

Qin, D. H., Liu, S. Y., and Li, P. J.: Snow cover distribution, variability, and response to climate change in western China, J. Climate, 19, 1820-1833, 2006.

Qiu, J.: The third pole, Nature, 454, 393-396, 10.1038/454393a, 2008.

Ramanathan, V., Li, F., Ramana, M. V., et al.: Atmospheric brown clouds: Hemispherical and regional variations in long-range transport, absorption, and radiative forcing, J. Geophys. Res., 112, D22S21, 10.1029/2006JD008124, 2007.

Sand, M., Berntsen, T. K., Seland, O., and Kristjansson, J. E.: Arctic surface temperature change to emissions of black carbon within Arctic or midlatitudes, J. Geophys. Res.-Atmos., 118, 7788-7798, 10.1002/Jgrd.50613, 2013.

Skiles, S. M., Painter, T. H., Deems, J. S., Bryant, A. C., and Landry, C. C.: Dust radiative forcing in snow of the Upper Colorado River Basin: 2. Interannual variability in radiative forcing and snowmelt rates, Water Resour. Res., 48, 10.1029/2012wr011986, 2012.

Takahashi, Y., Higashi, M., Furukawa, T., and Mitsunobu, S.: Change of iron species and iron solubility in Asian dust during the long-range transport from western China to Japan, Atmos. Chem. Phys., 11, 11237-11252, 10.5194/acp-11-11237-2011, 2011.

Wang, M., Xu, B., Cao, J., et al.: Carbonaceous aerosols recorded in a southeastern Tibetan glacier: analysis of temporal variations and model estimates of sources and radiative forcing, Atmos. Chem. Phys., 15, 1191-1204, 10.5194/Acp-15-1191-2015, 2015.

Wang, X., Doherty, S. J., and Huang, J. P.: Black carbon and other light-absorbing impurities in snow across Northern China, J. Geophys. Res.-Atmos., 118, 1471-1492, 2013.

Wang, X., Xu, B. Q., and Ming, J.: An overview of the studies on Black Carbon and Mineral Dust deposition in Snow and Ice Cores in East Asia, J. Meteorol. Res., 28, 354-370, 2014.

Wang, X., Pu, W., Ren, Y., Zhang, X., Zhang, X., Shi, J., Jin, H., Dai, M., and Chen, Q.: Observations and model simulations of snow albedo reduction in seasonal snow due to insoluble light-absorbing particles during 2014 Chinese survey, Atmos. Chem. Phys., 17, 2279-2296, 2017.

Warren, S. G., and Wiscombe, W. J.: A Model for the Spectral Albedo of Snow. Ⅱ: Snow Containing Atmospheric Aerosols, J. Atmos. Sci., 37, 2734-2745, 1980.

Warren, S. G.: Optical-Properties of Snow, Rev. Geophys., 20, 67-89, 1982.

Warren, S. G., and Wiscombe, W. J.: Dirty Snow after Nuclear-War, Nature, 313, 467-470, 10.1038/313467a0, 1985.

Wedepohl, K. H.: The Composition of the Continental-Crust, Geochim. Cosmochim. Ac., 59, 1217-1232, 1995.

Xu, B. Q., Yao, T. D., Liu, X. Q., and Wang, N. L.: Elemental and organic carbon measurements with a two-step heating-gas chromatography system in snow samples from the Tibetan Plateau, Ann. Glaciol., 43, 257-262, 2006.

Xu, B. Q., Cao, J. J., Hansen, J., Yao, T. D., Joswia, D. R., Wang, N. L., Wu, G. J., Wang, M., Zhao, H. B., Yang, W., Liu, X. Q., and He, J. Q.: Black soot and the survival of Tibetan glaciers, P. Natl. Acad. Sci. USA, 106, 22114-22118, 2009a.

Xu, B. Q., Wang, M., Joswiak, D. R., Cao, J. J., Yao, T. D., Wu, G. J., Yang, W., and Zhao, H. B.: Deposition of anthropogenic aerosols in a southeastern Tibetan glacier, J. Geophys. Res.-Atmos., 114, D17209, 10.1029/2008jd011510, 2009b.

Xu, B. Q., Cao, J. J., Joswiak, D. R., Liu, X. Q., Zhao, H. B., and He, J. Q.: Post-depositional enrichment of black soot in snow-pack and accelerated melting of Tibetan glaciers, Environ. Res. Lett., 7, 014022, 10.1088/1748-9326/7/1/014022, 2012.

Yang, K., Ding, B., Qin, J., Tang, W., Lu, N., and Lin, C.: Can aerosol loading explain the solar dimming over the Tibetan Plateau?, Geophys. Res. Lett., 39, 10.1029/2012GL053733, 2012.

Yao, T. D., Thompson, L., Yang, W., Yu, W. S., Gao, Y., Guo, X. J., Yang, X. X., Duan, K. Q., Zhao, H. B., Xu, B. Q., Pu, J. C., Lu, A. X., Xiang, Y., Kattel, D. B., and Joswiak, D.: Different glacier status with atmospheric circulations in Tibetan Plateau and surroundings, Nat. Clim. Change, 2, 663-667, 2012.

Yasunari, T. J., Koster, R. D., Lau, W. K. M., and Kim, K. M.: Impact of snow darkening via dust, black carbon, and organic carbon on boreal spring climate in the Earth system, J. Geophys. Res.-Atmos., 120, 5485-5503, 2015.

Zhang, R., Hegg, D. A., Huang, J., and Fu, Q.: Source attribution of insoluble light-absorbing particles in seasonal snow across northern China, Atmos. Chem. Phys., 13, 6091-6099, 2013a.

Zhang, R., Jing, J., Tao, J., Hsu, S. C., Wang, G., Cao, J., Lee, C. S. L., Zhu, L., Chen, Z., Zhao, Y., and Shen, Z.: Chemical characterization and source apportionment of PM 2.5 in Beijing: seasonal perspective, Atmos. Chem. Phys., 13, 7053-7074, 2013b.

Zhou, Y., Wang, X., Wu, X., Cong, Z., Wu, G., and Ji, M.: Quantifying light absorption of iron oxides and carbonaceous aerosol in seasonal snow across northern China, Atmosphere, 8, 63, 10.3390/atmos8040063, 2017.

Quantifying the light absorption and ~~its~~ source attribution of insoluble light-absorbing particles ~~in~~on Tibetan Plateau glaciers ~~from~~between 2013~~-~~ and 2015

Xin Wang[1,*], Hailun Wei[1], Jun Liu[1], Baiqing Xu[1,2,*], Mo Wang[2], Mingxia Ji[1], and Hongchun Jin[3]

[1] Key Laboratory for Semi-Arid Climate Change of the Ministry of Education, College of Atmospheric Sciences, Lanzhou University, Lanzhou, 730000, China

[2] Key Laboratory of Tibetan Environment Changes and Land Surface Processes, Institute of Tibetan Plateau Research, Chinese Academy of Sciences, Beijing 100085, China

[3] KuWeather Science and Technology, Haidian, Beijing, 100085, China

~~Correspondence to~~Corresponding authors: X. Wang (wxin@lzu.edu.cn~~),~~) and B. Xu (baiqing@itpcas.ac.cn)

Abstract. ~~Amounts~~The deposition of insoluble light-absorbing particles (ILAPs) ~~deposited on the surface of~~on snow and ice surfaces can significantly reduce ~~the snow~~ albedo~~ and accelerate~~, thereby accelerating the ~~snow~~ melting process. In this study, 67 ice samples were collected ~~in~~from seven glaciers ~~over~~located on the Tibetan Plateau (TP) ~~from~~between May 2013 ~~to~~and October 2015. The mixing ~~ratio~~ratios of black carbon (BC), organic carbon (OC), and mineral dust (MD) ~~was~~were measured ~~using~~with an integrating sphere~~/~~ / integrating sandwich spectrophotometer (ISSW) system~~ associated with the chemical analysis by assuming~~, which assumes that the light absorption of MD is due to iron oxide. ~~The~~Our results ~~indicated~~indicate that the mass~~-~~-mixing ratios of BC, OC, and MD ~~showed a large variation of~~exhibit considerable variability (BC: 10~~-~~–3100 ng g^{-1}~~,~~; OC: 10~~-17000~~–17,000 ng g^{-1}~~,~~; MD: 10~~-~~–3500 ng g^{-1}~~,~~) with respective mean values of 220~~±~~ ± 400 ng g^{-1}, 1360~~±~~ ± 2420 ng g^{-1}, and 240~~±~~ ± 450 ng g^{-1} ~~on TP glaciers during~~ over the course of the ~~entire ice~~ field campaign~~, respectively.~~. We ~~noted~~observed that ~~the averaged~~for wavelengths of 450–600 nm, the measured light absorption can be largely attributed to the average light absorption of BC (50.7%) and OC (33.2~~%) was largely responsible for the measured light absorption in the TP glaciers at the wavelengths of 450-600 nm. The chemical~~%). Chemical elements and ~~the~~ selected carbonaceous particles were also ~~analyzed~~analysed for ~~the~~ source attributions of ~~the~~ particulate light absorption, based on a positive matrix ~~factorization~~factorisation (PMF) receptor model. ~~On~~Our findings indicate that on average,~~ the~~ industrial pollution (33.1%), biomass/biofuel burning (29.4%), and ~~mineral dust~~MD (37.5%) ~~were~~constitute the ~~major~~principal sources of ~~the~~ ILAPs ~~in~~deposited on TP glaciers.

1 Introduction

~~Ample~~ The absorption efficiency of black carbon (BC) is higher in snow than in the atmosphere because of the higher degree of sunlight scattering in the former (Chylek et al., 1984), and a wealth of evidence ~~indicated~~confirms that the snow albedo is dominated by BC at visible wavelengths ~~is largely dominant by black carbon (BC)~~ (Warren and Wiscombe, 1980, 1985; Brandt et al., 2011; Hadley and Kirchstetter, 2012). For instance, a mixing ratio of 10 ng g^{-1} of BC in snow can reduce ~~snow~~ albedo by 1%, ~~which has a similar effect~~an amount equivalent to ~~that~~the impact of 500 ng g^{-1} of dust at 500 nm (Warren and Wiscombe, 1980; Warren, 1982; Wang et al., 2017~~). Chylek et al. (1984) indicated that the absorbing efficiency of BC is higher in snow than in the atmosphere due to more sunlight scattering in snow.~~), and Conway et al. (1996) ~~measured~~reported a ~~snow albedo~~ reduction in snow albedo of 0.21 and ~~a~~concomitant 50% increase in ~~the~~ ablation ~~rate of natural snow attributed to~~ due to 500 ng g^{-1} of BC contamination. ~~Liou et al. (2011) developed~~Similarly, in their experiments using a geometric-optics surface-wave approach ~~to demonstrate the snow~~, Liou et al. (2011) described an albedo reduction ~~by~~of as much as ~~∼~~5–10% ~~due to~~caused by small amounts of BC mixed internally ~~mixed~~ with snow grains. ~~Totally~~Overall, BC accounts for 85% of the total absorption by ~~all~~ insoluble light-absorbing impurities (ILAPs) in snow at ~~the wavelength~~wavelengths of 400–700 nm (Bond et al., 2013). ~~Due to the impact of BC on snow and ice albedos, the "efficacy"~~Furthermore, the 'efficacy' of this BC-~~snow~~ forcing is twice as effective as that of CO_2~~, at melting snow~~due to snow albedo change and may have contributed to ~~global~~the large-scale warming of the ~~past century in the~~ Northern Hemisphere over the last century (Hansen and Nazarenko, 2004).

The Tibetan Plateau (TP~~), known as the highest plateau in the world and its surrounding areas, contains~~) and neighbouring uplands together contain the largest ~~store~~area of snow and ice outside the polar regions (Qin et al., 2006). ~~[Please check that this is your intended meaning.]~~ However, over the last decade, ~82% of ~~the plateau's~~TP glaciers have retreated, and 10% of ~~its~~the permafrost ~~has degraded in the past decade~~ area has been lost as a result of climate warming (Qiu, 2008; Yao et al., 2012). Xu et al. (2009a, b) ~~indicated~~reported that the deposition of BC on snow and ice surfaces has potentially led to an earlier onset of the melting season, whereas the ~~BC deposited in snow and~~consequent loss of ice ~~potentially lead the melting seasons earlier, and the large retreat of these glaciers across the TP regions may affect the~~is projected to impact atmospheric circulation and ecosystem viability at regional and global scales and in multiple ways (Qian et al., 2011; Skiles et al., 2012; Sand et al., 2013). Therefore, ~~the~~ BC ~~content~~ is considered ~~one of the major absorbers~~ to ~~lead great decrease~~be a significant factor in ~~length and area~~the recent shrinkage of TP glaciers (Xu et al., 2006, 2009a; Qian et al., 2015; Li et al., 2016).

In addition to BC, organic carbon (OC) and mineral dust (MD) ~~recognized~~have also been identified as ~~the other types of~~ ILAPs ~~that substantially contribute~~contributing to springtime snowmelt and surface warming through ~~the~~ snow~~-~~-darkening effects (Painter et al., 2010, 2012; Huang et al., 2011; Kaspari et al., 2014; Wang et al., 2013, 2014; Yasunari et al., 2015). However, the optical properties of OC in snow are still ~~absent due to~~ largely unknown because of limited ~~small-scale~~ field ~~campaigns~~data and technical limitations. For instance, ~~the~~ pre-industrial OC concentrations ~~extracted at Antarctic~~ derived from sites in Antarctica are unexpectedly ~~higher ranging from~~ high (80 ~~to~~ –360 ng g^{-1} ~~than~~) relative to those reported ~~for~~from Greenland (10–40 ng g^{-1}) and ~~Alpine~~alpine sites (45–98 ng g^{-1} ~~) for pre-industrial ice~~) (Federer et al., 2008; Preunkert et al., 2011). ~~[Please check that this is your intended meaning.]~~ Furthermore, there ~~are still~~remain significant uncertainties in estimating the light~~-~~-absorption ~~by~~ capacities of different types of OC ~~associated with both~~from the chemical and optical ~~analyses from~~ analysis of new snow samples ~~across~~in western North America (Dang et al., 2014). Although the contribution of OC to ~~the global~~climate warming is generally lower than that of BC, ~~but still~~the impact of OC is nonetheless significant ~~mainly~~, particularly over southeastern Siberia, northeastern East Asia, and western Canada (Yasunari et al., 2015). As summarized by Flanner et al. (2009~~),~~) in relation to modelling future climate, consideration of the OC ~~in~~content of snow is ~~a~~ key ~~approach for~~to better estimating the ~~climate effects in global models due to the~~impact of ILAPs' absorption of solar radiation ~~by other ILAPs~~ from the ultraviolet to visible wavelengths.

It is well ~~known~~established that the light~~-~~-absorption capacity of MD ~~mainly depends on~~ is linked to the iron oxides (hereafter referred to as Fe) (Alfaro et al., 2004; Lafon et al., 2004, 2006; Moosmuller et al., 2012). The yellow-red colour of Fe (primarily hematite and goethite) ~~imparted a yellow-red color is a major component, which~~ affects the ability of mineral dust to absorb sunlight at short wavelengths~~, then~~ and alters ~~the dust's~~its radiative properties ~~and may influence the~~, potentially influencing climate (Takahashi et al., 2011; Jeong et al., 2012; Zhou et al., 2017). ~~Cong et al. (2018) indicated that the goethite was predominant form of Fe (81% to 98 % in mass fraction) among the glaciers in the TP regions.~~For example, Painter et al. (2007) ~~pointed out~~concluded that the duration of seasonal snow cover ~~duration in a seasonally snow-covered mountain was~~in alpine regions is shortened by 18 ~~to~~ –35 days ~~due~~owing to the ~~deposition~~redeposition of disturbed desert dust. ~~Wang et al. (2013) revealed that the light absorption was major dominated by OC across the grassland~~On the TP, goethite constitutes the dominant form of Fe (81%–98% mass) deposited on glacier surfaces (Cong et al., 2018). Over the grasslands of Inner Mongolia ~~across~~and northern China, ~~while~~light absorption is dominated by OC, whereas the snow~~-~~-particulate light absorption ~~was mainly contributed~~is provided primarily by local soil and desert dust ~~at~~derived from the northern ~~boundary of the~~ TP ~~regions.~~ (Wang et al., 2013). [~~Please check that this is your intended meaning.~~]

~~Due to the importance of the climate effects by ILAPs~~

To date, numerous ~~snow~~ surveys have ~~been conducted~~sought to ~~investigate~~evaluate the light~~-~~-absorption capacity of ILAPs (Xu et al., 2009a, b; Doherty et al., 2010; Huang et ~~a~~al., 2011; Wang et al., 2013; Dang et al., 2014~~)~~,) and their potential source attribution in snow and ice (Hegg et al., 2010; Zhang et al., 2013a; Doherty et al., 2014; Jenkins et al., 2016; Li et al., 2016; Pu et al., 2017). In their 2009 study, Hegg et al. ~~(2009) indicated~~(2010) used a positive matrix factorisation (PMF) receptor model to establish that ~~the light absorption by~~ ILAPs deposited in Arctic snow ~~is mainly originated~~originate predominantly from biomass burning, pollution, and marine sources ~~based on a positive matrix factorization (PMF) receptor model.~~. Similarly, Doherty et al. (2014) ~~found~~assessed chemical and optical data from 67 North American sites and concluded that the source attribution of particulate light absorption in seasonal snow is dominated by biomass/biofuel burning, soil dust, and fossil fuel pollution~~ based on the chemical and optical data from 67 North American sites~~.

~~Up to~~

Until now, ~~the~~ILAP light absorption and emission sources ~~of ILAPs remain~~for the TP have been poorly ~~understand.~~understood. ~~[Please check that this is your intended meaning.]~~ Increasing the in~~-~~ situ ~~measurements~~measurement of ILAPs in snow and ice is therefore crucial to assessing the ~~most urgent task to explore the~~ factors driving ongoing glacier retreat~~, especially in the TP regions. Here~~. Between 2013 and 2015, we ~~performed a large survey on collecting column~~collected ice samples ~~on~~from seven TP glaciers ~~in the TP regions~~ during both the ~~monsoon~~wet and ~~non-monsoon~~dry seasons ~~from 2013-2015.~~. By using an integrating sphere~~/~~/integrating sandwich spectrophotometer (ISSW) system ~~associated~~coupled with ~~the~~ chemical analysis, we evaluated the particulate light absorption ~~by~~of BC, OC, and MD ~~in TP glaciers was evaluated. Finally,~~before exploring the relative contributions of their respective emission sources ~~in these glaciers was explored based on~~via a PMF receptor model.

2 Site description and methods

2.1 Site description and sample collection

~~According to~~Figure 1 depicts the ~~second Chinese glacier inventory dataset, Fig. 1 exhibits the topographical maps in each glacier associated with the~~ topography and sampling locations of each glacier included in our study (Liu et al., 2014~~). Fig. S1 shows the pictures of the sampling locations in all seven glaciers, and all these glaciers are~~), arranged ~~from north to south according to their latitude and longitude in this study. Basically, the sampling locations are selected to be~~along a roughly north–south transect, and Figure S1 provides photographs of each sampling site. To minimise potential ILAP contamination from local sources, sampling sites were located at least 50 km apart from the main road and ~~the cities to minimize the effects of local sources. ~67 column~~adjacent city areas. During our 2013–2015 field seasons, we collected a total of 67 columnar ice samples ~~were gathered during monsoon and non-monsoon seasons along a south-north transect over the TP regions~~ from ~~2013-2015. It is worth noting that the seven glaciers can represent different climate~~the seven glacier surfaces. Owing to their broad geographic distribution, our glacial dataset represents climatic and land~~-~~-surface ~~types gradually~~conditions ranging from ~~the dry area~~

~~to wet area along~~ semi-arid in the northern ~~to the southern over the TP regions.~~ TP to humid in the southern. ~~[Please check that this is your intended meaning.]~~

Samples 1~~ to ~~–19 were collected from ~~2013 to 2015 during the monsoon season in the center of the~~ the centre of Qiyi ~~glacier~~ (QY~~,~~) Glacier (39°~~14'~~ 14′N, 97°~~45'~~ 45′E) (Fig. 1a)~~. The QY glacier~~) during the 2013–2015 wet seasons. QY Glacier is a small valley glacier~~, with the~~ (area ~~of~~ 2.98 km^2 ~~and the~~, length ~~of~~ 3.8 km~~. It is~~) located in the Qilian Mountains on the ~~north border of the~~northern TP ~~regions. This glacier~~and is ~~recognized~~classified as a typical ~~"~~'wet ~~island"~~island' in an otherwise arid region ~~due to~~ on account of its ~~multi-land~~multiple landcover types (e.g~~.~~., forests, ~~bushes~~bush/scrub, steppes, and meadows).

~~Samples~~ Further south, samples 20~~ to ~~–22 were collected ~~during the non-monsoon season in the southeast~~from the southeastern Qiumianleiketage ~~glacier~~ (QM~~,~~) Glacier (36°~~70'~~ 70′N, 90°~~73'~~ 73′E~~), which is originated from the~~) during the dry season. Located in the Kunlun Mountains of the ~~Qinghai-Tibet Plateau (Fig. 1b). The Tibetan Plateau~~TP ~~[In other cases, you use 'Tibetan Plateau' or the abbreviation 'TP'. Please check.]~~ (Fig. 1b), QM Glacier has a length of ~~the QM glacier is~~ 2.6 km~~,~~ and ~~the~~an area ~~is~~of 1.73 km^2.

Samples 23–32 were collected ~~in~~from the northern part of Meikuang ~~glacier during both monsoon and non-monsoon season~~ (MK~~,~~) Glacier (35°~~42'~~ 42′N, 94°~~12'~~ 12′E~~). The MK glacier is~~), located in the eastern Kunlun Mountains, ~~where is characterized~~during both the wet and the dry seasons. This region is characterised by alluvial deposits and sand dunes. ~~The~~ MK ~~glacier~~Glacier is 1.8 km ~~in length with an area of~~ long and 1.1 km^2 in area (Fig. 1c).

~~As shown in Fig. 1d~~ Immediately east of MK Glacier, samples 33–44 were collected ~~in~~from the ~~southwest~~southwestern reaches of Yuzhufeng ~~glacier~~ (YZF~~,~~) Glacier (35°~~38'~~ 38′N, 94°~~13'~~ 13′E~~). The YZF glacier is adjacent to MK glacier with~~), located on the highest peak ~~of~~ (6178 m ~~across~~) of the eastern Kunlun Mountains~~ at the northern margin of the TP regions. The glacier is surrounded by a small quantity of ferns, forests and some bushes due to the~~. This high-altitude ~~as well as the~~ region is characterised by a cold, arid climate and by fern, forest, and ~~arid climate.~~ scrubby vegetation. ~~[Please check that this is your intended meaning.]~~

Samples 45~~-~~–49 were ~~collected in~~obtained from the ~~center~~centre of Hariqin ~~glacier~~ (HRQ~~,~~) Glacier (33°~~14'~~ 14′N, 92°~~09'~~ 09′E), ~~which is~~a north-facing system located~~ at the headwaters of the Dongkemadi river~~ on the northern ~~slope~~flank of the Tanggula Mountains~~ in the~~, central ~~region of the~~ Qinghai~~-~~–Tibetan Plateau (Fig. 1e). ~~The~~ HRQ ~~glacier face north, with a mountain peak~~ Glacier drops from an elevation of 5820 m a.s.l. to its terminus ~~of~~at 5400 m~~ a.s.l.~~

~~Samples 50-60 were collected in the southern~~ , where it forms the headwaters of the Dongkemadi River. To the southwest of HRQ Glacier, the 2.8-km-long Xiaodongkemadi ~~glacier~~ (XD~~,~~) Glacier (33°~~04'~~ 04′N, 92°~~04'~~ 04′E~~). The XD glacier is adjacent to HRQ glacier, with~~) covers an area of 1.~~76~~77 km^2 and ~~2.8 km in length (Fig.~~ descends from 5900 m elevation~~1f). The elevations of the glacier from the peak~~ to its terminus ~~are 5900 and~~at 5500 m (Fig. 1f). ~~a.s.l., respectively. It has a~~ The surrounding landscape is predominantly cold steppe ~~landscape mainly surrounded by~~ and tundra. Samples 50–60 were collected from the southern reaches of XD glacier.

~~Samples 61-67 were collected in the eastern~~

Gurenhekou ~~glacier~~ (GR~~,~~) Glacier (30°~~19'~~ 19′N, 90°~~46'~~ 46′E~~). The GR glacier~~) is a relatively small ~~and cold alpine-type valley glacier in the central part of the southern TP, which is seated about 90 km northwest of Lhasa, the capital city of Tibet (Fig.~~ (area:~~1g). The glacier area is~~ 1.4 km^2~~, with a~~; length~~ and width of~~: 2.5 km~~ and~~; width: 0.6 km) cold-based alpine glacier located approximately 90 km north of Lhasa in southern Tibet (Fig. 1g). ~~, and the elevation is in the range of 5600 and 6000 m a.s.l.~~ ~~[Please check that this is your intended meaning.]~~ The glacier ranges in elevation from 6000 m to its terminus at 5600 m. Both Kang et al. (2009) and Bolch et al. (2010) ~~indicated~~suggested that ~~the Gurenhekou glacier~~GR is~~ mainly~~ influenced by both the continental climate of central Asia and the Indian monsoon system. Samples 61–67 were collected from the eastern part of the glacier.

According to Wang et al. (2015~~) pointed out that~~), the mean annual accumulation of snow/ice at ~~the~~our TP drilling ~~site over the TP glaciers was around~~sites is approximately 2 m~~ on average~~. Therefore, ~~a 1.2-m pure clean plastic bag with a diameter of 20 cm was put into a~~ for each glacier sampled between 2013 and 2015, we used a 1.2-m-long vertical tube lined with a clean, 20-cm-diameter plastic bag to collect ~~the~~ ice ~~samples~~deposited via both wet and dry deposition ~~during~~

~~monsoon and non-monsoon seasons in each sample location from 2013 to 2015 (Fig.~~ (Fig. 2). ~~Due~~Owing to ~~the~~their relatively high ~~altitudes of these glaciers, the~~altitude, wet deposition ~~in~~over these ~~areas were predominant~~glaciers is dominated by ~~new fallen snow, while much~~fresh snowfall, with considerably less ~~formed by~~derived from ~~precipitation~~rainfall. ~~However, most of the samples were gathered by column ice due to the multi-~~ ~~[Please note that snow is a form of precipitation. Do you mean 'rainfall' here?]~~ Nonetheless, the majority of samples consist of ice rather than snow, reflecting the prevalence of multiple melting processes. ~~Then, the column~~Following collection, ice samples were ~~kept frozen under -~~maintained at a temperature of −20 ~~°C and transported to laboratory facilities at~~°C during transportation to the State Key Laboratory of Cryospheric Sciences, Cold and Arid Regions Environmental and Engineering Research Institute in Lanzhou~~. Firstly, each sample was~~ , China.

In the laboratory, samples were cut vertically into four pieces ~~from the top to the bottom as shown in Fig. S2, and only one of the vertical samples was cut at 10 cm resolution~~ following established clean~~-~~sampling protocols~~, resulting in a total of 189 samples used in this study. It should be noted that if there is a significant dirty layer inside, then, this layer will be cut and analyzed separately. Another key issue is that some of the ice samples in the top layer is not~~ (Fig. S2), after which one of the four pieces was cut at 10-cm resolution. Where multiple melting events have produced a non-uniform ~~due to the multi-melting processes. Therefore, several samples were cut~~ surface layer (e.g., sites 13 and 26), we cut samples to be longer or shorter than the ~~other samples (e.g. sites 13 and 26). To minimize the losses~~average. Any dirty layers were cut and analysed separately. A total of 189 samples were used in this study. To minimise the loss of ILAPs to the container walls, each sample was ~~put into~~placed in a clean glass beaker and melted quickly in a microwave oven~~. The melted water then,~~, immediately after which the water was filtered through Nuclepore filters ~~with a~~ (pore size ~~of~~ 0.2 ~~-μm, as were used by~~ μm) following the procedure reported in Doherty et al. (2010). Further details ~~for filtrate processing can be found~~of the filtration process are given in Wang et al. (2013) and Doherty et al. (2014).

2.2 Optical analysis

~~An~~ To calculate the mass-mixing ratio of BC in our samples, we employed an updated integrating sphere~~/~~-/-integrating sandwich spectrophotometer (ISSW~~) was used to calculate the mass mixing ratio of BC in the ice samples, which is similar with the~~). Although this instrument is similar to that developed by Grenfell et al. (2011~~). Compared with the ISSW spectrophotometer developed by Grenfell et al. (2011), the major~~), a chief difference is that we used two integrating spheres to reduce diffuse radiation during measurement instead of the integrating sandwich diffuser ~~to reduce the diffuse radiation during the measuring process. This~~ employed by those authors. The ISSW spectrophotometer measures the light~~-~~-attenuation spectrum from 400 to 700 nm~~. The~~, with the total light~~-~~-attenuation spectrum ~~is~~being extended ~~over~~by linear extrapolation to cover the full spectral range ~~by linear extrapolation from 400 to~~ (300 ~~and from 700 to~~ –750 nm~~. Light~~). Nominally, light attenuation is ~~nominally only~~ sensitive solely to ILAPs trapped on the filter ~~because~~as a result of the diffuse radiation field and the sandwich structure of the two integrated spheres in the ISSW (Doherty et al., 2014). ~~Briefly, the~~ ~~[Please check that this is your intended meaning.]~~ Specifically, the system detects the light transmitted ~~light detected~~ by ~~the system for~~ an ice sample, S(λ), ~~is compared with the signal detected for~~and compares this value to that transmitted by a blank filter, S_0(λ~~), and the~~). The relative attenuation (Atn) is then expressed as:

$$Atn\cancel{=} = \ln[S_0(\lambda)/S(\lambda)] \qquad (1)$$

The mass absorption efficiency (MAE)~~MACs~~ and ~~the~~ absorption Ångström exponents (Å) employed here for BC, OC, and Fe ~~used~~are described in ~~this study could be found in~~ detail by Wang et al. (2013). ~~By using~~ ~~[Please consider spelling this term out in full where used first in the text.]~~ Using this technique, we ~~can~~are able to estimate the following parameters~~ included~~: equivalent BC (C_{BC}^{equiv}), maximum BC (C_{BC}^{max}), estimated BC (C_{BC}^{est}), the fraction of light absorption by non-BC ILAPs (f_{non-BC}^{est}), the absorption Ångström exponent of non-BC ILAPs ($\mathring{A}_{non\text{-}BC}$~~)~~), and the total absorption Ångström exponent ($\mathring{A}_{tot}$). These parameters are defined as follows: ~~[Your list of parameters in this sentence is in a different order from the list below. Please adjust.]~~

1. C_{BC}^{equiv} (ng g^{-1}): *equivalent BC* is the amount of BC that would be needed to produce absorption by all insoluble particles in snow for wavelengths of 300–750 nm.

2~~1~~. C_{BC}^{max} (ng g^{-1}): *maximum BC* is the maximum possible BC mixing ratio in snow ~~by~~, assuming that all light absorption is due to BC at ~~the~~ wavelengths of 650~~-~~–700 nm.

3~~2~~. C_{BC}^{est} (ng g^{-1}): *estimated BC* is the estimated true mass of BC in snow derived by separating the spectrally resolved total light absorption and non-BC fractions.

4. f_{non-BC}^{est} (%): the *fraction of light absorption by non-BC light-absorbing particles* is the integrated absorption due to non-BC light-absorbing particles. This value is weighted by the down-welling solar flux at wavelengths of 300–750 nm.

5. $Å_{non\text{-}BC}$: *non-BC absorption Ångström exponent*, derived from the light absorption by non-BC components for wavelengths of 450–600 nm.

~~3. C_{BC}^{equiv} (ng g^{-1}): *equivalent BC* is the amount of BC that would be needed to produce absorption of solar energy by all insoluble particles in snow for the wavelength-integrated from 300-750 nm.wavelengths of 300–750 nm. [Please consider rewording as your intended meaning is unclear.]~~

6~~4~~. $Å_{tot}$: *absorption Ångström exponent* ~~is~~, calculated for all insoluble particles deposited on the filter between 450 and 600 nm.

~~5. $Å_{non\text{-}BC}$: *non-BC absorption Ångström exponent* is, derived from the light absorption by non-BC components of the insoluble particles in snow between for wavelengths of 450-–600 nm.~~

~~6. f_{non-BC}^{est} (%): the *fraction of light absorption by non-BC light -absorbing particles* is the integrated absorption due to non-BC light -absorbing particles, which. This value is weighted by the down-welling solar flux at the wavelengths of 300-–750 nm.~~

~~It is well known that~~

Both the ~~aerosol~~ composition and the size distribution of aerosols are ~~key~~well-known parameters ~~that affect~~influencing the absorption Ångström exponent. ~~[You have already defined this as "$Å_{tot}$" just above. Please use the abbreviation both here and in instances below. Use "$Å_{tot}$ values" if needed to fit the various instances.]~~ Doherty et al. (2010) reported that the ~~value of the~~ absorption Ångström exponent of OC ~~was~~is close to 5, ~~which is~~ consistent with ~~previous studies with values ranging from 4-~~the previously reported range of 4–6 (Kirchstetter et al., 2004~~). Several~~), and several studies ~~indicated that the~~have included absorption Ångström ~~exponent~~exponents of 2–5 for ~~mineral dust ranged from 2 to 5[You have defined mineral dust as 'MD' above. Please therefore use the abbreviation both here and below.]~~MD (Fialho et al., 2005; Lafon et al., 2006; Zhou et al., 2017; Cong et al., 2018). ~~The variation of the~~Typical absorption

Ångström exponents for urban and industrial fossil fuel emissions ~~is typically in~~fall within the range ~~of~~ 1.0–1.5 (Millikan, 1961; Bergstrom et al., 2007), which is slightly lower than that of biomass-burning aerosols~~, which primarily falls in the range of~~ (1.5–2.5) (Kirchstetter et al., 2004; Bergstrom et al., 2007). In this study, we ~~noted~~note that the absorption Ångström exponent ($Å_{tot}$) ~~is due to the mix state of~~comprises both BC and non-BC impurities trapped on the filters~~, and the calculations~~. Calculations of $Å_{tot}$ and of $Å_{non\text{-}BC}$ ~~could be found in the study of~~are described by Doherty et al. (2014). ~~The~~Specifically, $Å_{non\text{-}BC}$ is calculated as a linear combination of the contributions to light absorption ~~due to~~made by OC and Fe~~, and the equation is listed as follows~~:

$$Å_{non\text{-}BC} = F_{OC} \times Å_{OC} + F_{Fe} \times Å_{Fe} \qquad (2)$$

2.3 Chemical analysis

~~The major~~Major metallic elements (Al, Cr, Mn, Fe, Ni, Cu, Zn, Cd, and Pb) were ~~analyzed by~~analysed on an X-7 Thermo Electrical inductively coupled plasma–mass ~~spectrometry~~spectrometer (ICP–MS~~, X-7 Thermo Elemental~~) at the Institute of Tibetan Plateau Research~~ in~~, Beijing, China. The detection limits are ~~Al,~~ 0.238 ng ml^{-1}~~; Cr~~ for Al, 0.075 ng ml^{-1}~~; Mn~~ for Cr, 0.006 ng ml^{-1}~~; Fe~~ for Mn, 4.146 ng ml^{-1}~~; Ni~~ for Fe, 0.049 ng ml^{-1}~~; Cu~~ for Ni, 0.054 ng ml^{-1}~~; Zn~~ for Cu, 0.049 ng ml^{-1}~~; Cd~~ for Zn, 0.002 ng ml^{-1}~~; Pb,~~ for Cd, and 0.002 ng ml^{-1}~~. Briefly, we acidified all~~ for Pb. Prior to measurement, melted samples ~~directly to~~ were acidified (pH $<$ 2) with ultra-pure ~~HNO_3, then let settled~~HNO_3 and left to settle for ~~48h~~48 hours. The relative deviation between most of the measured values and the standard reference values is within 10%. Details ~~on~~of these procedures are given in Li et al. (2009) and Cong et al. (2010).

~~Meanwhile, for the filtrated water samples, we measured the~~

We used a Dionex 320 ion chromatograph to measure major anions (Cl^-, NO_2^-, NO_3^-, ~~SO_4^{2-})~~ and SO_4^{2-}) and cations (Na^+, NH_4^+, K^+, Mg^{2+}, ~~Ca^{2+}~~ and Ca^{2+}) ~~with an ion chromatograph (Dionex 320; Dionex, Sunnyvale, CA) using a CS12 column for cations and an AS11 column for anions~~ in filtrated water samples. The apparatus, which is housed at the Institute of Tibetan Plateau Research in Beijing~~. All the~~, is equipped with a CS12 column for cations and an AS11 column for anions and has a detection limit ~~of the~~ for all measured ions ~~was~~of 1 ~~$\mu g \cdot l^{-1}$~~.

~~In addition, except for the anions and cations and trace elements,~~ μg · l^{-1}. We also measured concentrations of Sea ~~Cl~~ salt~~,~~ ~~[Please define this abbreviation.]~~ MD, and biosmoke K (~~$K_{Biosmoke}$) were determined~~ $K_{Biosmoke}$) to assess the mass contributions of the major components in ~~the~~our ice samples. Specifically, ~~Cl~~ Sea salt was estimated ~~as follows in accordance with~~ according to the protocol described by Pio et al. (2007~~),~~): ~~by adding to sodium, chloride, and sea-salt contributions of sodium, magnesium, calcium, potassium, and sulfate, as follows:~~sulphate: ~~[Please consider rewording as your intended meaning is unclear.] [Also, 'Cl salt' does not appear in either of the following equations. Please check.]~~

$$\cancel{Cl_{salt}=Na^{+}_{Ss}+Cl^{-}+Mg^{2+}_{S_s}+Ca^{2+}_{S_s}+K^{+}_{S_s}+SO^{2-}_{4S_s}}$$

$$\cancel{=Na^{+}_{Ss}+Cl^{-}+Cl_{salt}}\,\text{Sea salt} = Na^{+}_{Ss} + Cl^{-} + Mg^{2+}_{S_s} + Ca^{2+}_{S_s} + K^{+}_{S_s} + SO^{2-}_{4S_s}$$

$$= Na^{+}_{Ss} + Cl^{-} + 0.12 \times Na^{+}_{Ss} + 0.038 \times Na^{+}_{Ss} + 0.038 \times Na^{+}_{Ss} + 0.25 \times Na^{+}_{Ss} \quad (3)$$

$$Na_{Ss}\cancel{= Na_{Total}\text{-}Al\cdot(Na/Al)_{Crust}} = Na_{Total} - Al \times (Na/Al)_{Crust} \quad (4)$$

~~Where~~

where $(Na/Al)_{Crust} = 0.33$~~,~~ and represents the Na/Al ratio in the dust ~~materials~~material (Wedepohl, 1995).

The MD content ~~was~~is calculated ~~by a straightforward method, and the~~ assuming an Al concentration ~~in~~for dust ~~was estimated as~~of 7% (Zhang et al., 2013b):

$$MD = Al/0.07 \quad (5)$$

We determined $K_{Biosmoke}$ ~~as follows~~according to the following equation (Pu et al., 2017):

$$\cancel{K_{Biosmoke}=K_{Total}\text{-}K_{Dust}\text{-}K_{Ss} \quad (6)}$$

$$K_{Biosmoke} = K_{Total} - K_{Dust} - K_{Ss} \quad (6)$$

$$K_{Dust} = Al \times (K/Al)_{Crust} \quad (7)$$

$$K_{Ss} \cancel{= Na_{Ss}} = Na_{Ss} \times \cancel{\cdot}\, 0.038 \qquad (8)$$

~~Where~~~~[You use both "×" and "·" for multiplication in the equations. Please be consistent.]~~

where $(K/Al)_{Crust}$ is 0.37, ~~which represents~~representing the K/Al ratio ~~in~~of the dust ~~materials~~material (Wedepohl, 1995~~)~~), and Na_{Ss} is estimated ~~by Eq.~~using Equation (4).

2.4 Enrichment factor ~~(EF)~~

To evaluate the relative contributions of trace elements from natural (e.g., mineral and soil dust) versus anthropogenic sources (e.g., fossil fuels and vehicle exhaust), we conducted an inter-annual comparison of enrichment factor (EF) values, which represent the enrichment of a given element relative to its concentration in ~~the~~Earth's crust ~~of the earth.~~. The primary uncertainty in these calculations ~~is attributed to the~~originates from differences ~~between~~in chemical ~~compositions in the~~ composition between snow and the reference crustal ~~composition.~~material. ~~[Please check that this is your intended meaning.]~~ The ~~EF~~EF is defined as the concentration ratio of a given metal to that of Al, which is a reliable measure of crustal dust, ~~normalized~~normalised to the same concentration ratio characteristic of the upper continental crust (Wedepohl, 1995~~),~~). EF is calculated ~~with~~by the ~~following~~ equation:

$$EF = \cancel{\frac{(X/Al)_{snow}}{(X/Al)_{crust}}} = \frac{(X/Al)_{snow}}{(X/Al)_{crust}} \qquad (9)$$

2.5 Source apportionment

~~The Positive Matrix Factorization (~~PMF 5.0~~)~~ is ~~considered as~~ a ~~generally accepted~~ receptor model used to determine ILAP source apportionment ~~of the ILAPs~~ when source emission profiles are ~~unknown~~unavailable (Paatero and Tapper, 1994). ~~Details of the~~We employed a PMF procedure ~~used in this study are~~ similar to ~~the previous work as discussed in~~ that described by Hegg et al. (2009, 2010~~). Generally, the~~), in which mass ~~concentration~~ concentrations and ~~the uncertainties of the~~ chemical species ~~were used~~uncertainties are provided as the input. ~~The~~Our final data set ~~used for the PMF analysis~~ contained 189 samples with 18 elements~~whereby~~; only those elements ~~that~~

~~have~~with high recovery were used~~. The~~ for PMF analysis. For each sample, uncertainty values (Unc) for individual variables were estimated from an empirical equation expressed as:

$$\mathrm{Unc} = \sqrt{(\sigma \times \mathrm{c})^2 + (\mathrm{MDL}^2)} \qquad (10)$$

Where σ is the standard deviation, c represents the mass concentrations of the relative species, and the MDL depicts the method detection limited.

~~For each sample, uncertainty value of each variable in each sample was values for individual variables were estimated from an empirical equation. The PMF [Should you give more details about this?]~~ Although we ran the PMF model ~~was run~~ for ~~3 to 6~~between three and six factors~~ with 6~~, including six random seeds, ~~but only a three-factor solution could provide the~~ we found that the most meaningful results ~~of the ILAPS in TP glaciers. The~~for our TP sites were generated by a three-factor solution. Indeed, *Q* values (modified values) for ~~the 3~~this three-factor solution (both robust and true) were closest to the theoretical ~~*Q* value~~values of any ~~of the~~ factor ~~numbers~~number for which the model was run~~, suggesting that the 3-factor solution was optimal~~.

3~~.~~ Results and ~~Discussion~~discussion

~~[We note that your results were reported in the past tense. We have maintained that tense during editing except where the present or other tense is required. An alternative (and probably preferable) way would be to report the results using present tense throughout. Please consider.]~~

3.1 Aerosol optical depth ~~(AOD)~~

Aerosol optical depth (AOD) represents both the transport pathways and deposition of dry aerosols, which in turn provide vital information on potential ILAP sources. As shown in ~~Fig.~~Figure 3,~~ the~~ QY, QM, MK, and YZF glaciers are located ~~in~~on the northern ~~part of Tibetan Plateau, while~~TP, whereas XD, HRQ, and GR glaciers are located in the plateau's southern ~~part of Tibetan Plateau. It worth noting that the aerosol optical depth (AOD) can represent the dry aerosol deposition and its transport pathway, which could provide useful information about the possible sources of the ILAPs in the TP glaciers.~~regions. Therefore, to elaborate on the sources of ILAPs for each TP study site, we assessed the spatial distribution of ~~the~~ averaged ~~AOD at~~ 500 nm AOD, derived from Aqua-MODIS ~~were retrieved over the TP regions and its adjacent areas from~~ between 2013 ~~to~~and 2015. ~~Following the work of [Please check that this is your intended meaning.]~~

According to Ramanathan et al. (2007), ~~the~~ anthropogenic AOD~~, which is~~ also ~~called~~referred to as atmospheric brown ~~clouds~~cloud (ABC~~), was larger than 0.3~~) on the ~~southern~~south side of the Himalayas~~. Therefore~~ is greater than 0.3. Consequently, AOD (500 nm) values of >0.3 and <0.1 are considered ~~to present the~~representative of anthropogenic haze and background conditions, respectively.

We ~~found that~~observed considerably higher AOD over the ~~AOD was much larger across the~~ western TP than ~~that in~~over the central ~~part of~~ TP~~ regions. As a result, the AOD~~. For example, values ~~in the~~for QY, QM, MK, and YZF glaciers ~~were in the range of~~ranged from 0.25 to 0.3~~ could be highly influenced by human activities. The high values of AOD~~ , suggestive of anthropogenic influence, whereas values for HRQ, XD, and GR glaciers were considerably lower (<0.125). Although the elevated AOD over the western TP might ~~thus contribute~~serve to ~~the~~enhance glacial retreat ~~of Himalayan glaciers~~ there (Engling and Gelencser, 2010~~). In contrast, the lower values of AOD (<0.125) were observed near the HRQ, XD, and GR glaciers. However, the~~), we note that AOD over the TP ~~regions~~in general was ~~much~~significantly lower than ~~that over Southern~~ in southern Asia, ~~especially~~particularly over the Indo-Gangetic Plain during the cold season. This ~~is close to~~ pattern aligns closely with previous measurements ~~over the TP regions~~ (Cong et al., 2009; Ming et al., 2010; Yang et al., 2012; Lüthi et al., 2015).

3.2 Regional averages of ~~the~~ optical parameters

~~The general information of~~ Table 1 compiles the ice C^{est}_{BC}, C^{max}_{BC}, C^{equiv}_{BC}, $f^{est}_{non\text{-}BC}$, $\mathring{A}_{tot}$, and $\mathring{A}_{non\text{-}BC}$ ~~of the ice samples are given in Table 1~~ data for each glacier. The ~~lower~~lowest median ~~values of~~ C^{est}_{BC} ~~could be~~ (23~~ ng g^{-1}~~, 26 ng g~~$^{-1}$ during the monsoon season in the~~ $^{-1}$) was observed on HRQ and GR glaciers~~ on~~, southern TP, during the ~~south of~~wet season, whereas the ~~TP regions, while the higher~~highest values ~~of~~ (187~~ ng g^{-1} and~~ , 165 ng g~~$^{-1}$ found in the~~ $^{-1}$) occurred on MK and YZF glaciers on the central ~~part of the TP regions. Compared with the monsoon~~TP. Relative to the wet season, the ~~concentration~~measured concentrations of C^{est}_{BC} ~~increased very significantly in~~ were markedly higher during the dry season for all seven glaciers~~ than those values during the non-monsoon season. We found that the~~. The lowest overall BC concentration ~~of BC in the ice samples~~ was ~~found in the~~recorded on XD ~~glacier, with a value of~~ ~~C^{est}_{BC}~~ Glacier (C^{est}_{BC} = ~10 ng g^{-1}~~. In~~

~~contrast,~~), whereas the ~~highest~~maximum values of C_{BC}^{est}~~,~~ (3100 ng g^{-1}), C_{BC}^{max} ~~,~~ (3600 ng g^{-1}), and C_{BC}^{equiv} ~~were 3100 ng g^{-1}, 3600 ng g^{-1}, and~~ (4700 ng g~~$^{-1}$, respectively, taken in the~~ $^{-1}$) all corresponded to GR ~~glacier. Generally, the median of~~Glacier. Median $\mathring{A}_{tot}$ typically exceeded 1.0 at all ~~locations~~seven sites (Fig. 4, ~~and~~ Table 1).

The ice samples exhibited $\mathring{A}_{tot}$ and $\mathring{A}_{non\text{-}BC}$ ~~for all ice samples were in the range of~~ values of 1.4~~-~~–3.7 and 1.9~~-~~–5.8, respectively (Table S1). As shown in ~~Fig.~~ Figure 4a, the median values of $\mathring{A}_{tot}$ for QY, MK, XD, and GR glaciers were 2.62, 2~~,~~.64, 2~~,~~.18, and 2.46 ~~in the QY, MK, XD, and GR glaciers, associated with~~, respectively, and the estimated contributions of non-BC ILAPs to absorption ~~by non-BC ILAPs in these regions~~ were ~~~~~approximately 41%, 44%, 36%, and 48%, respectively. ~~Compared with these glaciers, the higher~~Relatively high values ~~of median $\mathring{A}_{tot}$~~ were ~~found~~observed in ~~the~~samples from QM (2.76), YZF (2.95), and HRQ (2.87) glaciers. ~~Correspondingly~~Accordingly, the estimated $f_{non\text{-}BC}^{est}$ values ~~in~~for those regions ~~is ~~~were 44%, 48%, and 48%, respectively. ~~Except~~With the exception of HRQ ~~glacier, the other glaciers showed an increased trend of the~~ Glacier, our data set exhibits a clear south-to-north increase in $\mathring{A}_{non\text{-}BC}$ ~~from the south to north regions in~~ over the TP ~~regions~~ (Fig. 4b). Histograms ~~of the~~depicting $\mathring{A}_{tot}$ by ~~regions~~region are shown in ~~Fig.~~ Figure 5. ~~We found that there was a large variation of $\mathring{A}_{tot}$ in the~~

XD ~~glacier~~Glacier exhibited the greatest degree of $\mathring{A}_{tot}$ variability, not only in the higher values (~2~~-~~–4), but also ~~for~~at the lower ~~values~~end of the range (<2). ~~The broadness of the $\mathring{A}_{tot}$~~This broad distribution is indicative of the complicated sources of particulate light absorption. For instance, Wang et al. (2013) ~~indicated~~reported that ~~the~~ higher $\mathring{A}_{tot}$ values ~~of $\mathring{A}_{tot}$ (~~~(approximately 3.5~~-~~–4.5) ~~was highly~~are strongly correlated with ~~the~~ local ~~soil source, while~~soils, whereas fossil fuel ~~burning may have~~combustion has an absorption Ångström exponent ~~lower than~~ of <2 (Millikan, 1961; Fialho et al., 2005). ~~Therefore, a~~A significant fraction of the total absorption ~~was not only~~ on XD Glacier, therefore, is attributed not only to BC (49~~%, shown in~~%; Fig. 7~~)~~;), ~~[Fig. 6 does not yet seem to have been mentioned. Please check through and ensure that each figure is mentioned in the text and that the first mentions are in ascending numerical order.]~~ but also ~~contributed by~~to non-BC absorbers (~~accounting for~~ 51%) ~~due~~linked to OC and MD ~~in the XD glacier.~~. In contrast, ~~a common feature in the~~ $\mathring{A}_{tot}$ values for all other ~~regions was that the major dominated values of $\mathring{A}_{tot}$~~

~~range from~~ sites typically ranged from 2 to 3. The valuesof$Å_{non\text{-}BC}$ and $Å_{tot}$ for each site ~~in each site~~ are ~~also given~~~~depicted as red dots and blue triangles, respectively,~~also given in ~~Fig. S3.~~Figure S3.~~.~~ ~~[Please consider putting this in the figure caption for S3.]~~

Figure 6 shows the regional ~~variations of~~ variability in BC, OC, and Fe ~~concentration in each glacier~~concentrations during ~~monsoon~~the wet and ~~non-monsoon~~dry seasons. Although ~~there were significant~~we observed clear differences ~~between the~~in median and average ~~values of~~ILAP concentrations among the ~~ILAPs concentration in each glacier~~seven glaciers, we ~~found~~also note that ~~all kinds of~~overall, ILAPs exhibited a similar ~~variation from the northern QY glacier to southern GR glacier. In addition~~pattern of variability throughout our study area. With the exception of QY and QM glaciers, we collected ~~the~~ ice samples during both ~~monsoon~~the wet and ~~non-monsoon~~the dry seasons ~~in five glaciers, only except the QY and QM glaciers.~~ . On average, ~~the~~ BC and OC concentrations ~~in the~~at HRQ, XD, and GR ~~glacier during non-monsoon season~~ glaciers were several orders of magnitude higher ~~than those in monsoon seasons. The result was highly~~during the dry season than during the wet season. This pattern is consistent with the ~~previous study by~~findings from the middle Himalayas of Cong et al. (2015), who ~~found that although the transport pathways of air masses arriving the middle Himalayas during monsoon and non-monsoon were similar,~~reported that the dry season is characterised by a distinctly higher carbonaceous aerosol level ~~was found only in~~than that of the ~~non-monsoon~~wet season~~.~~, despite similar air mass pathways.

Lüthi et al. (2015) ~~also exhibited~~ demonstrated that the atmospheric brown cloud over Southern ~~Asia can climb across the Himalayan and transport of polluted air mass, which may have serious implications of the cryosphere in the TP regions. However, there appeared to be~~~~[“southern”? Please be consistent; “southern” is probably better throughout because you are not referring to a political or official area of Asia.]~~ Asia can cross the Himalayas, transporting polluted air masses to the TP and potentially impacting regional glacier mass balance. ~~[Please check that this is your intended meaning.]~~ In our data set, however, there is no apparent difference in ~~the~~ILAP mixing ratios ~~of ILAPs~~ between ~~monsoon~~the wet and ~~non-monsoon~~dry seasons ~~in~~for two adjacent (MK and YZF) glaciers. ~~This can be mainly explained that,~~

~~except the~~We attribute this pattern to the fact that with the exception of long-range ~~transport of ILAPs~~pathways, local air pollutants ~~could~~can also ~~affect the ILAPs in~~impact ILAP availability on the central TP~~ regions.~~. ~~[Please check that this is your intended meaning.]~~ For instance, ~~Huang et al. (2018) investigated that the~~although the prevailing air masses ~~across~~over the MK and YZF glaciers ~~were originated~~originate from the arid western TP and Taklimakan ~~desert~~Desert regions, ~~and~~Huang et al. (2018) concluded that the concentration of trace elements ~~in the~~at YZF ~~glacier was~~Glacier, ~~is closer to those of the dust sources indicating that compared with XXX [Please complete the comparison at XXX.]~~ and thus that YZF ~~glacier was~~Glacier is less influenced by human ~~activities. The~~activity. In close agreement with Ming et al. (2013), our median values of ~~the~~ C_{BC}^{est} and C_{OC} (referred to as the mass concentration of OC) ~~obviously showed a slightly~~exhibit a gradually decreasing trend from ~~the~~north to south, and the mass concentrations of BC are higher for northern TP ~~to the southern TP. The mass concentration of BC in northern TP glaciers was higher than that in southern TP glaciers, which showed a good agreement with Ming et al. (2013).~~ glaciers than for their southern counterparts.

To help quantify the regional ILAP status of ~~ILAPs in~~ each glacier, ~~the~~Table 2 contains statistics ~~of the ILAPs in~~on snow and ice ~~in the studied TP glaciers and other related glaciers by~~ samples collected both during our present investigation and during previous studies ~~are shown in Table 2.~~ of TP glaciers. During ~~this field campaign,~~ our visit to YZF Glacier, we collected twelve ice samples ~~were collected in the YZF glacier. The~~ from depths ~~of these ice samples collected in the YZF glacier were ranging from~~ between 15 ~~to~~and 45 cm (Table S1). As shown in ~~Fig.~~Figure S4, ~~most values of C_{BC}^{est} in~~values for this region typically ranged from ~100~~-~~ to 1000 ng g^{-1}, with ~~a few~~several values ~~lower than~~ of <100 ng g^{-1}. ~~One notable~~A striking feature of this data set is ~~that~~ the ~~highest concentrations of~~ relatively high C_{BC}^{max} (1600 ng g^{-1}) and C_{OC} ~~for the surface layer were 1600 ng g^{-1} and~~ (9160 ng g^{-1}) in the surface layer at site 41. ~~We pointed out~~Judging by the high value of $f_{non\text{-}BC}^{est}$ (0.56) for this site, we suggest that ~~the~~ these data indicate that light absorption ~~in the surface glacier~~ at this site ~~41 was~~is influenced not only ~~influenced~~by BC but also potentially by ~~BC, but also possibly related to the~~ OC and MD~~ due to the high value of $f_{non\text{-}BC}^{est}$ (0.56). In the~~.

For YZF ~~glacier~~Glacier, $Å_{tot}$ ~~generally~~typically varied between ~2 and 3.7, and the average ~~value of~~ $f^{est}_{non\text{-}BC}$ ~~was~~is close to 50%, ~~so these results also revealed~~which together suggest that ~~the~~ ILAPs ~~in ice samples~~at this site are heavily influenced by anthropogenic air ~~pollutants. Large~~pollution. We also observed large variations ~~of~~in C_{OC} ~~were also observed,~~, with values ranging from ~10 to ~~1700~~17,000 ng g^{-1}. ~~Except~~With the exception of site 23, ~~the values of~~ C^{est}_{BC} ~~in the~~values for MK ~~glacier~~Glacier were ~~much~~considerably lower than those ~~in the YZF glacier, which were in the ranges of ~~~of YZF Glacier (range 20–670 ng g^{-1}~~, with a~~; median ~~value of~~ 130 ng g^{-1} ~~(~~; Fig. S5). ~~The~~ MK Glacier gave a median C_{OC} ~~was~~of ~600 ng g^{-1} ~~in~~, whereas the ~~MK glacier. The~~ fraction of total particulate light absorption ~~due~~attributable to non-BC constituents was typically ~16–62~~%, and~~%. $Å_{non\text{-}BC}$ (5.12) ~~in~~at this ~~region was highly~~site is very similar to that ~~found in the~~of YZF ~~glacier~~Glacier (5.06).

~~In the QY glacier (Fig. S6), the~~

C^{est}_{BC} ~~were much~~values for QY Glacier (Fig. S6) are similar ~~with~~to those ~~in the~~of MK ~~glacier, with values~~Glacier, ranging from ~20 to 720 ng g^{-1}~~, which did not include~~ (excluding the highest value of 1900 ng g^{-1} at site 13~~.~~). The fraction of total particulate light absorption due to the non-BC constituent $f^{est}_{non\text{-}BC}$ was typically ~20–70%, with a median value of 41%. ~~This information along~~Together with the lower $Å_{tot}$ (2.6~~) indicated~~), this information indicates that BC ~~played the~~plays a dominant role in influencing ~~the~~ light absorption in this region. Compared with the other TP glaciers, we ~~noted~~note that the vertical ILAP profiles ~~of ILAPs in the~~on QY ~~glacier~~Glacier were collected ~~in~~during the ~~monsoon season from~~ 2014 ~~to~~and 2015 wet seasons (Table S1). ~~[Or do you mean 'In contrast to'? If so, please consider replacing.]~~ The mixing ratios of OC and Fe ~~ranged from~~were 80~~-10100~~–10,100 ng g^{-1} and 20–340 ng g^{-1}, respectively. ~~Fig.~~Figure S7 shows that the vertical profiles of the mass-mixing ratios of BC, OC, and Fe ~~for the ice samples in the XD glacier~~ were more variable for XD Glacier than ~~those~~ for the other ~~regions~~six glaciers. With the exception of the surface layer at sites 53 and 54, ~~most values of~~ C^{est}_{BC} typically ranged from 10 to 280 ng g^{-1} ~~in the~~, indicating that XD ~~glacier; therefore, this glacier was~~Glacier is the cleanest ~~region among all the studied glaciers.~~site in our study. At sites 56–58, $f^{est}_{non\text{-}BC}$ was ~~lower~~less than 38%, and $Å_{tot}$ ranged from 1 to 2.5~~. These results were~~, consistent with the ~~fossil fuel~~ combustion ~~source~~of fossil fuels due to industrial ~~activities~~activity.

3.3 Scavenging and washing efficiencies

Previous studies have ~~illustrated that the~~demonstrated how ILAPs ~~could~~ become trapped and integrated ~~at the surface of~~ into the snowpack ~~due to~~ as a result of melting and sublimation ~~to enrich the~~, thereby enriching surface concentrations of these particles (Conway et al., 1996; Painter et al., 2012; Doherty et al., 2013). For instance, Doherty et al. (2013) ~~found~~reported that ~~the ILAPs could be scavenged with the~~ILAP scavenging by snow meltwater ~~to lead to a much higher~~ leads to elevated concentrations of BC in the surface layer. Similarly, Flanner et al. (2007, 2009) concluded that amplified ablation due to the concentration of BC in ~~the surface snow. Flanner et al. (2007, 2009) indicated that the melt amplification due to concentrated BC in melted~~ melting snow serves to further reduce the snow ~~would amplify snow~~ albedo ~~reduction, and therefore provide~~, thus providing a positive feedback to radiative forcing. However, ~~it still~~the impact of multiple melting processes on ILAPs located at greater depths in the glacier surface remains unclear ~~what happens~~.

On QY Glacier, we observed a marked increase in ILAP mixing ratios with depth. Although this result may appear inconsistent with those of Doherty et al. (2013), we note that Xu et al. (2012) observed high concentrations of BC at the snow surface and at depth, which those authors attributed to meltwater percolation and the deposition of superimposed ice in the snowpack. A further prominent feature in our data set is the elevated surface mixing ratio of C_{BC}^{est} at sites 52–54 on XD Glacier, relative to deeper layers, which we attribute to the ~~vertical~~dry/wet deposition of BC on the surface samples. We propose that the clear difference in vertical profiles between QY and XD glaciers is a function of ILAP deposition. Specifically, QY Glacier was sampled during the wet season, when higher temperatures and stronger melting potentially serve to concentrate ILAPs in the basal layers. In contrast, because we sampled XD Glacier during both the wet and dry seasons, ILAP concentrations decrease with depth during the dry season as a function of scavenging (Figs. S7a–~~gd, f, h–j~~) but increase during the wet season because of the concentration effect (Figs. S7h~~, ~~–j). ~~[Please check that these ranges correspond correctly to the number of panels in Fig. S7.]~~ Because the single-layer samples are not shown, ~~[The meaning of this is unclear. Please rephrase. Shown where?]~~ the vertical profiles of C_{BC}^{est} ~~deeper layer of snow and ice during the multi-melting processes due to limited in-situ observations~~for QM, HRQ, and GR glaciers are plotted in Figure S8. With the exception of those sites included in Figure S8d–e, i, and h, the sampled glaciers exhibit the trapping and scavenging effects of a higher surface-layer BC content resulting from melting processes. ~~In this study, the mixing ratios of ILAPs in most of the ice samples increased remarkably from the top to the bottom in QY glacier. This result seemed inconsistent with a previous study by Doherty et al. (2013). However, Xu et al. (2012) observed that the concentrations of BC were higher not only at the snow surface, but also found at the bottom due to the percolation time of meltwater and superimposed ice by the temperature decline in the snowpack. Another notable feature was that the surface mixing ratios of~~ $\cancel{C_{BC}^{est}}$ ~~at sites 52-54 in the XD glacier were significantly larger than those in the sub-surface layers, possibly because of the accumulation of BC via dry/wet deposition on the surface samples. We found that the mechanism of the ILAPs in the vertical ice samples in the QY and XD glacier could be difference. The ice samples in the QY glacier were collected in the monsoon season. Due to the higher temperature in the monsoon season, the strong melting processes could wash out the ILAPs in ice samples to lead a higher concentration in the bottom layer in QY glaciers. In contrast, the ice samples were collected in XD glacier in both monsoon and monsoon seasons. Therefore, it can be seen clearly that a decreasing trend of the ILAPs in the ice samples was found from the top to the bottom in XD glacier due to the high scavenging effect during the non-monsoon season (Fig. S7a-S7f, only except Fig. S7e and S7g), while a opposite trend due to the washing effect during the monsoon season (Fig. S7h and Fig. S7j). Because the single layer samples are not shown,~~

~~the vertical profiles of~~ $\cancel{C_{BC}^{est}}$ ~~are plotted in Fig. S8 for all ice samples, which were collected in the QM, HRQ, and GR glaciers. Except for the sites in Fig. S8d, S8e, S8i, and S8h, the other sites revealed the trapping and scavenging effects of a higher mass concentration of BC in the surface layer due to the melting processes.~~

3.4 ~~Contributions~~ILAP contributions to particulate light absorption ~~by ILAPs~~

The fractional contributions ~~to total absorption by~~ of BC, OC, and Fe (~~assumed to be~~presumably in the form of goethite) ~~at~~ to total absorption (450 nm ~~in~~) are depicted for each glacier ~~are shown~~ in ~~Fig.~~Figure 7, ~~and~~with further details of ~~the concentrations of~~ BC, OC, and Fe ~~are~~ concentrations given in Table S1. BC ~~played~~plays a dominant role in particulate light absorption, with average values ranging from ~44~~%-~~% to 54% ~~in~~across all seven glacier ~~regions.~~sites. Although OC ~~was~~represents the second highest absorber ~~in glacier regions, and there are large variations of~~ , we noted significant variability (between 25% and 46% on average) in its contribution to total light absorption ~~of OC~~ during the 2013–2015 field campaign~~ (~25%-46%~~. For those glaciers located on ~~average). The~~the eastern TP (QY, YZF, and HRQ glaciers), the relative contributions of BC and OC to total absorption ~~due to BC and OC were relatively comparable in the QY, YZF and HRQ, which are located in the eastern TP regions.~~are broadly similar. The highest fraction of BC (54%) was ~~accounting for 54% in the~~measured on QM ~~glaciers, which is located in~~Glacier, on the western TP ~~regions. So the~~.

Complementing the BC and OC contributions, light absorption ~~due to ILAPs in the TP glacier regions was not only from BC and OC, but also with a small contribution from~~ on TP glaciers is also influenced by Fe. ~~The~~According to our data, the average fraction of total light ~~absorption due to Fe was ~11%~~ absorbed by Fe ranges from approximately 11% to 31% ~~in~~across all seven glaciers, with the highest ~~light absorption of Fe in the GR glacier. The relative contributions to total light absorption by BC, OC, and Fe for surface ice samples in each sampling location are also shown in Fig. S9 and Table 1. This result was an indication~~values recorded on GR Glacier. This finding indicates that ~~mineral dust~~MD ~~played~~plays a key role in ~~affecting~~ the spectral absorption properties of ILAPs ~~in ice samples from the TP glaciers.~~ on TP glaciers. The relative contributions of BC, OC, and Fe to total light absorption for all surface-ice samples are presented in Figure S9 and Table 1.

3.5 Enrichment factor ~~(EF)~~

~~Briefly, the~~ EF values ranging from 0.1 to 10 ~~indicate~~represent significant input from crustal sources~~. Conversely, EF~~, whereas values ~~that larger than~~ of >10 ~~exhibit a~~indicate major ~~contribution~~contributions from anthropogenic ~~activities. Referring~~activity. According to ~~the~~our EF analysis (Fig. ~~8), the mean EF of Fe < 5 in each glacier can be assumed to customarily originate from crustal sources. Recent studies have also indicated~~8), mean values for Fe are less than 5 for all seven glaciers, suggesting a primarily crustal origin. This result supports the findings of previous studies in northern China (Wang et al., 2013) and North America (Doherty et al., 2014), which indicate that light-absorbing particles in snow are dominated by local soil dust~~ in some typical regions over northern China (Wang et al., 2013), and northern America (Doherty et al., 2014).~~

~~Comparable with Fe, the~~. Similar to Fe, other trace metals with ~~the~~ mean EF values of ⩾5.0 ~~were~~are moderately~~-~~-to~~-~~-highly enriched ~~from~~because of anthropogenic emissions (Hsu et al., 2010). For example, Pacyna and Pacyna (2001) reported that ~~fossil fuel~~Cr is derived chiefly from the combustion ~~is a major~~of fossil fuels, which is also a primary source of ~~Cr.~~ Cu~~ primarily originates from emissions from fossil fuel combustion and industrial processes, while~~. Pb and Zn, however, are ~~known~~linked to~~ be drawn from the~~ traffic-related ~~activities~~combustion and coal burning (Christian et al., 2010; Contini et al., 2014). ~~Hence~~In summary, the high EF values ~~observed~~ for Cu, Zn, and Cd in our ice samples ~~clearly suggested~~provide clear evidence that ~~the~~ TP glaciers ~~have already been polluted~~are being affected by ~~human activities, such as biomass burning, fossil fuel burning, and the coal burning~~anthropogenic pollution.

3.6 Source apportionment

~~Given the importance of the climate effect in our understanding of the ILAPs in TP glaciers, we applied a PMF receptor model to analyze the source attribution of ILAPs light absorption in these glaciers. In this study, the~~We employed mass concentrations of ~~the chemical components~~principal elements and ~~the~~ ILAPs~~ in ice associated~~, together with ~~the uncertainty datasets were used~~their respective uncertainties, to ~~run~~populate the PMF 5.0 model~~. The~~, the details of ~~the techniques have already been illustrated~~which are described by Hegg et al. (2009, 2010) and Pu et al. (2017). ~~The~~ ~~[Please check that this is your intended meaning.]~~ Model-derived factor loadings (defined as the apportionment of species mass to individual factors) for the ~~3~~three-factor solution of ~~the~~each source ~~profiles based on the PMF 5.0 model~~profile are ~~given~~shown in ~~Fig.~~Figure 9~~ (in~~, both as measured mass ~~concentration~~concentrations and the % total mass allocated to each factor~~). It was evident that the~~. The first factor (top panel) ~~was obviously characterized by~~exhibits relatively high loadings of Cl^-, Cl salt, SO_4^{2-}, and NO_3^-, which are well~~-~~-known markers for ~~the~~ urban and/or local industrial ~~pollutions~~pollution (Alexander et al., 2015). Although Cl^- and~~to~~ Na^+ ~~[“and”?]~~ are usually considered ~~as a~~ potential ~~product of emission source~~products of sea salt, ~~but also a~~ high ~~loading~~loadings of Cl^- relative to Cl salt~~, reflecting another~~ reflect a further source~~ in addition to sea salt~~, such as industrial ~~emission and~~emissions or coal combustion

(Hailin et al., 2008; Kulkarni, 2009). ~~Additionally, the highest loading~~High concentrations of NH_4^+ ~~is~~are also ~~suggested as an indicator of~~linked to coal combustion (Pang et al., 2007).

Compared with the first factor, Al (90.3%) and Fe (87.3%) ~~usually~~are generally regarded as ~~major~~chief indicators ~~for the~~of urban and/or regional ~~mineral dust~~MD (Pu et al., 2017~~). Therefore,~~), and the second factor ~~was easily interpretable~~ can therefore be readily interpreted as a natural ~~mineral dust~~MD source. ~~It was notable~~We note that C_{BC}^{max} ~~showed~~exhibits a high mass loading ~~in~~on this factor. Since both K^+ and $K_{Biosmoke}$ are ~~the major~~primary indicators of biomass burning (Zhang et al., 2013a~~). Therefore, it was easily interpretable that~~), we attribute the highest loadings of K^+ and $K_{Biosmoke}$ ~~were well representative for the biomass burning~~to this source (Fig. 9c). ~~However~~Nonetheless, the lowest mass loading of C_{BC}^{max} in this factor ~~is a bit~~was unexpected~~. Indeed, the~~, as C_{BC}^{max} is related not only ~~attributed~~ to ~~the~~ biomass burning ~~emission,~~ but also ~~associated with the industrial activities associated with the~~to local ~~mineral dust~~MD associated with industrial activity (Bond et al., 2006). ~~Therefore~~Consequently, we ~~interpreted~~interpret the third factor ~~normally considered a predominantly biomass burning product.~~ as representing primarily the burning of biomass. ~~[Please check that this is your intended meaning.]~~

~~Finally,~~

Figure 10 illustrates the chemical composition and mean ILAP source apportionment ~~of~~for the ~~ILAPs to the three sources in the~~seven TP glaciers ~~were given in Fig. 10. Note~~. We reiterate that the apportionment ~~was~~refers to the amount of ~~the~~ light ~~absorption~~absorbed by insoluble particles ~~in~~on the glacier surface ~~glaciers~~. On average, the observed source ~~appointment of the ILAPs in all TP glaciers~~apportionment by ~~mineral dust~~MD ~~was~~is close to 37.5%, ~~while the~~with industrial ~~emission~~emissions and biomass burning ~~contributed~~contributing 33.1% ~~[Please use one decimal place precision here, like the other two values in the sentence. Please be consistent throughout for each measure.]~~ and 29.4%, respectively. Specifically, the largest biomass ~~burning~~ contribution ~~of the~~to light~~-~~ absorption ~~of ILAPs was~~is found ~~in the~~on QY ~~glacier~~Glacier, which is located close to ~~the~~centres of human ~~activity regions~~land use (Guan et al., 2009; Li et al., 2016). ~~In the~~For MK, QM, GR, and XD glaciers, the ~~mineral dust~~MD contribution ~~of light absorption was much~~is significantly larger (>47.9%) than ~~that~~those of industrial pollution and biomass burning, ~~especially~~particularly in the case of MK ~~glacier~~Glacier. In these regions, the ~~percent~~percentage of

~~the ~~light absorption due to soil dust ~~ranged~~ranges from 20.4~~-~~% to 31.1%, ~~while the~~whereas light absorption ~~by~~due to biomass burning ~~was in the range of ~~is 18.5~~-~~% to 35.8%.

Industrial pollution ~~constituted~~is a major ~~fraction in the YZF glacier. Chemical analysis showed that the percentages of the chemical species in the~~component of apportionment for both YZF and MK glaciers~~ were much similar. The ~~, where the attribution of ~~the ~~total anions by chloride, nitrate, and sulphate ~~were~~is significantly higher than ~~the~~that of other chemical species~~ in the YZF and MK glaciers. In the~~. ~~[Please check that this is your intended meaning.]~~ On HRQ ~~glacier~~Glacier, the largest contribution of ~~the ~~sulphate ~~was up to~~is 45.4%. As ~~shown~~depicted in ~~Fig.~~Figure 10, the ~~source~~primary sources of ~~the ~~light absorption by insoluble surficial particles ~~in the surface glaciers was dominated by~~are ~~mineral dust~~MD and ~~the ~~industrial pollution~~ in most glaciers.~~. The ~~only~~sole exception ~~was the~~is YZF ~~glacier where~~Glacier, which exhibits a relatively large ~~fraction of~~ contribution from the ~~light absorption was due to biomass ~~burning ~~in the YZF glacier. These~~of biomass. Together, these results ~~were~~are highly consistent with ~~the~~those of previous studies (Andersson et al., 2015~~). They found~~), which reported that ~~the contributions of coal ~~BC deposited on TP glaciers is derived overwhelmingly from the combustion~~-sourced BC are the most significant for the TP glaciers~~ of coal.

4 Conclusions

~~In this study, the ILAPs observations in seven glacier regions across the Tibetan Plateau were presented using~~We employed the ISSW technique~~ along~~, coupled with chemical analysis~~.~~, to assess ILAPs at seven glacier sites on the Tibetan Plateau. Specifically, we analysed 67 vertical profiles ~~of~~in ice samples collected during both the ~~monsoon~~wet and ~~non-monsoon~~dry seasons ~~from~~between 2013~~-~~ and 2015~~ were analyzed. On~~. Our findings from HRQ, XD, and GR glaciers show that on average, ~~the ~~BC and OC concentrations ~~in the HRQ XD, and GR glacier during non-monsoon season ~~were several orders of magnitude higher during the dry season than ~~those in monsoon seasons. However, it~~during the wet season. It remains unclear~~ that~~, however, whether the ILAPs in the MK and YZF glaciers were comparable during the monsoon and non-monsoon seasons, ~~which could be investigated by future survey studies across these regions. By excluding some of the highest ~~and thus we suggest this as a suitable focus for future research. ~~[Please consider~~

~~rewording as your intended meaning is unclear.] After excluding anomalously high ILAPs values in the ice samples, thefrom our data set, we reported mass concentration ofconcentrations for BC, OC, and Fe ranged fromof 100–1000 ng g^{-1}, 10–2700 ng g^{-1}, and 10–1000 ng g^{-1}, respectively. Among the samples, the lower[Please check that this is your intended meaning.]~~ The lowest concentrations of BC ~~were found~~ in ~~the~~our data set originate from XD, HRQ and GR glaciers, ~~with the~~which give median concentrations of 33 ng g^{-1}, 24 ng g^{-1}, and 28 ng g^{-1}, respectively. ~~We found that the ILAPs in the ice samples was decreased from the top to the bottom in~~Moreover, we observed a pronounced decline in ILAP concentration with depth on XD ~~glacier due~~Glacier, which we attribute to ~~the~~ scavenging ~~effect during the non-monsoon season, while a opposite trend due to the washing effect by high temperature~~ during the ~~monsoon~~wet season. An opposite trend, driven by meltwater ‘washing’ effects, characterises the warmer wet season.

Both BC ~~played a dominant role~~and OC play central roles in particulate light absorption on TP glaciers, with average values ~~ranging from~~of ~44~~%~~–54% ~~in these glaciers, while~~and ~25~~%~~–46~~% for OC.~~%, respectively. By using a PMF receptor model, we ~~found~~ascertained that the ~~ILAPs across the~~ ILAP budget of northern ~~glaciers is heavy polluted due to human activities, but the major emissions~~ TP glaciers reflects a significant portion of ~~the light absorption by~~anthropogenic pollutants. The largest contributors of light-absorbing insoluble particles ~~in~~for TP glaciers ~~originated from the~~, however, include local ~~mineral dust~~MD and industrial pollution sources, followed by the ~~biomass~~ burning ~~source. Therefore, the~~of biomass. In summary, both natural ~~mineral dust~~MD ~~source~~ and anthropogenic ~~emission source are both~~emissions constitute non-negligible ~~to the~~sources of ILAPs ~~in the~~for TP glaciers.

Data availability. All datasets and codes used in this study can be obtained by contacting Xin Wang (wxin@lzu.edu.cn).

~~**5 Data availability**~~

The Supplement related to this article is available online at https://XXXX-supplement.

Author contributions. BX and MW designed the experiments. XW prepared the manuscript with contributions from all co-authors.

~~All datasets and codes used to produce~~in ~~this study can be obtained by contacting Xin Wang (wxin@lzu.edu.cn).~~

Competing interests. The authors declare that they have no conflicts of interest.

~~*Acknowledgements*. This research was supported by the Foundation for Innovative Research Groups of the National Natural Science Foundation of China (41521004), the National Natural Science Foundation of China under grant (~~~~(grants 41775144 and 41522505), and the Fundamental Research Funds for the Central Universities (lzujbky-2018-k02).~~**Acknowledgements.** This research was supported by the National Key Research and Development Program on Monitoring, Early Warning and Prevention of Major Natural Disaster (2018YFC1506005), the National Natural Science Foundation of China (grants 41775144, 41522505, 41771091, 41675065 and 41875091), and the Fundamental Research Funds for the Central Universities (lzujbky-2018-k02).

Edited by: Mark Flanner

Reviewed by: two anonymous referees

Table 1. Statistics of the ILAPs in each glacier measured using an ISSW spectrophotometer associated with the chemical analysis.

Region	Latitude	Longitude		C_{BC}^{equiv}	C_{BC}^{max}	C_{BC}^{est}	$f_{non\text{-}BC}^{est}$	$\mathring{A}_{tot}$	OC	AI	Fe
	(N)	(E)		(ng g^{-1})	(ng g^{-1})	(ng g^{-1})	(%)		(ppm)	(ppm)	(ppm)
Qiyi glacier	39°14’28”	97°45’27”	average	414	299	238 (116, 313)	42 (15, 66)	2.59	1.21	0.19	0.18
			median	176	128	94 (29, 124)	41 (17, 70)	2.62	0.66	0.08	0.09
			minimum	26	29	25 (13, 35)	21 (—, 53)	0.8	0.08	0.01	0.02
			maximum	2651	2230	1877 (1182, 2100)	73 (41, —)	3.73	11.59	3.35	2.41
Qiumianleiketage glacier	36°41’47”	90°43’44”	average	421	296	238 (139, 402)	44 (24, 81)	2.80	1.43	0.21	0.23
			median	307	215	172 (64, 218)	44 (24, 81)	2.76	1.06	0.15	0.18
			minimum	139	93	62 (19, 93)	37 (12, 64)	2.45	0.54	0.09	0.11
			maximum	995	662	558 (143, 678)	56 (27, 86)	3.08	3.97	0.55	0.63
Meikuang glacier	35°40’24”	94°11’10”	average	493	328	260 (119, 331)	42 (15, 37)	2.65	2.14	0.19	0.22
			median	197	156	133 (76, 153)	44 (16, 69)	2.64	0.61	0.09	0.13
			minimum	24	23	19 (17, 24)	16 (—, 17)	1.37	0.13	0.02	0.03
			maximum m	4696	2817	2292 (109, 2938)	62 (23, 85)	3.56	16.89	1.36	1.22
Yuzhufeng glacier	35°38’43”	94°13’36”	average	457	312	233 (94, 295)	51 (—, 37)	2.84	1.51	0.17	0.44
			median	317	201	160 (116, 204)	48 (26, 87)	2.95	1.02	0.10	0.21
			minimum	52	35	24 (8, 35)	15 (—, 37)	1.82	0.07	0.02	0.05
			maximum	2630	1608	1169 (72, 1603)	110 (6, 49)	3.7	9.16	0.81	3.51
Hariqin glacier	33°08’23” ”””””	92°05’34”	average	476	327	256 (100, 385)	48 (26, 82)	2.79	1.59	0.17	0.17
			median	54	37	23 (9, 30)	48 (26, 82)	2.87	0.22	0.04	0.05
			minimum	36	24	13 (4, 22)	19 (—, 41)	1.96	0.08	0.01	0.03
			maximum	3990	2702	2131 (682, 2784)	64 (32, 84)	3.52	9.64	1.11	1.05
Xiaodongkemadi	33°04’08”	92°04’24”	average	253	171	152 (76, 177)	37 (15, 63)	2.28	0.95	0.13	0.17

Region	Latitude	Longitude		C_{BC}^{equiv}	C_{BC}^{max}	C_{BC}^{est}	$f_{non\text{-}BC}^{est}$	$\mathring{A}_{tot}$	ISOC	Al	Fe
	(N)	(E)		(ng g^{-1})	(ng g^{-1})	(ng g^{-1})	(%)		(ppm)	(ppm)	(ppm)
			median	62	47	53 (37, 65)	36 (13, 59)	2.18	0.19	0.03	0.06
			minimum	13	12	9 (6, 18)	8 (—, 19)	1.08	0.01	0.01	0.01
			maximum	2770	1849	1637 (596, 2031)	86 (25, 90)	3.63	6.97	2.40	2.13
Gurenhekou glacier	30°11'17"	90°27'23"	average	382	292	247 (212, 591)	46 (16, 71)	2.42	0.62	0.15	0.18
			median	61	46	30 (19, 44)	48 (18, 75)	2.46	0.13	0.05	0.10
			minimum	28	23	15 (10, 24)	27 (7, 52)	1.34	0.02	0.01	0.03
			maximum	4674	3634	3080 (1876, 2884)	61 (26, 85)	2.92	5.22	1.35	0.91

Table 2. Statistics of the ILAPs in snow and ice in the studied TP glaciers and other related glaciers.

Glacier name	Sampling time	Season	Altitude/ m a.s.l.	BC (ng g^{-1})	OC (ng g^{-1})	MD (μg g^{-1})	Sample type	References
Qiyi	2005.7	Monsoon	4850	22±2	——	——	Snow pit	Ming et al., 2009
	2001.7-8	Monsoon	4600	6.65±3.3	87.52±37.59	——	Fresh snow	Xu et al., 2006
	2001.7-8	Monsoon	4600	52.64±17.83	195.5±85	——	Aged snow	Xu et al., 2006
	2013.8-9	Monsoon	4700	238±349	1210±2023	1.42±1.17	Ice	This study
Qiumianleiketage	2014.5	Non-monsoon	5300	238±168	1431±1130	2.92±2.09	Ice	This study
Meikuang	2001.7-8	Monsoon	5200	446	124	——	Surface snow	Xu et al., 2006
	2015.10	Monsoon	5050	290±241	3745±5100	5.27±6.81	Ice	This study
	2015.5	Non-monsoon	5050	250±468	1718±3639	1.85±2.38	Ice	This study
Yuzhufeng	2014,2015.10	Monsoon	5350	265±270	1596±2052	2.93±3.19	Ice	This study
	2014.5	Non-monsoon	5350	213±188	1421±1173	1.9±1.77	Ice	This study
Hariqin	2015.10	Monsoon	5650	91±126	930±1880	1.23±1.77	Ice	This study
	2015.5	Non-monsoon	5650	1077±1489	4860±6759	8.38±10.59	Ice	This study
Xiaodongkemadi	2014.8-2015.7	Monsoon	5400-5750	41.77±6.36	157.97±42.3	1.89±0.92	Fresh snow	Li et al., 2017
		Monsoon	5400-5750	246.84±118.3	611.45±467.7	39.43±24.35	Aged snow	Li et al., 2017
		Monsoon	5400-5750	3335±3767	9857±10923	880±1038	Granular ice	Li et al., 2017
	2015.10	Monsoon	5600	57±37	250±233	0.68±0.3	Ice	This study
	2013-2015.5	Non- monsoon	5600	178±381	1174±2014	2.18±6.15	Ice	This study
Gurenhekou	2015.10	Monsoon	5610	85±177	330±648	1.17±1.49	Ice	This study
	2014.5	Non-monsoon	5610	1116±1700	2148±2668	7.7±9.99	Ice	This study
Palong-Zanbu-	1998-2005	Monsoon	4800-5600	5.27±2.23	70.8±39.3	——	Ice core	Xu et al., 2009a
No. 4		Non-monsoon	4800-5600	11.51±4.7	97.5±49.9	——	Ice core	Xu et al., 2009a
Zuoqiupu	1956-2006	Monsoon	5100-5400	2.37±1.55	11.55±11.5	——	Ice core	Xu et al., 2009b
		Non-monsoon	5100-5400	8.33±3.29	26.71±13.74	——	Ice core	Xu et al., 2009b
Zhadang	2012.8	Monsoon	5500-5800	51.9±7.2	——	6.38±1.54	Snow pit	Qu et al., 2014
	2014.6	Monsoon	5800	79	515.08	——	Snow pit	Li et al., 2016
	2015.5	Non-monsoon	5790	303	822	——	Snow pit	Li et al., 2018
	2015.6-9	Monsoon	5570-5790	281	743	——	Surface snow	Li et al., 2018
Urumqi No.1	2004.7-8	Monsoon	4130	500	1200	——	Surface snow	Xu et al., 2012
	2013.8	Monsoon	3800-4100	30±5	——	17±6	Fresh snow	Ming et al., 2016
Muji	2012.6-10	Monsoon	4700-5500	375±3	175±15	——	Snow pit	Yang et al., 2015
Qiangyong	2001	——	5400	43.1	117.3	——	Surface snow	Xu et al., 2006
Kangwure	2001	——	6000	21.8	161.1	——	Surface snow	Xu et al., 2006
Namunani	2004	——	5780-6080	4.4±2.1	51.1±20.6	——	Surface snow	Xu et al., 2006
Demula	2014.5	Non-monsoon	5404	17	185	——	Snow pit	Li et al., 2016

Yulong	2015.5	Non-monsoon	4400-4800	372±58	2003±308	9.47±2.36	Aged snow	Niu et al., 2017
	2015.8	Monsoon	4400-4800	2309±125	3211±168	97.12±50.78	Aged snow	Niu et al., 2017
Laohugou No. 12	2015.8	Monsoon	4400-4800	2198±1004	2190±1203	114±67	Aged snow	Zhang et al., 2017
	2015.10	Non-monsoon	4400-4800	1218±212	504±50	63±2	Aged snow	Zhang et al., 2017

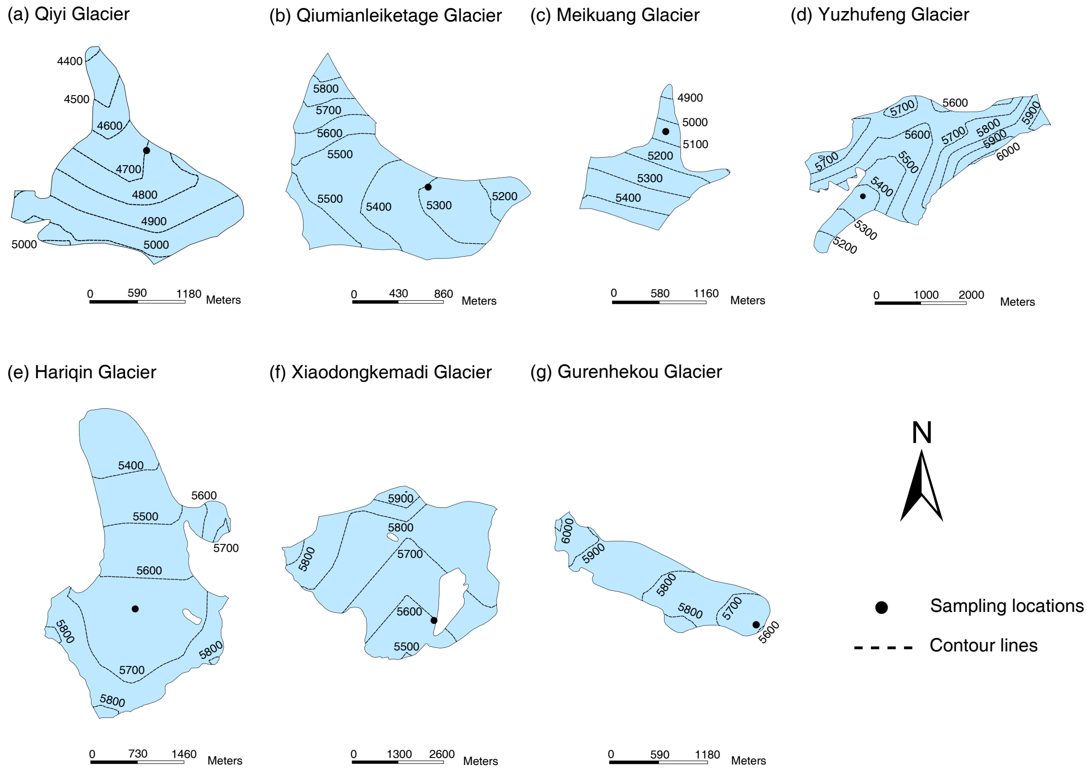

Figure 1. Geographical locations of (a) Qiyi ~~glacier (97.76° E,~~ Glacier (39.24°~~–~~N, 97.76°E), (b) Qiumianleiketage ~~glacier (90.73° E,~~ Glacier (36.70°~~-~~N, 90.73°E), (c) Meikuang ~~glacier (94.19° E,~~ Glacier (35.67°~~-~~N, 94.19°E), (d) Yuzhufeng ~~glacier (94.23° E,~~ Glacier (35.65°~~-~~N, 94.23°E), (e) Hariqin ~~glacier (92.09° E,~~ Glacier (33.14°~~-~~N, 92.09°E), (f) Xiaodongkemadi ~~glacier (92.07° E,~~ Glacier (33.07°~~-~~N, 92.07°E), (g) Gurenhekou ~~glacier (90.46° E,~~ Glacier (30.19°~~-~~N, 90.46°E). The black ~~dot is the~~ dots indicate sampling locations. ~~[Please note that the British spelling of 'metres' should be used in the scales for each glacier (instead of 'meters').]~~

Figure 2. The equipment for collecting new snow samples ~~in~~from the surfaces of the seven studied TP glaciers**.**

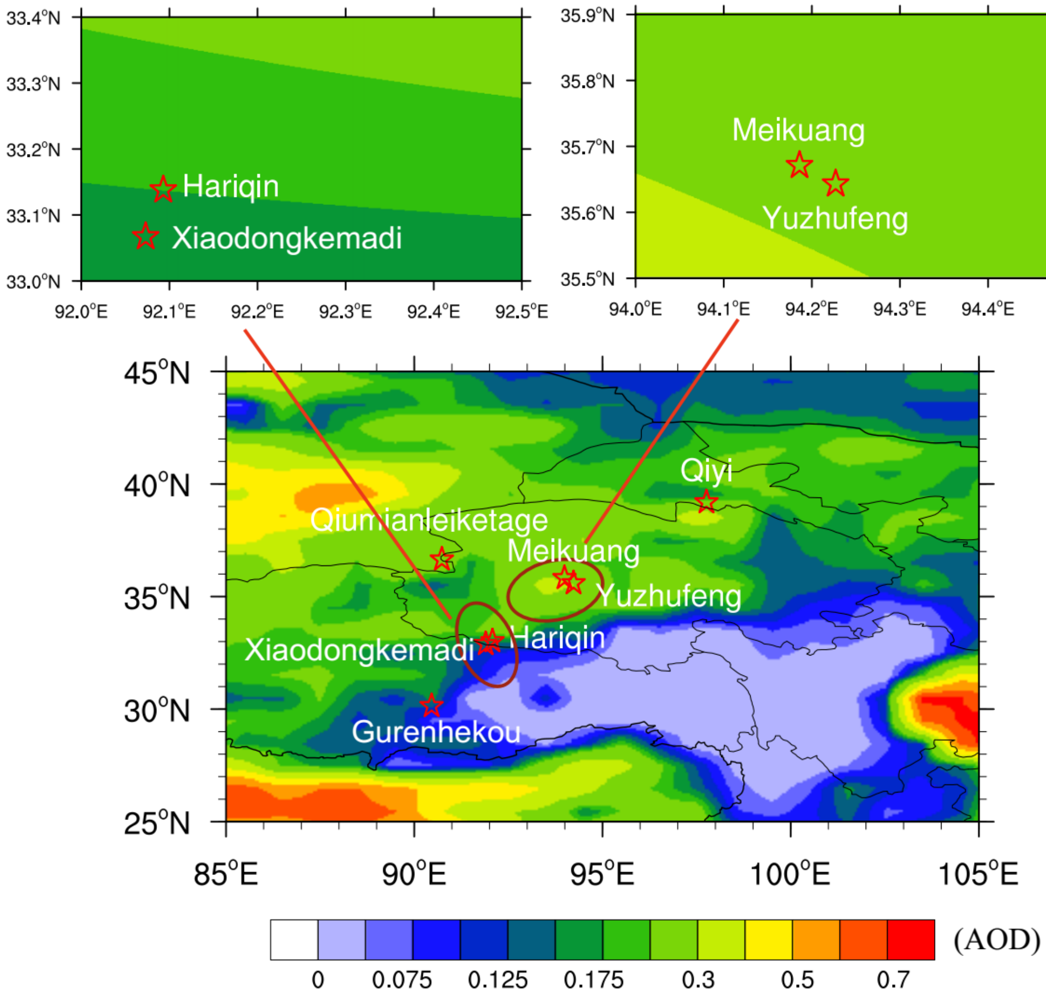

Figure 3. Spatial distribution of the averaged AOD over the TP between 2013 and 2015, retrieved from Aqua-MODIS at 500 nm ~~over Tibetan Plateau from 2013 to 2015.~~. The red stars ~~are the~~represent sampling locations (see also Table 1~~):~~).

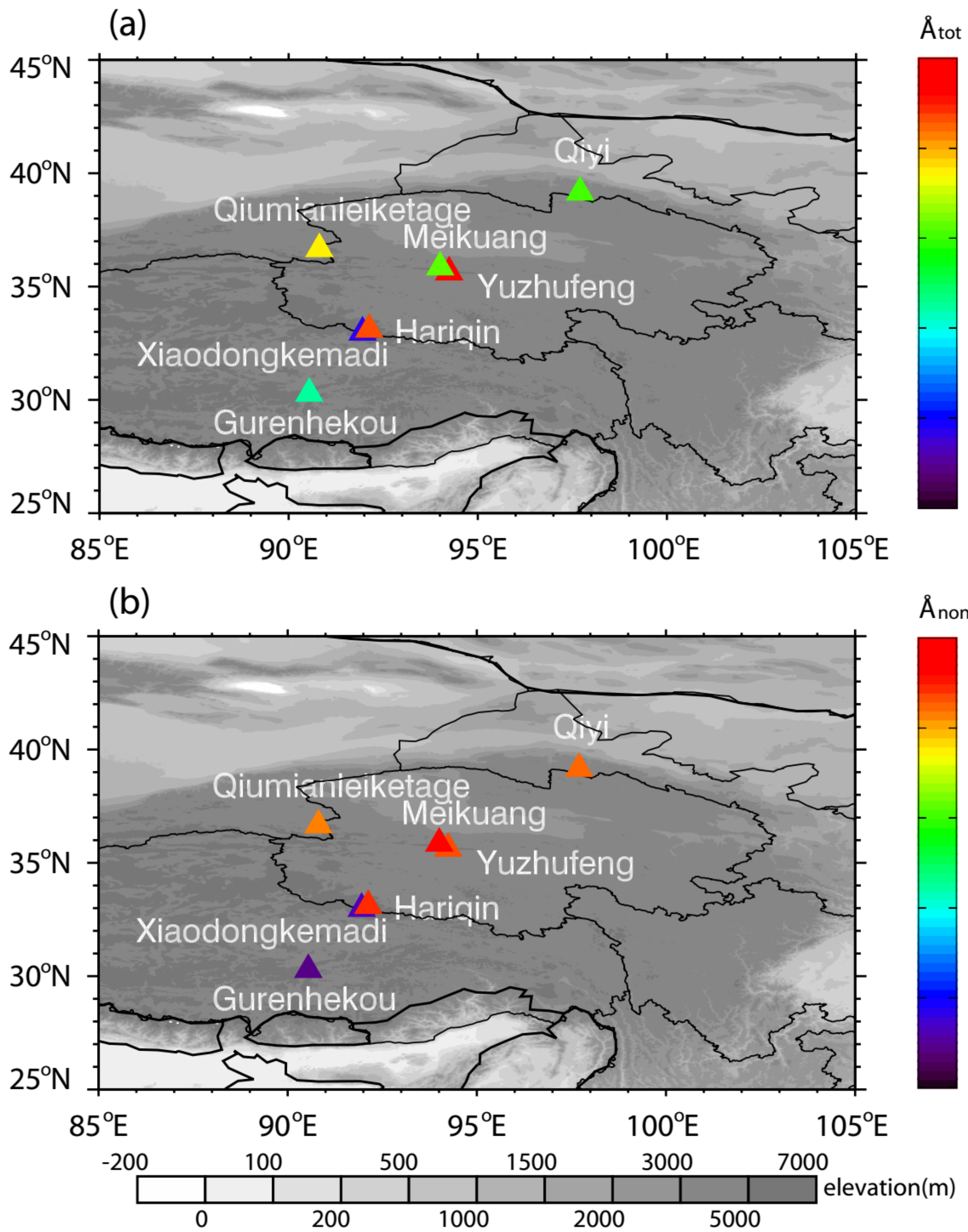

(a)
Åtot
3.0
2.8
2.6
2.4
2.2
2.0
45°N
40°N
35°N
30°N
25°N
85°E
90°E
95°E
100°E
105°E
Qiyi
Qiumianleiketage
Meikuang
Yuzhufeng
Hariqin
Xiaodongkemadi
Gurenhekou
(b)
Ånon-BC
5.2
5.0
4.8
4.6
4.4
4.2
45°N
40°N
35°N
30°N
25°N
85°E
90°E
95°E
100°E
105°E
Qiyi
Qiumianleiketage
Meikuang
Yuzhufeng
Hariqin
Xiaodongkemadi
Gurenhekou
-200
100
500
1500
3000
7000
elevation(m)
0
200
1000
2000
5000

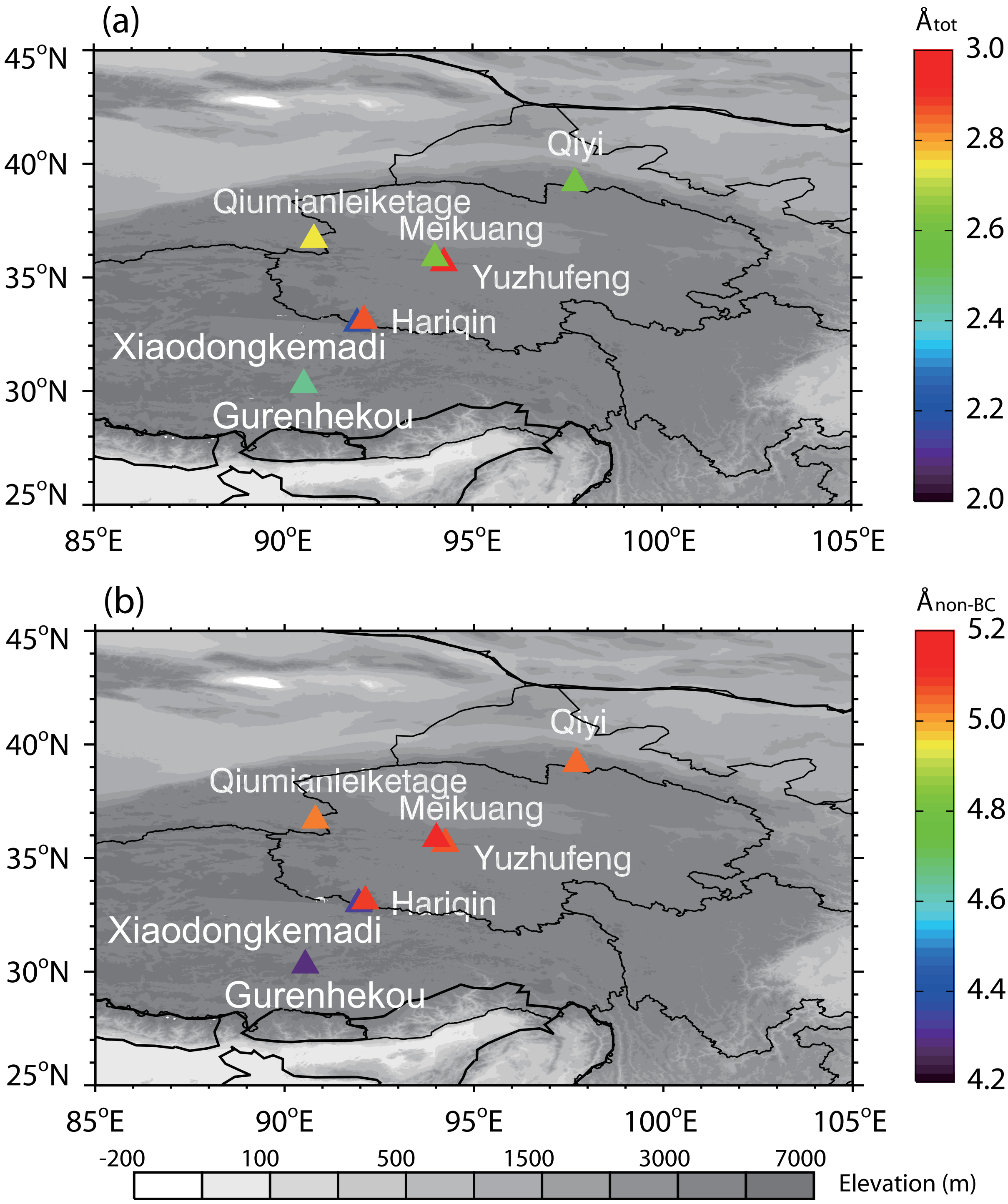

Figure 4. ~~The spatial~~Spatial distribution of the median absorption Ångström exponent for (a) total particulate constituents ($Å_{tot}$), and (b) non-BC particulate constituents ($Å_{non\text{-}BC}$) ~~in each glacier.~~ for each glacier. ~~[Please consider adding a space between the terms 'elevation' and '(m)' in your scale, both here and in Figures 7 and 10. Also, 'Elevation' is preferable to 'elevation'.]~~

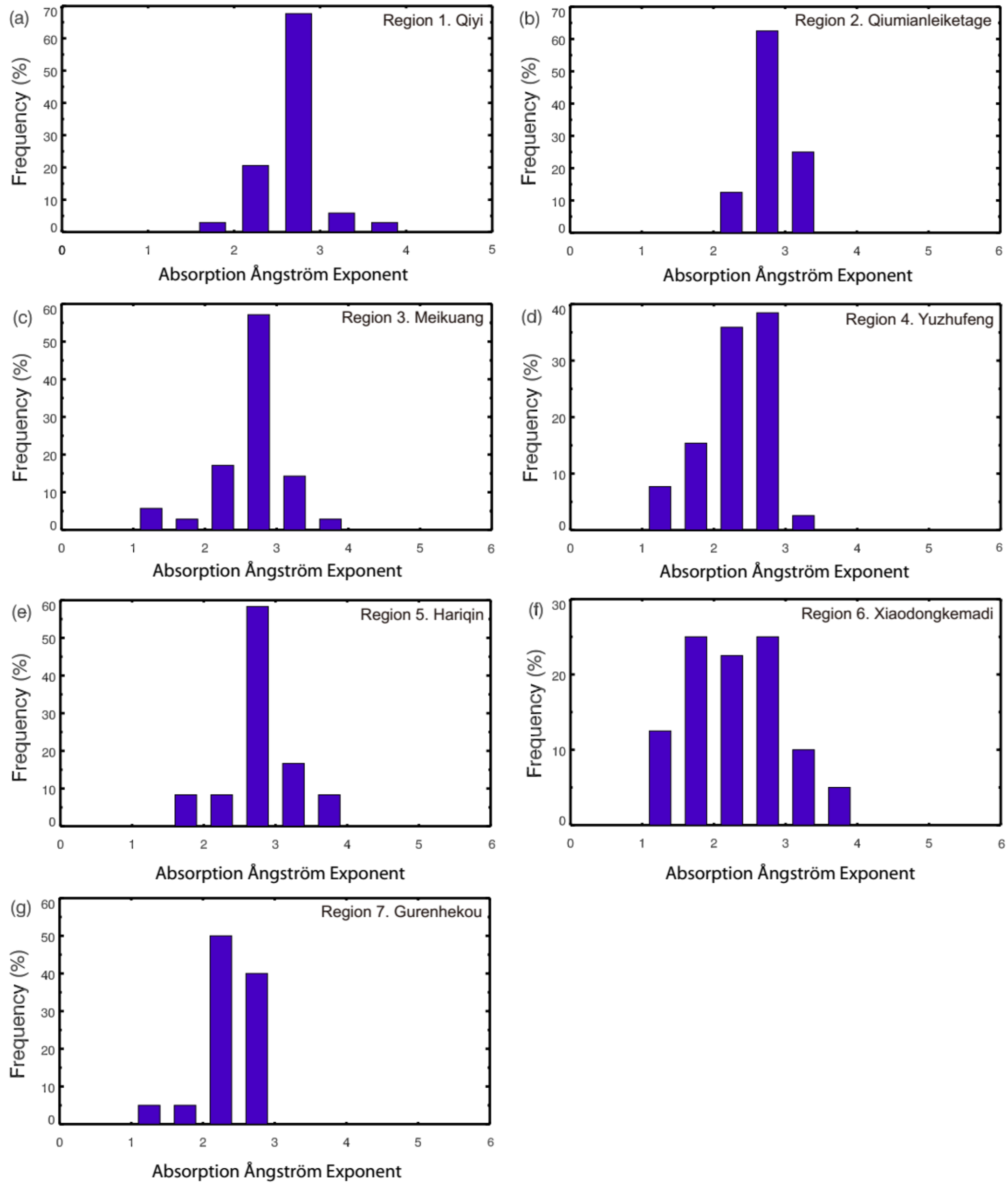

Figure 5. Histograms of the frequency of $\mathring{A}_{tot}$ (450~~-~~–600 nm) ~~for~~in ice ~~samples in~~from each ~~of the~~ glacier ~~region~~. Samples from all vertical profiles are included.

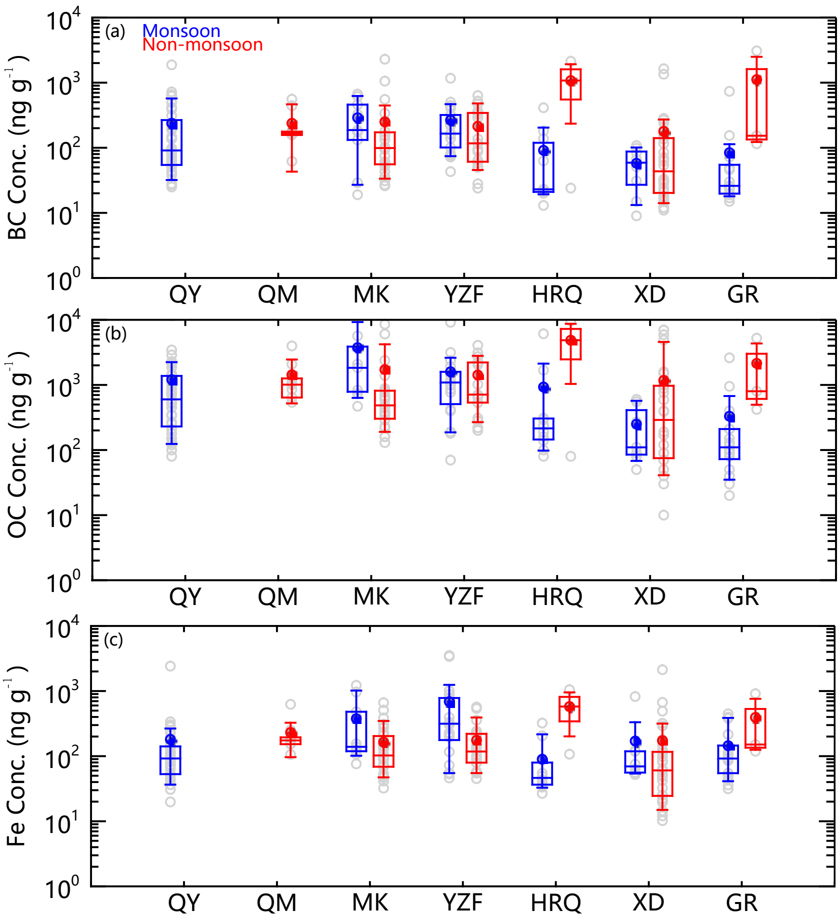

Figure 6. Box plots ~~of~~depicting the regional ~~variations~~variability in (a) BC concentration, (b) ISOC concentration, and (c) Fe concentration ~~of~~on the seven glaciers. ~~Error~~ The solid dots represent the average ILAP concentrations for each glacier, and the bars ~~are~~represent the 10th, 25th, median, 75th, and 90th percentiles of the data. ~~The dot symbol represents the average concentrations of the ILAPs in ice samples in each glacier.~~ ~~[Please check that this is your intended meaning.]~~

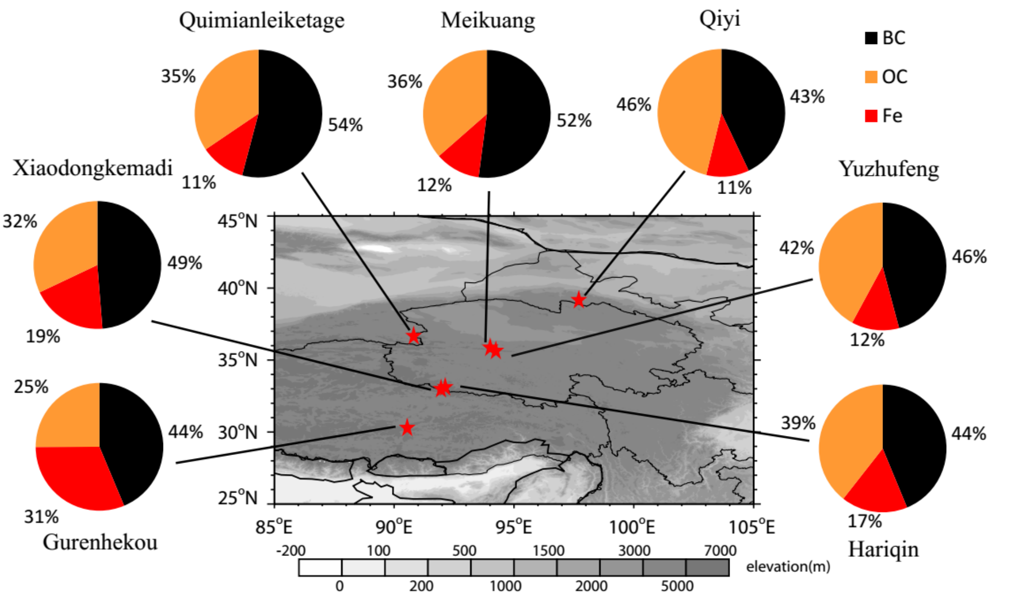

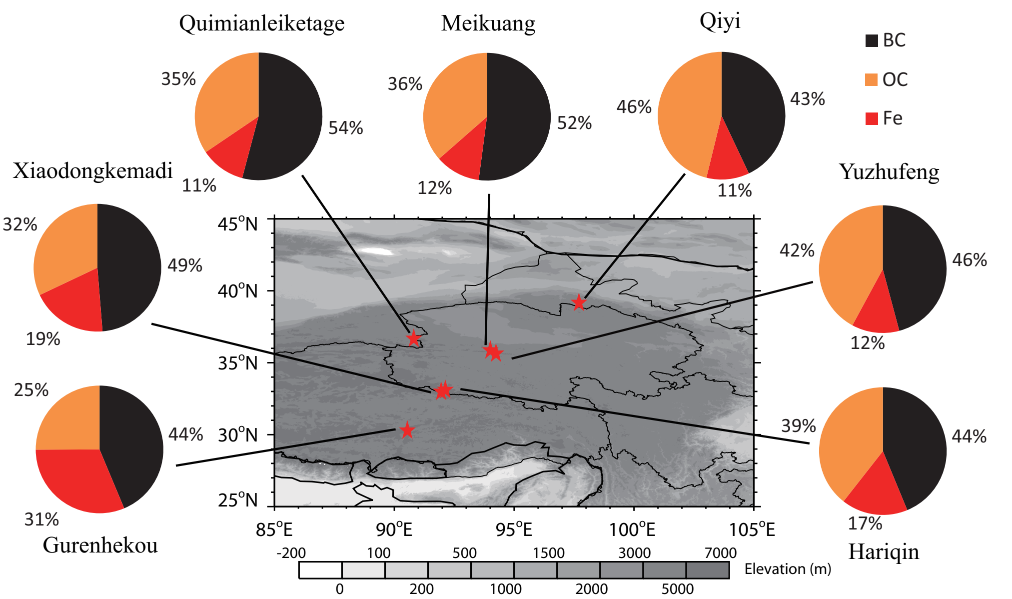

Figure 7. The median ~~of~~ relative contributions of BC, OC, and Fe to ~~total~~ light absorption ~~by BC, OC, and Fe~~ for ~~ice samples in~~ each glacier.

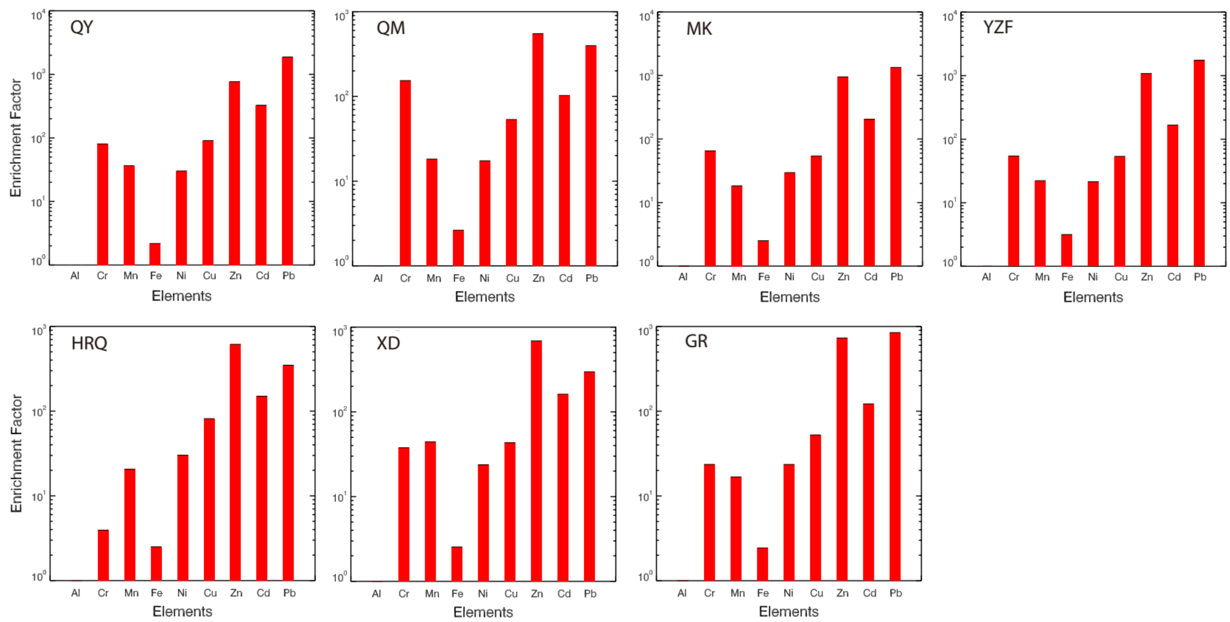

Figure 8. ~~Average~~The average enrichment factors of trace metals in surface-~~-~~ice samples ~~at~~from each ~~region~~glacier.

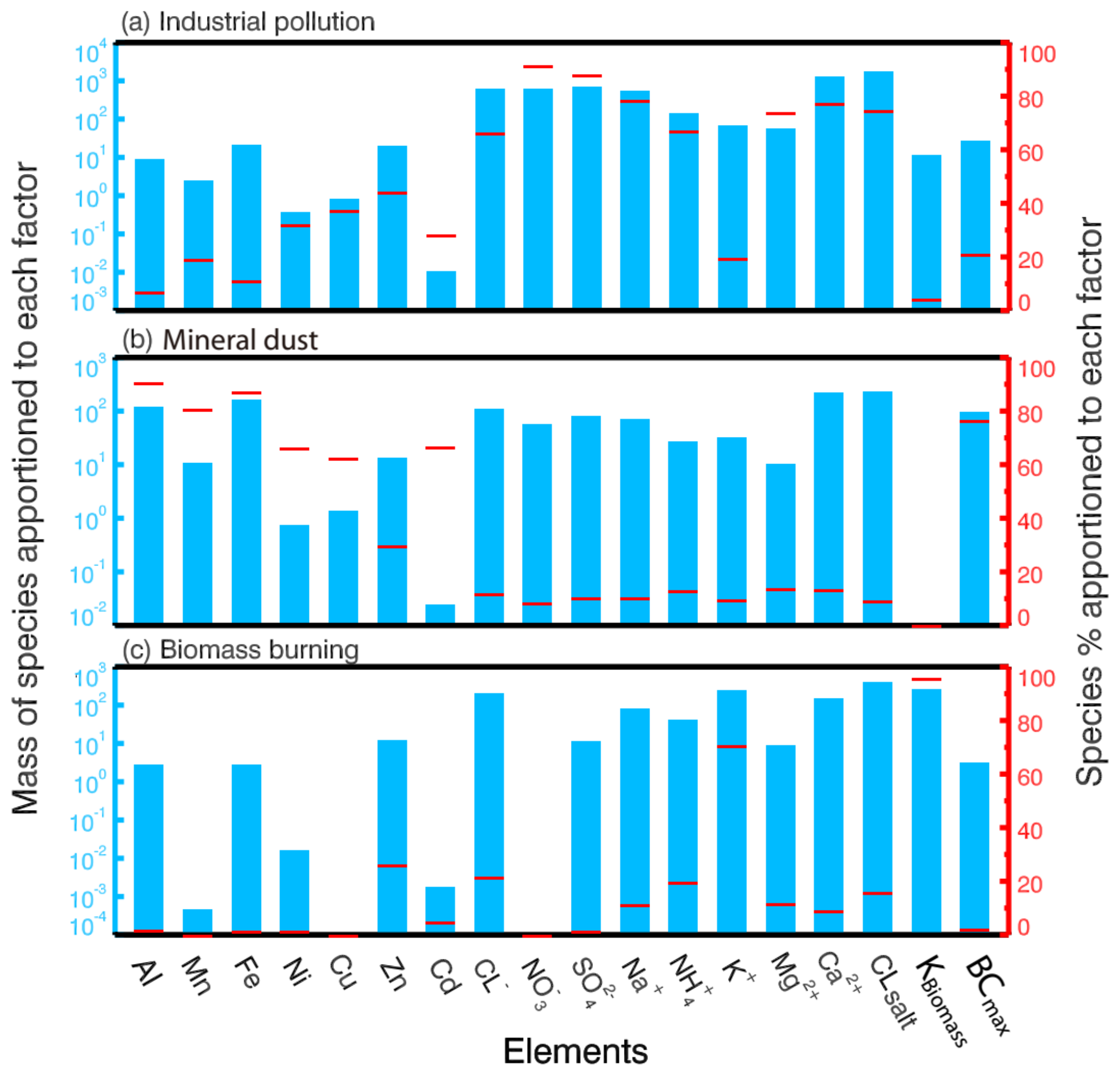

Figure 9. Source profiles for the three factors/sources that were resolved by the PMF 5.0 model. The blue columns and red horizontal bars depict the mass and percentage of the relative species, respectively. ~~[Consider explaining/defining what the blue columns and red horizontal bars depict.]~~

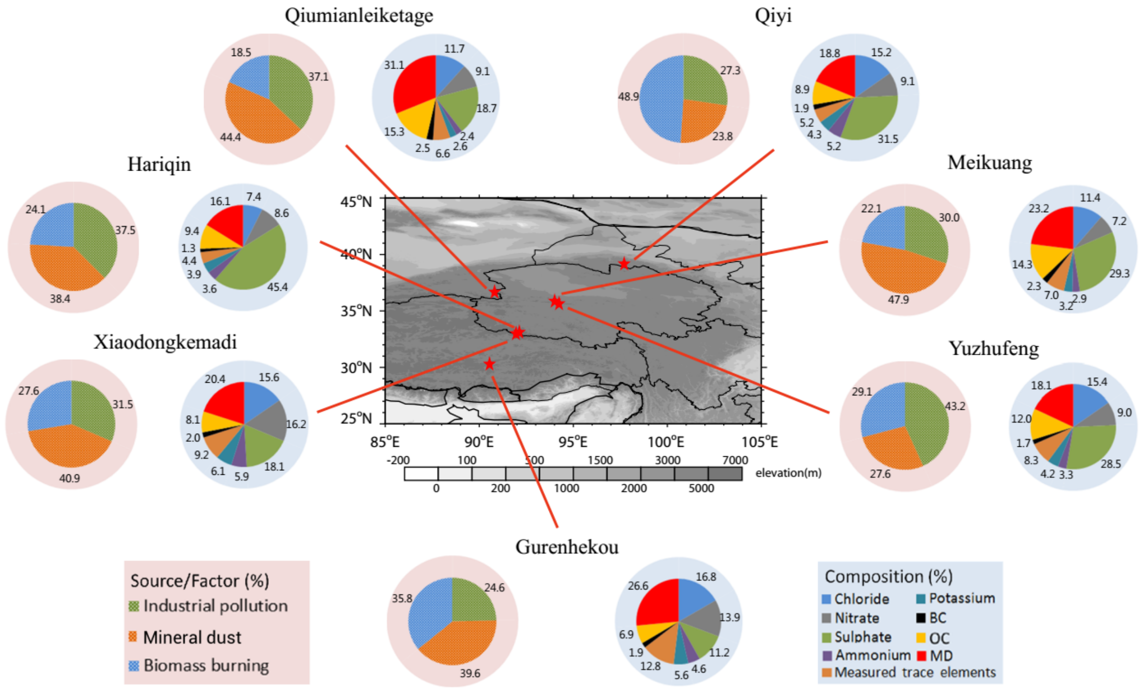

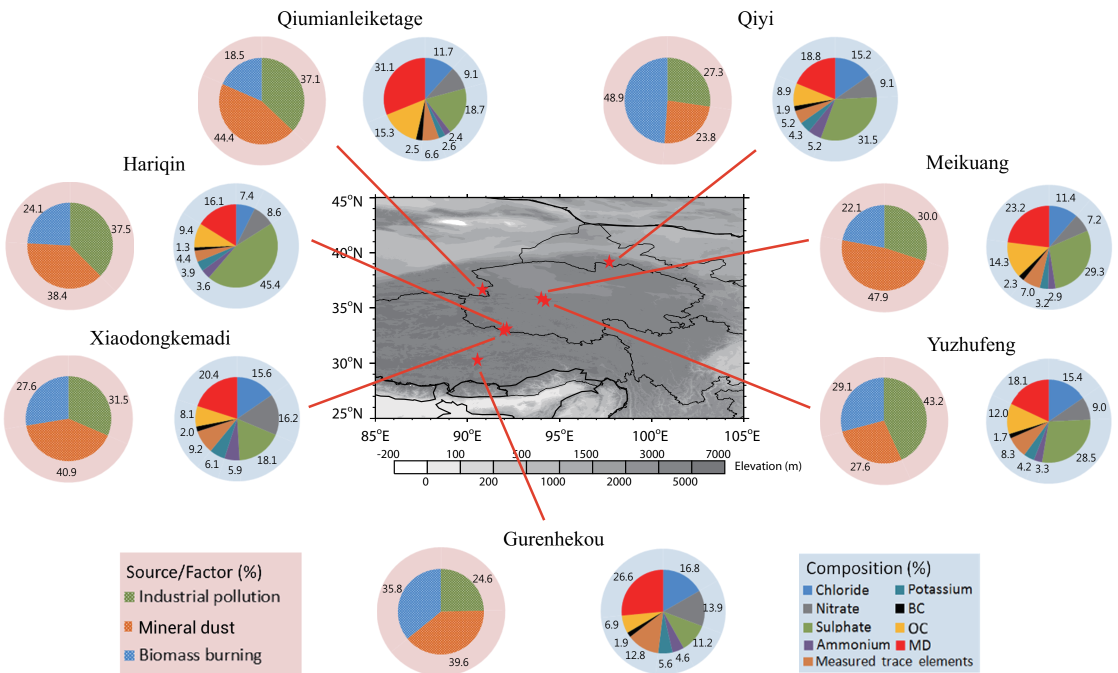

Figure 10. Chemical composition and source apportionment for the seven TP glaciers~~ in the TP regions.~~. Note that the apportionment ~~is of~~applies to the light ~~absorption~~absorbed by insoluble particles ~~in~~on the ~~surface glaciers~~glacier surfaces.

References

Alexander, B., and Mickley, L. J.: Paleo-perspectives on potential future changes in the oxidative capacity of the atmosphere due to climate change and anthropogenic emissions, Current Pollution Reports, 1, 57-69, 2015.

Alfaro, S. C., Lafon, S., Rajot, J. L., Formenti, P., Gaudichet, A., and Maille, M.: Iron oxides and light absorption by pure desert dust: An experimental study, J. Geophys. Res.-Atmos., 109, Artn D08208, 10.1029/2003jd004374, 2004.

Bergstrom, C.: Measuring the value and prestige of scholarly journals, College and Research Libraries News, 68, 314-316, 2007.

Bolch, T., Yao, T., Kang, S., Buchroithner, M. F., Scherer, D., Maussion, F., Huintjes, E., and Schneider, C.: A glacier inventory for the western Nyainqentanglha Range and the Nam Co Basin, Tibet, and glacier changes 1976–2009, The Cryosphere, 4, 419-433, https://doi.org/10.5194/tc-4-419-2010, 2010.

Bond, T. C., and Bergstrom, R. W.: Light absorption by carbonaceous particles: An investigative review, Aerosol Sci. Technol., 40, 27-67, 2006.

Bond, T. C., Doherty, S. J., Fahey, D. W., et al.: Bounding the role of black carbon in the climate system: A scientific assessment, J. Geophys. Res.-Atmos., 118, 5380-5552, 2013.

Brandt, R. E., Warren, S. G., and Clarke, A. D.: A controlled snowmaking experiment testing the relation between black carbon content and reduction of snow albedo, J. Geophys. Res.-Atmos., 116, Artn D08109, 10.1029/2010jd015330, 2011.

Christian, T. J., Yokelson, R. J., Cárdenas, B., Molina, L. T., Engling, G., and Hsu, S. C.: Trace gas and particle emissions from domestic and industrial biofuel use and garbage burning in Central Mexico, Atmos. Chem. Phys., 10, 565-584, 2010.

Chylek, P., Ramaswamy, V. & Srivastava, V.: Graphitic carbon content ofaerosols, clouds and snow, and its climatic implications, Sci. Total Environ., 36, 117–120, 1984.

Cong, Z., Gao, S., Zhao, W., Wang, X., Wu, G., Zhang, Y., Kang, S., Liu, Y., and Ji, J.: Iron oxides in the cryoconite of glaciers on the Tibetan Plateau: abundance, speciation and implications, The Cryosphere, 12, 3177-3186, 10.5194/tc-12-3177-2018, 2018.

Cong, Z. Y., Kang, S. C., Smirnov, A., and Holben, B.: Aerosol optical properties at Nam Co, a remote site in central Tibetan Plateau, Atmos. Res., 92, 42-48, 10.1016/J.Atmosres.2008.08.005, 2009.

Cong, Z. Y., Kang, S. C., Zhang, Y. L., and Li, X. D.: Atmospheric wet deposition of trace elements to central Tibetan Plateau, Appl. Geochem., 25, 1415-1421, 2010.

Cong, Z., Kang, S., Kawamura, K., Liu, B., Wan, X., Wang, Z., Gao, S., and Fu, P.: Carbonaceous aerosols on the south edge of the Tibetan Plateau: concentrations, seasonality and sources, Atmos. Chem. Phys., 15, 1573-1584, 2015.

Contini, D., Cesari, D., Genga, A., Siciliano, M., Ielpo, P., and Guascito, M. R.: Source apportionment of size-segregated atmospheric particles based on the major water-soluble components in Lecce (Italy), Sci. Total Environ., 472, 248-261, 2014.

Conway, H., Gades, A., and Raymond, C. F.: Albedo of dirty snow during conditions of melt, Water Resour. Res., 32, 1713-1718, 10.1029/96wr00712, 1996.

Dang, C., and Hegg, D. A.: Quantifying light absorption by organic carbon in Western North American snow by serial chemical extractions, J. Geophys. Res.-Atmos., 119, 10.1002/2014jd022156, 2014.

Doherty, S. J., Warren, S. G., Grenfell, T. C., Clarke, A. D., and Brandt, R. E.: Light-absorbing impurities in Arctic snow, Atmos. Chem. Phys., 10, 11647-11680, 2010.

Doherty, S. J., Grenfell, T. C., Forsström, S., Hegg, D. L., Brandt, R. E., and Warren, S. G.: Observed vertical redistribution of black carbon and other insoluble light-absorbing particles in melting snow, J. Geophys. Res.-Atmos., 118, 5553-5569, 2013.

Doherty, S. J., Dang, C., Hegg, D. A., Zhang, R. D., and Warren, S. G.: Black carbon and other light-absorbing particles in snow of central North America, J. Geophys. Res.-Atmos., 119, 12807-12831, 2014.

Engling, G. and Gelencser, A.: Atmospheric Brown Clouds: From Local Air Pollution to Climate Change, Elements, 6, 223-228, 2010.

Federer, U., Kaufmann, P. R., Hutterli, M., Schüpbach, S., and Stocker, T. F.: Continuous flow analysis of total organic carbon in polar ice cores, Environ. Sci. Technol., 42, 8039–8043, 2008.

Fialho, P., Hansen, A. D. A., and Honrath, R. E.: Absorption coefficients by aerosols in remote areas: a new approach to decouple dust and black carbon absorption coefficients using seven-wavelength Aethalometer data, J. Aerosol Sci., 36, 267-282, 2005.

Flanner, M. G., Zender, C. S., Randerson, J. T., and Rasch, P. J.: Present-day climate forcing and response from black carbon in snow, J. Geophys. Res.-Atmos., 112, D11202, doi: 10.1029/2006jd008003, 2007.

Flanner, M. G., Zender, C. S., Hess, P. G., Mahowald, N. M., Painter, T. H., Ramanathan, V., and Rasch, P. J.: Springtime warming and reduced snow cover from carbonaceous particles, Atmos. Chem. Phys., 9, 2481-2497, 2009.

Grenfell, T. C., Doherty, S. J., Clarke, A. D., and Warren, S. G.: Light absorption from particulate impurities in snow and ice determined by spectrophotometric analysis of filters, Appl. Opt., 50, 2037-2048, 2011.

Guan, X., Huang, J., Guo, N., Bi, J., and Wang, G.: Variability of soil moisture and its relationship with surface albedo and soil thermal parameters over the Loess Plateau, Adv. Atmos. Sci., 26, 692-700, 2009.

Hadley, O. L., and Kirchstetter, T. W.: Black-carbon reduction of snow albedo, Nat. Clim. Change, 2, 437-440, 2012.

Hansen, J., and Nazarenko, L.: Soot climate forcing via snow and ice albedos, P. Natl. Acad. Sci. USA, 101, 423-428, 2004.

Hegg, D. A., Warren, S. G., and Grenfell, T. C.: Source attribution of black carbon in Arctic snow, Environ. Sci. Technol., 43, 4016-4021, 2009.

Hegg, D. A., Warren, S. G., and Grenfell, T. C.: Sources of light-absorbing aerosol in arctic snow and their seasonal variation, Atmos. Chem. Phys., 10, 10923-10938, 2010.

Hsu, S. C., Liu, S. C., Arimoto, R., et al.: Effects of acidic processing, transport history, and dust and sea salt loadings on the dissolution of iron from Asian dust, J. Geophys. Res.-Atmos., 115, 2010.

Huang, J., Li, Y. F., Li, Z., and Xiong, L. F.: Spatial variations and sources of trace elements in recent snow from glaciers at the Tibetan Plateau, Environ. Sci. Pollut. R., 25, 7875-7883, 2018.

Huang, J. P., Fu, Q., Zhang, W., Wang, X., Zhang, R. D., Ye, H., and Warren, S. G.: Dust and Black Carbon in Seasonal Snow across Northern China, Bull. Amer. Meteor. Soc., 92, 175-181, 2011.

Jenkins, M., Kaspari, S., Kang, S. C., Grigholm, B., and Mayewski, P. A.: Tibetan plateau geladaindong black carbon ice core record (1843-1982): recent increases due to higher emissions and lower snow accumulation, Advances in Climate Change Research, 7(3), 132-138, 2016.

Jeong, D., Kim, K., and Choi, W.: Accelerated dissolution of iron oxides in ice, Atmos. Chem. Phys., 12, 11125-11133, 10.5194/acp-12-11125-2012, 2012.

Kang, S., Chen, F., Gao, T., Zhang, Y., Yang, W., Yu, W., and Yao, T.: Early onset of rainy season suppresses glacier melt: a case study on Zhadang glacier, Tibetan Plateau, J. Glaciol., 55(192), 755–758, 2009.

Kaspari, S., Painter, T. H., Gysel, M., Skiles, S. M., and Schwikowski, M.: Seasonal and elevational variations of black carbon and dust in snow and ice in the Solu-Khumbu, Nepal and estimated radiative forcings, Atmos. Chem. Phys., 14, 8089-8103, 2014.

Kirchstetter, T. W., Novakov, T., Hobbs, P. V.: Evidence that the spectral dependence of light absorption by aerosols is affected by organic carbon, J. Geophys. Res.-Atmos., 109, D21, 10.1029/2004JD004999, 2004.

Kulkarni, S.: Assessment of source-receptor relationships of aerosols: an integrated forward and backward modeling approach, Dissertations and Theses-Gradworks, 2009.

Lafon, S., Rajot, J. L., Alfaro, S. C., and Gaudichet, A.: Quantification of iron oxides in desert aerosol, Atmos. Environ., 38, 1211-1218, 10.1016/J.Atmosenv.2003.11.006, 2004.

Lafon, S., and Lee, A. B.: Diffusion maps and coarse-graining: a unified framework for dimensionality reduction, graph partitioning and data set parameterization, IEEE T. Pattern anal., 28, 1393-1403, 2006.

Li C. L., Kang S. C., Zhang Q.: Elemental composition of Tibetan Plateau top soils and its effect on evaluating atmospheric pollution transport, Environ. Pollut., 157, 8-9, 2009.

Li, C. L., Bosch, C., Kang, S. C., Andersson, A., Chen, P. F., Zhang, Q. G., Cong, Z. Y.,Chen, B., Qin, D. H., and Gustafsson, O.: Sources of black carbon to the Himalayan-Tibetan Plateau glaciers, Nat. Commun., 7, 12574, 10.1038/ncomms12574, 2016.

Liou, K. N., Takano, Y., and Yang, P.: Light absorption and scattering by aggregates: Application to black carbon and snow grains, J. Quant. Spectrosc. Ra., 112, 1581-1594, 10.1016/J.Jqsrt.2011.03.007, 2011.

Liu S. Y., Guo, W. Q., Xu J. L., et al.: The Second Glacier Inventory Dataset of China (Version 1.0), Cold and Arid Regions Science Data Center at Lanzhou, 10.3972/glacier.001.2013.db, 2014.

Lüthi, Z. L., Škerlak, B., Kim, S.-W., Lauer, A., Mues, A., Rupakheti, M., and Kang, S.: Atmospheric brown clouds reach the Tibetan Plateau by crossing the Himalayas, Atmos. Chem. Phys., 15, 6007-6021, https://doi.org/10.5194/acp-15-6007-2015, 2015.

Millikan, R. C.: Optical properties of soot, J. Opt. Soc. Am., 51, 698-699, 1961.

Ming, J., Xiao, C. D., Du, Z. C., and Yang, X. G.: An overview of black carbon deposition in High Asia glaciers and its impacts on radiation balance, Adv. Water Resour., 55, 80-87, 2013.

Ming, J., Xiao, C. D., Sun, J. Y., Kang, S. C., and Bonasoni, P.: Carbonaceous particles in the atmosphere and precipitation of the Nam Co region, central Tibet, J. Environ. Sci., 22, 1748-1756, 10.1016/S1001-0742(09)60315-6, 2010.

Moosmuller, H., Engelbrecht, J. P., Skiba, M., Frey, G., Chakrabarty, R. K., and Arnott, W. P.: Single scattering albedo of fine mineral dust aerosols controlled by iron concentration, J. Geophys. Res.-Atmos., 117, Artn D11210, 10.1029/2011jd016909, 2012.

Paatero, P., and Tapper, U.: Positive matrix factorization: a non-negative factor model with optimal utilization of error estimates of data values, Environmetrics, 5, 111-126, 1994.

Pacyna, J. M. and Pacyna, E. G.: An assessment of global and regional emissions of trace metals to the atmosphere from anthropogenic sources worldwide, Environ. Rev., 9, 269-298, 2001.

Painter, T. H., Barrett, A. P., Landry, C. C., Neff, J. C., Cassidy, M. P., Lawrence, C. R., McBride, K. E., and Farmer, G. L.: Impact of disturbed desert soils on duration of mountain snow cover, Geophys. Res. Lett., 34, L12502, 10.1029/2007gl030284, 2007.

Painter, T. H., Deems, J. S., Belnap, J., Hamlet, A. F., Landry, C. C., and Udall, B.: Response of Colorado River runoff to dust radiative forcing in snow, P. Natl. Acad. Sci. USA, 107, 17125-17130, 2010.

Painter, T. H., Bryant, A. C., and Skiles, S. M.: Radiative forcing by light absorbing impurities in snow from MODIS surface reflectance data, Geophys. Res. Lett., 39, L17502, 10.1029/2012gl052457, 2012.

Pang, H., He, Y., Theakstone, W. H., and Zhang, D. D.: Soluble ionic and oxygen isotopic compositions of a shallow firn profile, Baishui glacier No. 1, southeastern Tibetan Plateau, Ann. Glaciol., 46, 325-330, 2007.

Pio, C. A., Legrand, M., Oliveira, T., Afonso, J., Santos, C., Caseiro, A., Fialho, P., Barata, F., Puxbaum, H., Sanchez-Ochoa, A., Kasper-Giebl, A., Gelencser, A., Preunkert, S., and Schock, M.: Climatology of aerosol composition (organic versus inorganic) at nonurban sites on a west-east transect across Europe, J. Geophys. Res., 112, D23S02, 10.1029/2006JD008038, 2007.

Preunkert, S., Legrand, M., Stricker, P., Bulat, S., Alekhina, I., Petit, J. R., Hoffmann, H., May, B., and Jourdain B.: Quantification of Dissolved Organic Carbon at very low levels in natural ice samples by a UV induced oxidation method, Environ. Sci. Technol., 45, 673–678, 2011.

Pu, W., Wang, X., Wei, H. L., Zhou, Y., Shi, J. S., Hu, Z. Y., Jin, H. C., and Chen, Q. L.: Properties of black carbon and other insoluble light-absorbing particles in seasonal snow of northwestern China, The Cryosphere, 11, 1213-1233, 2017.

Qian, Y., Flanner, M. G., Leung, L. R., and Wang, W.: Sensitivity studies on the impacts of Tibetan Plateau snowpack pollution on the Asian hydrological cycle and monsoon climate, Atmos. Chem. Phys., 11, 1929-1948, 2011.

Qian, Y., Yasunari, T. J., Doherty, S. J., Flanner, M. G., Lau, W. K. M., & Jing, M.: Light-absorbing particles in snow and ice: measurement and modeling of climatic and hydrological impact, Adv. Atmos. Sci., 32, 64-91, 2015.

Qin, D. H., Liu, S. Y., and Li, P. J.: Snow cover distribution, variability, and response to climate change in western China, J. Climate, 19, 1820-1833, 2006.

Qiu, J.: The third pole, Nature, 454, 393-396, 10.1038/454393a, 2008.

Ramanathan, V., Li, F., Ramana, M. V., et al.: Atmospheric brown clouds: Hemispherical and regional variations in long-range transport, absorption, and radiative forcing, J. Geophys. Res., 112, D22S21, 10.1029/2006JD008124, 2007.

Sand, M., Berntsen, T. K., Seland, O., and Kristjansson, J. E.: Arctic surface temperature change to emissions of black carbon within Arctic or midlatitudes, J. Geophys. Res.-Atmos., 118, 7788-7798, 10.1002/Jgrd.50613, 2013.

Skiles, S. M., Painter, T. H., Deems, J. S., Bryant, A. C., and Landry, C. C.: Dust radiative forcing in snow of the Upper Colorado River Basin: 2. Interannual variability in radiative forcing and snowmelt rates, Water Resour. Res., 48, 10.1029/2012wr011986, 2012.

Takahashi, Y., Higashi, M., Furukawa, T., and Mitsunobu, S.: Change of iron species and iron solubility in Asian dust during the long-range transport from western China to Japan, Atmos. Chem. Phys., 11, 11237-11252, 10.5194/acp-11-11237-2011, 2011.

Wang, M., Xu, B., Cao, J., et al.: Carbonaceous aerosols recorded in a southeastern Tibetan glacier: analysis of temporal variations and model estimates of sources and radiative forcing, Atmos. Chem. Phys., 15, 1191-1204, 10.5194/Acp-15-1191-2015, 2015.

Wang, X., Doherty, S. J., and Huang, J. P.: Black carbon and other light-absorbing impurities in snow across Northern China, J. Geophys. Res.-Atmos., 118, 1471-1492, 2013.

Wang, X., Xu, B. Q., and Ming, J.: An overview of the studies on Black Carbon and Mineral Dust deposition in Snow and Ice Cores in East Asia, J. Meteorol. Res., 28, 354-370, 2014.

Wang, X., Pu, W., Ren, Y., Zhang, X., Zhang, X., Shi, J., Jin, H., Dai, M., and Chen, Q.:

Observations and model simulations of snow albedo reduction in seasonal snow due to insoluble light-absorbing particles during 2014 Chinese survey, Atmos. Chem. Phys., 17, 2279-2296, 2017.

Warren, S. G., and Wiscombe, W. J.: A Model for the Spectral Albedo of Snow. Ⅱ: Snow Containing Atmospheric Aerosols, J. Atmos. Sci., 37, 2734-2745, 1980.

Warren, S. G.: Optical-Properties of Snow, Rev. Geophys., 20, 67-89, 1982.

Warren, S. G., and Wiscombe, W. J.: Dirty Snow after Nuclear-War, Nature, 313, 467-470, 10.1038/313467a0, 1985.

Wedepohl, K. H.: The Composition of the Continental-Crust, Geochim. Cosmochim. Ac., 59, 1217-1232, 1995.

Xu, B. Q., Yao, T. D., Liu, X. Q., and Wang, N. L.: Elemental and organic carbon measurements with a two-step heating-gas chromatography system in snow samples from the Tibetan Plateau, Ann. Glaciol., 43, 257-262, 2006.

Xu, B. Q., Cao, J. J., Hansen, J., Yao, T. D., Joswia, D. R., Wang, N. L., Wu, G. J., Wang, M., Zhao, H. B., Yang, W., Liu, X. Q., and He, J. Q.: Black soot and the survival of Tibetan glaciers, P. Natl. Acad. Sci. USA, 106, 22114-22118, 2009a.

Xu, B. Q., Wang, M., Joswiak, D. R., Cao, J. J., Yao, T. D., Wu, G. J., Yang, W., and Zhao, H. B.: Deposition of anthropogenic aerosols in a southeastern Tibetan glacier, J. Geophys. Res.-Atmos., 114, D17209, 10.1029/2008jd011510, 2009b.

Xu, B. Q., Cao, J. J., Joswiak, D. R., Liu, X. Q., Zhao, H. B., and He, J. Q.: Post-depositional enrichment of black soot in snow-pack and accelerated melting of Tibetan glaciers, Environ. Res. Lett., 7, 014022, 10.1088/1748-9326/7/1/014022, 2012.

Yang, K., Ding, B., Qin, J., Tang, W., Lu, N., and Lin, C.: Can aerosol loading explain the solar dimming over the Tibetan Plateau?, Geophys. Res. Lett., 39, 10.1029/2012GL053733, 2012.

Yao, T. D., Thompson, L., Yang, W., Yu, W. S., Gao, Y., Guo, X. J., Yang, X. X., Duan, K. Q., Zhao, H. B., Xu, B. Q., Pu, J. C., Lu, A. X., Xiang, Y., Kattel, D. B., and Joswiak, D.: Different glacier status with atmospheric circulations in Tibetan Plateau and surroundings, Nat. Clim. Change, 2, 663-667, 2012.

Yasunari, T. J., Koster, R. D., Lau, W. K. M., and Kim, K. M.: Impact of snow darkening via dust, black carbon, and organic carbon on boreal spring climate in the Earth system, J. Geophys. Res.-Atmos., 120, 5485-5503, 2015.

Zhang, R., Hegg, D. A., Huang, J., and Fu, Q.: Source attribution of insoluble light-absorbing particles in seasonal snow across northern China, Atmos. Chem. Phys., 13, 6091-6099, 2013a.

Zhang, R., Jing, J., Tao, J., Hsu, S. C., Wang, G., Cao, J., Lee, C. S. L., Zhu, L., Chen, Z., Zhao, Y., and Shen, Z.: Chemical characterization and source apportionment of PM 2.5 in Beijing: seasonal perspective, Atmos. Chem. Phys., 13, 7053-7074, 2013b.

Zhou, Y., Wang, X., Wu, X., Cong, Z., Wu, G., and Ji, M.: Quantifying light absorption of iron oxides and carbonaceous aerosol in seasonal snow across northern China, Atmosphere, 8, 63, 10.3390/atmos8040063, 2017.